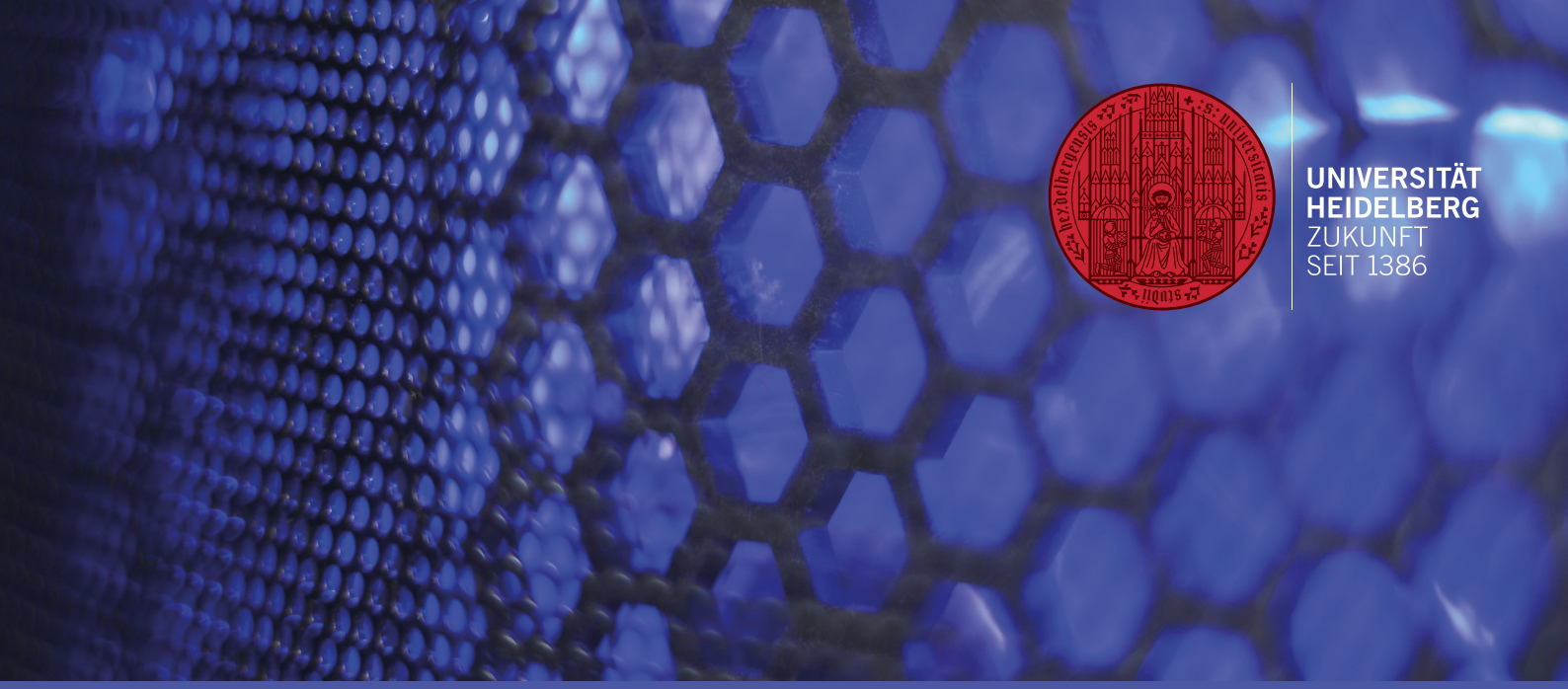

UNIVERSITÄT HEIDELBERG
ZUKUNFT SEIT 1386

# Proceedings of the 3rd bwHPC-SYMPOSIUM

**Heidelberg 2016**

UNIVERSITÄTS-BIBLIOTHEK HEIDELBERG

# Proceedings of the 3rd bwHPC-Symposium

## October 12th 2016 / Heidelberg

Edited by
S. Richling
M. Baumann
V. Heuveline

UNIVERSITÄTS-
BIBLIOTHEK
HEIDELBERG

**The Editors**

**Sabine Richling** is a research associate at the Heidelberg University Computing Centre (URZ) with focus on data intensive and energy efficient computing.

**Martin Baumann** is the head of the service unit „Future IT - Research & Education“ (FIRE) at the Heidelberg University Computing Centre (URZ). This service unit develops and provides IT services for science, e.g. for high-performance computing, for storage of large scientific data, and for scientific visualization.

**Vincent Heuveline** is the Director of the Heidelberg University Computing Centre (URZ). As full professor at Heidelberg University he leads the Engineering Mathematics and Computing Lab (EMCL) under the roof of the Interdisciplinary Centre for Scientific Computing (IWR). Furthermore, he is the group leader of the research group “Data Mining and Uncertainty Quantification” at the Heidelberg Institute for Theoretical Studies (HITS gGmbH).

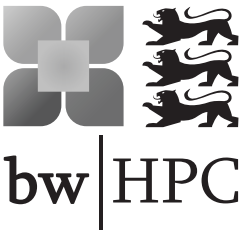


**Bibliographic information published by the Deutsche Nationalbibliothek**
The Deutsche Nationalbibliothek lists this publication in the Deutsche Nationalbibliografie; detailed bibliographic data are available on the Internet at http://dnb.dnb.de.




The online version of this publication is freely available on the ebook-platform of the Heidelberg University Library heiBOOKS http://books.ub.uni-heidelberg.de/heibooks (open access).
urn: urn:nbn:de:bsz:16-heibooks-book-308-7
DOI: 10.11588/heibooks.308.418



Cover Image: Server grill with blue light (https://www.flickr.com/photos/bigpresh/7389234452)
© David Precious. Published under CC BY-SA 2.0 (https://creativecommons.org/licenses/by/2.0)

ISBN: 978-3-946531-70-8 (PDF)

# Contents

**Chemistry**



**Earth Sciences**



**Poster Contributions**

# Welcome to the 3rd bwHPC-Symposium

Vincent Heuveline[1,2,3]

[1]Computing Centre, Heidelberg University
[2]Interdisciplinary Center for Scientific Computing, Heidelberg University
[3]Heidelberg Institute for Theoretical Studies

The bwHPC initiative manages and harmonizes the usage, administration, and (future) setup of supercomputers at higher education institutions and research facilities in the state of Baden-Württemberg. Based on this initiative, researchers are not just limited to using the HPC resources at their home institutions, but are guaranteed fair and easy access to supercomputers all across the state. As maintained by the bwHPC guidelines, many of these supercomputers cater to the individual requirements and special needs of specific disciplines or fields of research. To offer additional support and guidance for all users, the bwHPC-C5 project has been established as an integral part of the bwHPC network.

The bwHPC-Symposium is an annual gathering of administrators and users of this bwHPC network. It fosters a lively exchange between the users and administrators of supercomputers, serving as a platform to discuss experiences, problems, and innovations in a very hands-on manner. As a provider and administrator of one of those supercomputers, we at the Heidelberg University Computing Centre were more than happy to be able to host this event, and we are delighted to share its proceedings with a wider audience through this publication.

High performance computing has become a key asset in modern research. This volume shows just how ubiquitous, how diverse and how interdisciplinary the application of supercomputers has become. The articles in this volume encompass topics from the sciences and the humanities, ranging from physics to earth sciences to economics and engineering.

Figure 1: Welcome to the 3rd bwHPC-Symposium at the Marsilius-Kolleg in Heidelberg.

As we walk further into the digital age of research, we see many changes and challenges looming on the horizon: more digitization in all disciplines (even in the most conservative fields), larger and larger amounts of raw data to store, process, and archive, and research questions that, by their very nature, go far beyond the processing power of the human brain.

Supercomputers are the crucial tool for this digital age. They help us to examine processes of tremendous complexity, from the population patterns of water fleas to the formation of stars in far-off galaxies. To be able to harness their full potential, we need initiatives like bwHPC that help us to use and enhance these powerful research tools in a sensible and proficient way, and these wonderful proceedings of the 3rd bwHPC-Symposium show that we are definitely on the right track.

## Acknowledgements

Many thanks to the Ministry of Science, Research and the Arts Baden-Württemberg (MWK) for the financial support through the bwHPC-C5 project. Furthermore, I would like to thank all participants and contributors of this exciting event, all members of the bwHPC competence centers in Baden-Württemberg for the cooperation in setting up the agenda and for reviewing the contributions of the proceedings, and the members of the bwHPC competence center MLS&WISO for the active support in the execution of the symposium. Special thanks go to the members of the service unit Future IT – Research & Education (FIRE) of the Heidelberg University Computing Centre for the strong support in the preparation and execution of the event and of the proceedings.

Figure 2: Participants of the 3rd bwHPC-Symposium 2016 in Heidelberg.

# High-Performance Computing and Coordinated Compute Cluster Competence Centers in Baden-Württemberg

Robert Barthel

Steinbuch Centre for Computing, Karlsruhe Institute of Technology

Baden-Württemberg's initiative on high-performance computing (**bwHPC**) has been establishing a permeable HPC ecosystem throughout all performance levels (i.e., tiers) including a federated and purpose customized, multi-cluster entry level as well as state-wide coordinated HPC support and competence centers. Clusters, implementation activities and support services are co-funded by Baden-Württemberg's Ministry of Science, Research and the Arts and largely coordinated by the corresponding project **bwHPC-C5**. Driven by a successful and positively reviewed transition phase (i.e., from 2013 until 2015) the project bwHPC-C5 Phase 2 aims between 2016 and 2018 for continuation and expansion of Baden-Württemberg's HPC tier-3 services.

## 1 Introduction

High-performance computing in the state of Baden-Württemberg has a long tradition. The current implementation concept for Baden-Württemberg's high-performance computing from 2013 until 2018, officially labelled **bwHPC** [1], has been aiming for the implementation of HPC clusters covering all HPC performance and scalability levels, i.e., HPC tiers, (Fig. 1) for permeability throughout all HPC tiers, differentiation/customization of tier-3 services to the requirements of scientific areas, and providing federated HPC support via competence centers. The initiative bwHPC recommended by the German Research Foundation (DFG) for funding is considered a model concept for Germany advancing the impact of HPC.

The accompanying state-wide project of bwHPC – officially labelled "bwHPC-C5" which is short for bwHPC: Coordinated Compute Cluster Competence Centers [2] – coordinates all associated provisions and activities to establish HPC competence centers and cooperative HPC operations, unify user environment, pool HPC expertise, as well as identify and implement HPC innovations. Moreover, bwHPC-C5 raises awareness of Baden-Württemberg's HPC, helps to embed the scientific communities into the HPC world and creates synergies for the development of state-wide user support. The project bwHPC-C5 is co-funded by Baden-Württemberg's Ministry of Science, Research and the Arts (MWK).

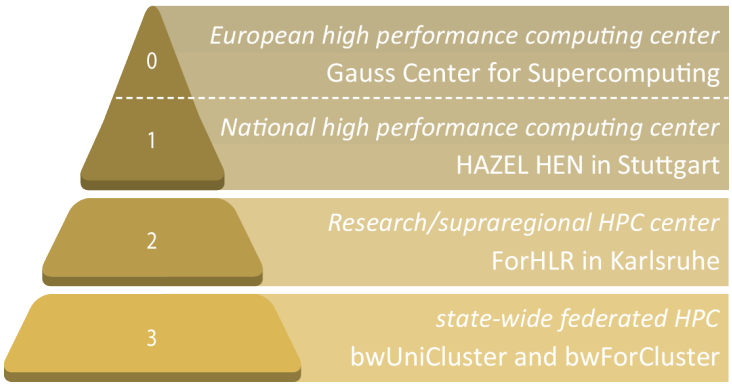


Figure 1: HPC performance pyramid in the state of Baden-Württemberg, Germany: from top (tier 0) to bottom (tier 3) with decreasing scalability and performance level.

## 2 Federated HPC tier-3

Since late 2016 all clusters of Baden-Württemberg's HPC tier-3 are operational. The HPC entrance level consists of the bwUniCluster (bw = Baden-Württemberg, Uni = Universal/University) and 4 bwForClusters (For = Forschung, German for Research). The latter ones are tailored to the needs of particular scientific communities and their specific applications while the former one provides the resources of Baden-Württemberg's universities for general purpose computing covering teaching and all science communities without a dedicated bwForCluster (Tab. 1).

| Cluster | Location | Start date | Purpose |
|---|---|---|---|
| bwUniCluster | Karlsruhe | Jan 2014 | General purpose, teaching |
| bwForCluster JUSTUS | Ulm | Dec 2014 | Computational chemistry; high I/O, large MEM jobs |
| bwForCluster MLS&WISO | Heidelberg / Mannheim | Dec 2015 | Molecular life science, economics and social science; method development |
| bwForCluster NEMO | Freiburg | Sep 2016 | Neuro science, elementary particle physics, micro systems engineering; VM image deployment |
| bwForCluster BinAC | Tübingen | Nov 2016 | Astrophysics, bioinformatics; 60 dual GPU nodes |

Table 1: bwHPC tier-3 clusters: location, operational start date and their main purpose.

## 3 Services and achievements of bwHPC-C5

bwHPC-C5 offers a comprehensive and demand-oriented service for users in Baden-Württemberg for the existing HPC systems. The bwHPC-C5 project assembles a team of more than 30 people from 11 Baden-Württemberg universities[1].

[1] Universities of Freiburg, Tübingen, Ulm, Heidelberg, Hohenheim, Konstanz, Mannheim, Stuttgart, the KIT and the universities of applied sciences in Stuttgart and Esslingen.

**Access services:** bwHPC-C5 is committed to install new levels of federated service management which in particular provides enhancement for users. For logging into bwHPC clusters via home organisation credentials bwHPC-C5 has integrated Baden-Württemberg's federated identity management (bwIDM) in the cluster infrastructure. To transparently apply the usage policies of bwHPC, hence process compute project applications for all bwForClusters, the bwHPC-C5 team has developed and is using the central application site (ZAS) [3] as well as assembled the cluster assignment team.

**Software services:** bwHPC-C5 has managed to set up the same environment and behaviour throughout all tier-3 HPC clusters. Moreover, comprehensive HPC software stacks – in case of bwUniCluster and bwForCluster JUSTUS over 200 and 100 software modules, respectively – together with extensive help built-ins and installation description have been installed which have been expanding upon demands and user requests.

**Support services:** Competence centers for bwHPC, which have been established by the project bwHPC-C5, play a central role in the science specific HPC support as these centers unite technical experts and field specialists and coordinate the high-level support projects (aka tiger team projects). bwHPC competence centers match the scientific fields of the bwForClusters, but also cover areas of expertise without dedicated cluster resources (Fig. 2). Tiger team projects are

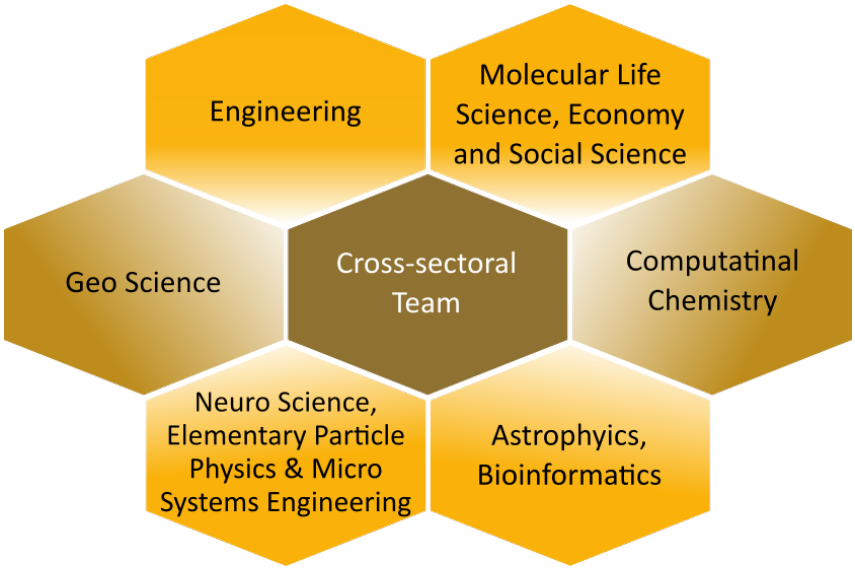


Figure 2: bwHPC competence centers covering the dedicated scientific areas of the bwForClusters, but also three areas of expertise without cluster resources.

the project's most elaborated support activities resulting in 30 collaborations with the scientific communities since 2013 [4]. Other support activities of the bwHPC competence centers are: providing online best practice and user guides [5], aiding in parallelization of application codes and in accessing HPC or traversing to higher HPC tiers, provisioning development tools and scientific software on the HPC systems, and providing tools to manage scientific data. Together with other members of the bwHPC-C5 team HPC courses (incl. materials) [6] have been organized and held at the Baden-Württemberg universities with 36 HPC introductory, 7 programming, 21 HPC tools, 25 parallel programming, 3 visualization, and 7 compiler and debugging courses

since 2014. Furthermore, the current support infrastructure of bwHPC-C5 has more than 20 state-wide HPC support units dealing with all kind of HPC related second level support issues.

**Dissemination:** bwHPC-C5 has been publishing all results of bwHPC (e.g. user's publications [7]), reporting and answering to the (user) steering committees as well as promoting the bwHPC infrastructure to raise awareness of HPC (and bwHPC in particular) to all science communities. To enhance the impact of the scientific communities on bwHPC, the bwHPC-C5 team provides the platform for an annual meeting between users and support/operations teams, namely the bwHPC symposium.

## Acknowledgements

bwHPC-C5 has been co-funded by the Ministry of Science, Research and the Arts of the state of Baden-Württemberg, Germany and the universities of Freiburg, Heidelberg, Hohenheim, Konstanz, Mannheim, Stuttgart, Tübingen and Ulm, the Karlsruhe Institute of Technology, as well as the universities of applied sciences in Stuttgart and Esslingen.

## References

[1] Hartenstein, H., T. Walter, and P. Castellaz. "Aktuelle Umsetzungskonzepte der Universitäten des Landes Baden-Württemberg für Hochleistungsrechnen und datenintensive Dienste." Praxis der Informationsverarbeitung und Kommunikation, Band 36, Heft 2 (2013): 99-108. http://dx.doi.org/10.1515/pik-2013-0007

[2] Barthel, R., T. König. "Landesprojekt "bwHPC-C5" gestartet: Föderative Fachkompetenzzentren unterstützen Landesnutzer beim Einstieg ins Hochleistungsrechnen". SCC-News, 02-2013, pp 6-9.

[3] http://www.bwhpc-c5.de/en/ZAS

[4] http://www.bwhpc.de/en/tiger_team_projects.php

[5] http://www.bwhpc.de/wiki

[6] http://training.bwhpc.de

[7] http://www.bwhpc.de/en/user_publications.php

# The importance and need for system monitoring and analysis in HPC operations and research

Florina M. Ciorba

Department of Mathematics and Computer Science
University of Basel, Switzerland

In this work, system monitoring and analysis are discussed in terms of their significance and benefits for operations and research in the field of high performance computing (HPC). HPC systems deliver unique insights to computational scientists from different disciplines. It is argued that research in HPC is also computational in nature, given the massive amounts of monitoring data collected at various levels of an HPC system. The vision of a comprehensive system model developed based on holistic monitoring and analysis is also presented. The goal and expected outcome of such a model is an improved understanding of the intricate interactions between today's software and hardware, and their diverse usage patterns. The associated modeling, monitoring, and analysis challenges are reviewed and discussed. The envisioned comprehensive system model will provide the ability to design future systems that are better understood before use, easier to maintain and monitor, more efficient, more reliable, and, therefore, more productive. The paper is concluded with a number of recommendations towards realizing the envisioned system model.

## 1 Introduction

Each of the four pillars (experiments, theory, simulation, and data) of the scientific method produce and consume large amounts of data. Breakthrough science will occur at the interface between empirical, analytical, computational and data-based observation. Parallel computing systems are the workhorse of the third pillar: simulation science. These systems are highly complex ecosystems, with multiple layers, ranging from the hardware to the application layer (Fig. 1). Monitoring solutions exist at every single layer. Access to the monitoring data varies between the different communities, which also have different interests in the data. For instance, computational scientists in general have access to the monitoring data from the application layer and in certain cases also from the application environment layer. Their interests may include the running time of their applications but also understanding the application performance by profiling or tracing. Computer scientists may have access to monitoring data from application environment and cluster software layers. They are typically interested in performance data from both software and hardware components and subsystems. System administrators typically have access to data monitored at the hardware, system software, and cluster software layers. The

interests regard more the operational aspects of the system, including availability, fair usage, etc. Accessing and sharing of data based on the actual community interests (as depicted by the arrows in Fig. 1) may require bilateral agreements between the communities or public release of data.

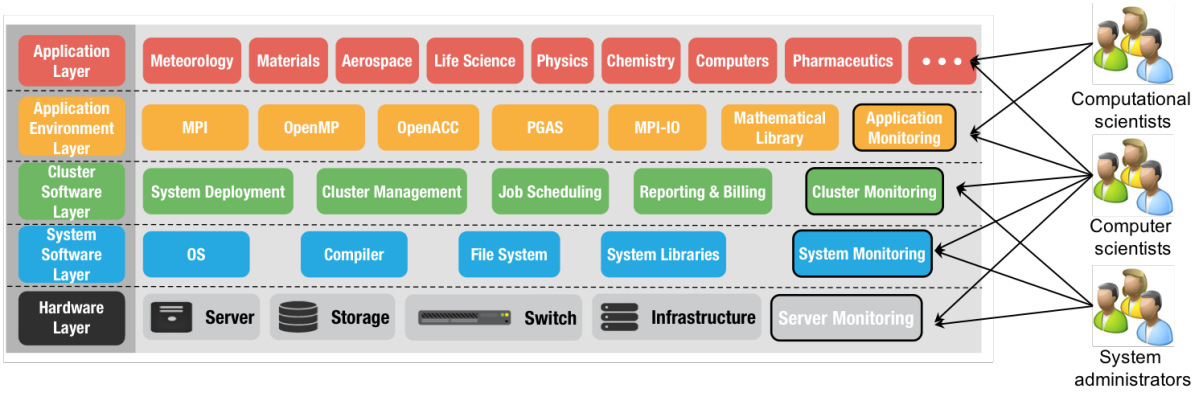


Figure 1: The HPC ecosystem and the monitoring interests of the different communities.

Understanding the interaction between the software running on parallel computers and the underlying hardware is a notorious challenge, especially given the fact that the hardware models and designs change very often. This is due to the rapid advances in computing technologies. Studying the interaction between hardware and software in this context will require integration of monitoring solutions from the different system layers. System monitoring relates to data science (the fourth pillar) in the sense that monitoring applications and systems generates a large amount of data from various sources, at various rates, and under various formats. This brings about all the data-related challenges also faced in other domains that require a data science approach. Thus, scientific research in high performance computing that involves very large amounts of monitoring data becomes *computational computer science*. Conducting research in computational computer science is challenging due to the fact that the "physical world" to be modeled is changing with every new software and hardware release. Specifically, modeling system behavior is a significant challenge for the following reasons: (1) The hardware architecture is heterogeneous. (2) The system stack is also heterogeneous. (3) There exist multiple types of execution environment.

This paper describes the importance and need of holistic system monitoring in view of developing a comprehensive model of the system behavior, wherein "system" denotes both hardware and software components. It is argued that such monitoring and modeling will have positive impacts and ramifications in HPC operations and research, not only for existing systems, but most importantly for the design, procurement, operation, productivity, and maintenance of future HPC systems. A review of existing monitoring and analysis solutions of the different system layers is also presented. The envisioned system model requires a comprehensive view of the applications and the system that captures and integrates activities from all system layers (Fig. 1).

## 2 Current Monitoring and Analysis Solutions

The process of monitoring and analysis consists of three stages: data collection, data processing, and data visualization and analysis. Monitoring and analysis is employed at various layers of

the HPC ecosystem, as illustrated in Fig. 1. Below is a brief review of monitoring solutions for each layer, in a top-down manner, followed by pointers to system-wide monitoring and analysis efforts. The purpose of this review is rather illustrative and not meant to be comprehensive.

## 2.1 Single-Layer Monitoring and Analysis

**Application Layer** The monitoring and analysis solutions described herein pertain both to the *application* and *application environment* layers (Fig. 1). The Virtual Institute for High Productivity Supercomputing (VI-HPS) also provides a great overview and guide in selecting application level productivity tools[1].

*A. Automatic profile and trace analysis*: The Periscope tuning framework[2] enables automatic analysis and tuning of parallel applications. TAU[3] is a set of tuning and analysis utilities that offer an integrated parallel performance system. Score-P[4] is a community-developed instrumentation and measurement infrastructure, targeting both performance and energy. Extra-P[5]: automatic performance-modeling tool that supports the user in the identification of scalability bugs. mpiP[6] is an MPI profiling tool, while mpiPview[7] is an MPI performance profile analysis and viewer. Open|SpeedShop[8] is an integrated parallel performance analysis environment. IPM[9] is an integrated performance monitoring profiling tool.

*B. Visualization and analysis*: Vampir[10] is an interactive graphical trace visualization and analysis tool supporting identification of performance hotspots. Paraver/Dimemas/Extrae[11] form a suite of tools allowing the profiling, tracing and sampling of an application, supported by graphical trace visualization and analysis. Scalasca[12] a tool for large-scale parallel program performance analysis supporting identification of performance bottlenecks. Allinea PR[13] provides performance reports that show the behavior of parallel HPC application runs.

*C. Optimization*: Rubik[14] is a tool that generates topology-aware mapping of processes, optimized for IBM Blue Gene machines. MAQAO[15] is a solution for analyzing and optimizing binary codes on single nodes, supporting Intel64 and Xeon Phi architectures.

*D. Debugging, error and anomaly detection*: MUST[16] is a runtime error detection tool for MPI applications Archer[17] is a low overhead data race detector for OpenMP programs. STAT[18] is a tool for identifying errors in code running at full system scale. Allinea Forge tools[19] includes DDT and MAP, and provides a single interface for debugging, profiling, editing and building code on local and remote systems. RogueWave TotalView[20] is a parallel debugging tool that allows fault isolation, memory optimization, and dynamic visualization for high-scale HPC applications.

**Cluster Layer** The solutions employed at cluster level are either used for cluster management or job scheduling and reporting.

[1] http://www.vi-hps.org/tools/
[2] http://periscope.in.tum.de
[3] http://www.cs.uoregon.edu/research/tau/
[4] http://www.score-p.org
[5] http://www.scalasca.org/software/extra-p
[6] https://computing.llnl.gov/code/mpip-llnl.html
[7] https://computation.llnl.gov/casc/tool_gear/mpipview.html
[8] https://openspeedshop.org/
[9] http://ipm-hpc.sourceforge.net
[10] https://www.vampir.eu
[11] http://www.bsc.es/computer-sciences/performance-tools
[12] http://www.scalasca.org
[13] https://www.allinea.com/products/allinea-performance-reports
[14] https://github.com/LLNL/rubik
[15] http://www.maqao.org
[16] http://www.itc.rwth-aachen.de/MUST
[17] https://github.com/PRUNER/archer
[18] http://www.paradyn.org/STAT/STAT.html
[19] https://www.allinea.com/products/develop-allinea-forge
[20] http://www.roguewave.com/products/totalview.aspx

*A. Cluster management*: Nagios[21] represents the industry standard in IT infrastructure monitoring, including critical components, log server, and network. Ganglia[22] is a scalable and distributed monitoring system used in approximately 90% of HPC shops. It represents data in XML, uses XDR for compact and portable data transfer, and stores and visualizes data using the RRDtool. Supermon[23] is a high-speed cluster monitoring system, that emphasizes low perturbation and high sampling rates. Zenoss[24] provides event-based IT monitoring and analytics for cloud, virtual and physical IT environments. Cerebro[25] is a collection of cluster monitoring tools and libraries, not yet scaling to a full host level. Splunk[26] is a collection of software for searching, monitoring, and analyzing machine-generated big data, via a web-style interface and team dashboards. RUR[27] (resource utilization reporting) is an administrator tool for gathering statistics on how system resources are being used by applications, developed by Cray for its HPC systems. RUR runs before or after applications collecting system statistics.

*B. Job scheduling and reporting*: SysMon[28] is a Windows-based system service that logs system activity in XML format; it is also a batch system monitor plugin for Eclipse PTP. Other batch scheduling systems (e.g., SLURM, UNIVA Grid Engine, PBS/Pro, LSF, Moab/Torque) provide statistics from batch jobs by running daemons on the compute nodes during application execution.

**System Layer** Current solutions for system monitoring and analysis mainly target the operating system and storage/file system behavior.

*A. Operating system*: Collectd[29] is a system statistics collection daemon, which collects performance metrics periodically and can interface with Nagios (see above) and LMT (see below). Perf[30] is a lightweight profiling command line tool for Linux 2.6+ systems (included in the kernel tools); it abstracts CPU hardware differences. Collectl[31] is a comprehensive OS-level monitoring tool which gathers information about Linux system resources: CPU, memory, network, inodes, processes, nfs, tcp, sockets, and others. ProcMon[32] is an advanced monitoring tool for Windows (part of Sysinternals), which shows real-time file system, Registry and process/thread activity.

*B. Storage/File system*: LMT (Lustre Monitoring Tool, http://wiki.lustre.org/Lustre_Monitoring_Tool) is an open-source tool for capturing and displaying of Lustre file system activity. It monitors Lustre file system servers, collects data using the Cerebro monitoring system in a MySQL database. Lltop (https://github.com/jhammond/lltop is a command line utility that monitors file system load (Lustre I/O statistics) and is integrated with job assignment data from cluster batch schedulers. GPFS Monitor Suite (https://sourceforge.net/projects/gpfsmonitorsuite/) uses Perl scripts and Ganglia to monitor IBM's general parallel file system (GPFS) multi-cluster environments, and can interface with Nagios.

**Server Layer** The solutions employed at the server level target the different node-level (and not only) subsystems: CPU, memory, network, I/O, and storage, respectively.

*A. Node/CPU*: PAPI[33] (performance API) is an interface to hardware performance counters found in most microprocessors. Syslog[34] is a Linux system logging utility, which has become

[21] https://www.nagios.org
[22] http://ganglia.info
[23] http://supermon.sourceforge.net
[24] https://www.zenoss.com/
[25] https://github.com/chaos/cerebro
[26] https://www.splunk.com/
[27] http://pubs.cray.com/#/00241000-FA/FA00240785
[28] http://ss64.com/nt/sysmon.html
[29] https://collectd.org
[30] https://perf.wiki.kernel.org/
[31] http://collectl.sourceforge.net
[32] https://technet.microsoft.com/en-us/sysinternals/bb896645.aspx
[33] http://icl.cs.utk.edu/papi/
[34] https://linux.die.net/man/8/syslogd

standard for message logging, applied to various facilities: kernel, user, mail, printer, network, and others.

*B. Memory*: Callgrind[35] is an open-source profiler using execution-driven cache simulation. It is accompanied by KCachegrind, a visualization GUI that provides various views of performance data (annotated call graphs and tree maps, annotated source and machine code). Memchecker[36] a framework integrated within Open MPI that finds hard-to-catch memory errors in parallel applications.

*C. Network*: Monitoring of fabric (e.g., InfiniBand, OmniPath) counters is performed with operating system-level tools such as collectl (see above). Pandora FMS, OpenNMS, NetXMS, and Zabbix are open source network management systems which also perform network performance monitoring. They have recently been compared in a recent article published by Network World[37].

*D. I/O*: SIONlib[38] is a scalable I/O library for parallel access to task-local files that uses shared files for task-local data, written through collective I/O operations. Darshan (http://www.mcs.anl.gov/research/projects/darshan/) is a characterization tool of the I/O behavior of scalable HPC applications. IOTA[39] (I/O tracing and allocation library) is a lightweight scalable tracing tool for diagnosing poorly performing I/O operations to parallel file systems, especially Lustre.

*E. Storage*: DirectMon[40] is a configuration and monitoring solution for DDN storage devices. Iostat[41] is part of the sysstat family of Linux tools, which reports statistics for CPU, input and output storage devices, partitions, and network file systems.

**Remarks** Most of the solutions described above are released under open-source licenses while certain are licensed commercially (e.g., tools from Allinea, Splunk, Zenoss). The majority of the tools are also interoperable (e.g., those included in the VI-HPS Tools Guide[42]). One can observe that more and more tools are being developed and released per layer over time. Truly needed, however, are efforts that integrate these or other tools ideally across all four layers (with respect to Fig. 1), such that a *holistic view* of the behavior of the applications, the software they employ, as well as the hardware on which they run can become feasible.

## 2.2 System-Wide Monitoring and Analysis

The following efforts employ, to different extents, solutions for system-wide or, in some cases, integrated monitoring and analysis of HPC applications and systems.

Elastic Stack[43] consists of Elasticsearch, which along with Logstash and Kibana, provides a powerful platform for indexing, searching and analyzing the data stored in logs. It also includes Beats, an open source platform for building lightweight data shippers for log files, infrastructure metrics, network packets, and more.

Graylog[44] is a powerful open source log management and analysis platform, that has many use cases, from monitoring SSH logins and unusual activity to debugging applications. It is based on Elasticsearch, Java, MongoDB, and Scala.

[35] http://kcachegrind.sourceforge.net/html/Home.html
[36] http://www.open-mpi.org/
[37] http://www.networkworld.com/article/3142061/open-source-tools/pandora-fms-wins-open-source-management-shootout.html
[38] http://www.fz-juelich.de/SIONlib
[39] https://bitbucket.org/mhowison/iota
[40] www.ddn.com/products/storage-management-directmon/
[41] https://linux.die.net/man/1/iostat
[42] http://www.vi-hps.org/upload/material/general/ToolsGuide.pdf
[43] https://www.elastic.co
[44] https://www.graylog.org

Perfsuite[45] is an accessible, open source performance analysis environment for Linux. It consists of a collection of tools, utilities, and libraries for software performance analysis that are easy to use, comprehensible, interoperable, and simple. It serves as starting point for more detailed analyses and for selection of other more specialized tools/techniques.

The SUPReMM[46] project targeted integrating monitoring and modeling of HPC systems usage and performance of resources of XSEDE cluster, and was jointly carried out between the University at Buffalo and Texas Advanced Computing Center (TACC) from 2012-2015. One outcome of this project is TACC stats.

TACC Stats[47] is a package providing tools for automated system-wide resource-usage monitoring and analysis of HPC systems at multiple levels of resolution.

Decision HPC[48] is an analytics and monitoring tool developed by X-ISS, hooks into existing HPC schedulers (e.g., Torque, PBS Pro, LSF, CJM, and Univa Grid Engine) and can interface with common (e.g., Ganglia) or custom cluster monitoring tools. It displays a live dashboard for real-time monitoring in a single pane of glass view.

OVIS[49] is an open source modular software system for data collection, transport, storage, analysis, visualization, and response in HPC systems under active development at Sandia National Laboratories and Open Grid Computing[50]. It provides real-time, intelligent monitoring of the performance, health and efficiency of large scale computing systems.

"Holistic, Measurement-Driven Resilience: Combining Operational Fault and Failure Measurements and Fault Injection for Quantifying Fault Detection and Impact"[51] (HDMR) is a collaboration between the University of Illinois at Urbana-Champaign; Sandia, Los Alamos, and Lawrence Berkeley National Laboratories; and Cray Inc. The goal is to determine fault-error-failure paths in extreme scale systems of today, to help improve those and future systems.

The NSF project "Computer System Failure Data Repository to Enable Data-Driven Dependability"[52] (CSFDR) (2015-2018) will address the need for an open failure data repository for large and diverse computing infrastructures that will provide enough information about the infrastructures and the applications that run on them.

**Remarks** All these efforts address the challenge of system-wide monitoring and analysis in different manners. System-wide monitoring is not necessarily equivalent to *comprehensive* or *holistic* system monitoring. The failure data repository (CSFDR) and resiliency modeling (HMDR) projects take a comprehensive and holistic, respectively, approach to fault monitoring and modeling. However, modeling faulty behavior alone may leave out significant aspects such as logical reconfigurability, heterogeneity, performance variability, utilization of resources, and others. Therefore, all above efforts are a strong source of inspiration and motivation for considering all aspects of applications and system behavior holistically.

## 3 Modeling System Behavior based on Holistic System Monitoring

The author's vision is that system behavior can be modeled comprehensively based on insights and information obtained by holistic system monitoring. In this context, *system* is understood as the entirety of all its software (the four upper layers in Fig. 1) and hardware (the bottom layer

[45] http://perfsuite.ncsa.illinois.edu
[46] https://github.com/ubccr/supremm
[47] https://github.com/TACC/tacc_stats
[48] https://www.hpcwire.com/2014/09/18/modernizing-hpc-cluster-monitoring/
[49] https://ovis.ca.sandia.gov/mediawiki/index.php/Main_Page
[50] https://www.opengridcomputing.com
[51] http://portal.nersc.gov/project/m888/resilience/
[52] https://www.nsf.gov/awardsearch/showAward?AWD_ID=1513197

in Fig. 1) components. Studying system behavior based on single-layer monitoring data limits the insight to the extent corresponding to that particular layer. A model of *system behavior* captures the intricate relation between the behavior of the components in each layer and across layers (Fig. 2). This intricate relation can only be observed and understood, by a "diagnosis team", through *holistic system monitoring* (Fig. 3). Such monitoring will offer a holistic view of the system and facilitate the comprehensive understanding of the system behavior.

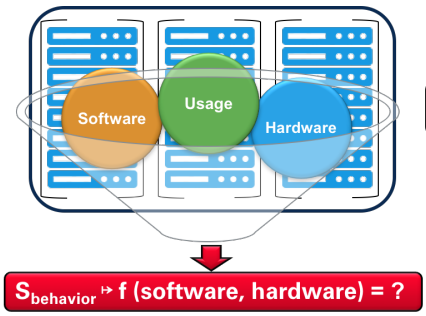


Figure 2: Vision of a system model.

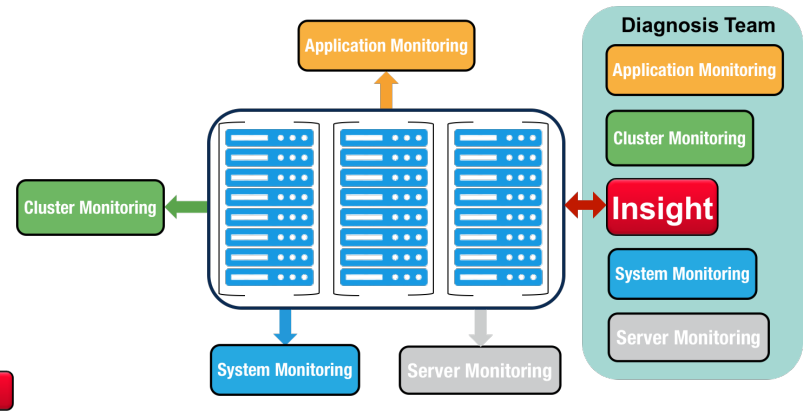


Figure 3: Holistic system monitoring.

The envisioned system model will allow the systematic investigation of the interaction between hardware, software and operating conditions in high performance computers. Moreover, it will provide the ability to study the behavior and efficiency of high performance computers on application, cost, performance, and operational levels.

## 3.1 Challenges

**Modeling** Capturing the complex behavior of computer systems in a *model* is highly challenging because the "physical world" to be modeled is always changing, with every new software and hardware release. Since the interaction between newly released software and/or hardware components cannot be foreseen *a priori*, this interaction needs to be studied by observation *in situ*. In this context, the integration of monitoring solutions from the different system layers is the only path forward. Verification and validation of computer system models is a challenging and rewarding task. The same holds for the verification and validation of the envisioned system model, and will require experiments, simulation, and analytical work.

**Monitoring** Applications and systems *monitoring* generates large amounts of data from various sources (i.e., the system layers of Fig. 1), at various rates, and under various formats.

The data generated by different layers is "owned" by the different communities. For instance, application performance data is "owned" by the computational scientists, while system performance data is "owned" by the system administrators. Computer scientists may "own" data from the application environment layer. However, accessing data from higher or lower layers is not a trivial pursuit. In most cases, such data can be accessed either based on bilateral agreements between the computer scientists and computational scientists/system administrators, or if the data is publicly available.

Holistic monitoring and analysis requires a unified real-time view of all cluster(s) activities, presented in a comprehensive way. This implies that monitoring data needs to be gathered

from application, cluster, system, and server levels, and integrated accordingly. In addition to the data ownership challenge mentioned earlier, data processing challenges include filtering, de-noising, curating, and de-identifying all the data, in view of extracting system behavior.

In terms of infrastructure, larger computing systems require correspondingly larger monitoring infrastructure(s). Consequently, the following questions arise naturally: (1) How can monitoring infrastructures be budgeted and funded? (2) How and where is the monitoring infrastructure hosted? (3) How does the quality of the monitoring hardware influence the quality of the monitoring information? (3) Does the monitoring infrastructure need any form of monitoring? (4) How can the monitoring data be collected on shared resources (e.g., network, storage, etc.) without requiring additional investments? (5) Can comprehensive monitoring be realized in a light-weight manner, to ensure minimal perturbation in system behavior?

**Analysis** The goal of monitoring applications and systems is to gain insight into their behavior by *analyzing* the empirically collected data, ultimately resulting in an analytical behavioral model. The data analysis process faces the following challenges: (1) De-identification and anonymization of sensitive data (e.g., user identifiers and activities, malfunctions, and security vulnerabilities). (2) Extracting value from monitoring data, such as job and project level statistics. This challenge is closely coupled with the choice of relevant metrics, which can be different for across systems. (3) Support of various types of analyses (e.g., qualitative, quantitative). (4) Correlation of data sources, in the form of e.g., integrated databases, multiple databases due to multiple data types. (5) Storing and near-real time indexing of monitoring metrics and logs storing. (6) Concerns about bandwidth consumption on shared resources and denial of service attacks.

**Other Challenges** There are several other challenges on the path to modeling system behavior through holistic monitoring and analysis. (1) Finding the best monitoring and analysis solution for a given HPC system, given that not all comprehensive monitoring solutions will work in practice for all HPC systems. (2) Diagnosing system behavior (including performance) without the right data available is difficult. (3) Data collection and processing noise needs to be minimum (e.g., system logs are quite "noisy" as they collect most of the activities).

## 3.2 Importance and Value

**Importance** Comprehensive system monitoring is important as it provides the basis for maintaining good management and facilitating improvements of HPC systems operations. Understanding the current usage and behavior of HPC systems is the prerequisite for designing and purchasing future systems.

**Value and Benefits** Comprehensive system monitoring can be analogized to personalized system health and has a high value for the HPC stakeholders. More productive HPC operations and research at decreased costs is for the benefit of all scientists, system owners, administrators, and sponsors.

## 3.3 Expected Outcome and Impact

**Outcome** The expected outcome of the envisioned system mode based on comprehensive monitoring and analysis is the ability to (1) Give a personalized system diagnosis. (2) Identify application and system performance variation. (3) Detect contention for shared resources and

assess impacts. (4) Discover misbehaving users and system components. (5) Reduce operational cost. (6) Improve system reliability. Ideally, these analyses should be automated. The system model will offer an improved understanding of the intricate interactions between today's software and hardware, and their diverse usage patterns.

**Impact** The impact of holistic system monitoring and analysis includes: a broader application and project performance assessment, historical trends of applications and systems, estimates of job and operational costs, as well as a positive impact on more targeted future HPC system procurements.

The impact of a comprehensive system model is providing the ability to *design future systems* that are: (1) Better understood before they are deployed and released for production use. (2) Easier to maintain and monitor, right from the start, decreasing the operational and maintenance costs. (3) Larger, more efficient (in terms of performance and energy), more reliable, and, therefore, more productive.

## 4 Summary and Conclusions

**Summary** System monitoring and analysis are important topics of high relevance to a wide range of stakeholders, ranging from system administrators to sponsors, and including computer and computational scientists, that share different interests. The importance of these topics is also supported by the increasing number of workshops, bird-of-a-feather session, panels and discussion events organized at different venues, as well as by the large ongoing and several new funding grants. Remarkable monitoring and analysis efforts exist for different system layers, as well as several system-wide efforts. In this paper, a vision for a system model describing the behavior and interaction between the software and hardware components is presented. The model is based on insights and information obtained by holistic system monitoring. Such monitoring offers a holistic view of the system to a "diagnosis team" which analyzes the information and captures the system behavior in a comprehensive model. The envisioned system model will allow systematic investigation of the interaction between hardware, software and operating conditions in high performance computers. Moreover, it will provide the ability to study the behavior and efficiency of high performance computers on application, cost, performance, and operational levels. A number of challenges have been identified regarding holistic system monitoring as well as comprehensive system modeling. The importance, value, expected outcome, and impact of the envisioned model have also been outlined.

**Recommendations** To conclude the paper, a set of recommendations for going forward are enumerated below. (1) Transform all challenges described herein as opportunities to gain better systems insights that will lead to better systems designs and happier stakeholders. (2) Include the design of the monitoring infrastructure and associated costs as part of the system design, procurement, and maintenance process. Monitoring is often excluded from this process, and seldom designated for performance. (3) Monitor both software and hardware. (4) Decide what aspects are important to record and analyze. (5) Perform a holistic, versus a disjoint, analysis of the monitoring data originating both in software and hardware. (6) Understand the behavior of current (smallest-to-largest) systems before building and using the next (largest) system.

## Acknowledgements

The author acknowledges Prof. Wolfgang E. Nagel, Director of the Center for Information Services and High Performance Computing at TU Dresden, for his support in establishing a system monitoring infrastructure on Taurus[53]. Thanks also go to Dr. Sadaf Alam, Associate Director at the Swiss National Supercomputing Centre, for establishing a system monitoring infrastructure to collect monitoring data on CSCS machines[54]. Acknowledgements also go to Dr. Ann Gentile and Dr. Jim Brandt for building a community site for monitoring large-scale HPC systems collaborations[55] and exchange of ideas. The author further acknowledges the HPC Team, Rechenzentrum, Universität Freiburg, lead by Prof. Gerhard Schneider for welcoming the idea of monitoring the bwForCluster NEMO[56] in view of collecting failure information and optimizing application performance.

[53] https://doc.zih.tu-dresden.de/hpc-wiki/bin/view/Compendium/SystemTaurus

[54] http://www.cscs.ch/computers/index.html

[55] https://sites.google.com/site/monitoringlargescalehpcsystems/

[56] https://www.hpc.uni-freiburg.de/nemo

# Modeling the Dynamics of the Interstellar Medium

Ralf S. Klessen[1], Simon C. O. Glover[1], Rowan J. Smith[2], Paul C. Clark[3], and Volker Springel[1,4]

[1]Zentrum für Astronomie, Universität Heidelberg
[2]Jodrell Bank Centre for Astrophysics, University of Manchester
[3]School of Physics and Astronomy, Cardiff University
[4]Heidelberger Institut für Theoretische Studien

Stars and star clusters are the fundamental visible building blocks of galaxies. They form by gravitational collapse in regions of high density in the complex multi-phase interstellar medium. The process of stellar birth is controlled by the intricate interplay between the self-gravity of the star-forming gas and various opposing agents, such as supersonic turbulence, magnetic fields, radiation pressure, and gas pressure. We approach the problem employing high-resolution multi-physics multi-scale simulations. We report some recent results from our research activities making use of the high-performance computing infrastructure in Baden-Württemberg.

## 1 Introduction

Understanding the formation of stars together with their subsequent evolution and identifying the physical processes that govern the dynamics of the interstellar medium (ISM) are central research themes in astronomy and astrophysics. Knowledge of stellar birth is a prerequisite for deeper insights into the assembly of planets and planetary systems and for the search for our own origins. Stars and star clusters are fundamental building blocks of the galaxies we observe. Understanding the formation and evolution of galaxies, their chemical enrichment history, and their observational properties throughout the cosmic ages are key research areas in extragalactic astronomy and cosmology that also depend on a deep understanding of ISM physics.

Dynamical processes in the ISM are the central engine of galaxy evolution, and determine where and at what rate stars form. There are close links between large-scale phenomena, such as spiral arms or tidal perturbations, and the local process of star birth. Conversely, the energy and momentum input from stars is an important driver of ISM dynamics and turbulence. Stellar radiation and winds as well as supernova explosions determine the chemical and thermal state of the ISM, which in turn affects subsequent star formation. The dynamical evolution of the ISM is governed by the complex interplay between matter and radiation, turbulent motions, magnetic fields, self-gravity, and local variations in the chemical composition.

Shedding light on the fundamental physical processes that control the formation and evolution of stars and galaxies at different cosmic epochs and identifying and characterizing the various feedback loops that link these together are research activities at the Center for Astronomy in Heidelberg (ZAH) and the Heidelberg Institute for Theoretical Studies (HITS). Here, we report some recent findings that make use of the high-performance computing infrastructure in Baden-Württemberg as well as national supercomputing facilities.

## 2 Numerical Approach

The formation of stars and the dynamics of the ISM can only be understood by considering self-gravity, turbulence, magnetic fields, the coupling between matter and radiation, chemical reactions, stellar feedback, cosmic rays, as well as the galactic environment consistently and simultaneously. This lies at the very forefront of computational astrophysics, and only recently have researchers begun to truly face this complexity through the development of sophisticated computer codes capable of simulating these processes self-consistently.

In this proceedings I focus on an investigation by Rowan Smith and collaborators [13], in which we use the moving mesh code Arepo developed by Volker Springel and his group at the Heidelberg Institute for Theoretical Studies [14]. Arepo solves the hydrodynamical equations on an unstructured mesh defined by the Voronoi tessellation of a set of mesh-generating points. These points can be kept static or can move with the local gas flow. In the latter case, the method becomes similar to a mesh-based Lagrangian scheme, but one which avoids the severe mesh distortions that have hampered the application of previous mesh-based Lagrangian schemes to complex three-dimensional gas flows. With moving mesh points, the scheme naturally adapts its spatial resolution to account for local accumulation of gas, in a similar fashion to the widely-used smoothed particle hydrodynamics (SPH) approach. However, unlike SPH, the fact that the method is mesh-based allows modern high-order shock-capturing schemes to be used, allowing strong shocks and other discontinuities to be treated more accurately than in SPH (see e.g. [1], [12] for examples of flows treated more accurately by Arepo than by SPH). The Arepo mesh can be refined or de-refined simply by adding or subtracting mesh points, allowing the study of problems with an extremely large dynamical range of densities and length scales. Together, these properties make Arepo a superb tool for modeling the formation of dense molecular gas in spiral galaxies.

The chemical evolution of the gas in our simulations is modeled using a highly simplified hydrogen-carbon-oxygen chemical network designed to follow the formation and destruction of the two main molecular species in the ISM, $H_2$ and CO [7, 8, 11]. Full details of this network can be found in [5], with some additional discussion in [10]. We account for the photodissociation of $H_2$ and CO by the interstellar radiation field (ISRF), which we assume to have a similar strength and spectrum to the values measured in the solar neighborhood [4]. The attenuation of this radiation field in dense gas owing to molecular self-shielding and dust absorption is treated using the TreeCol algorithm developed by Clark and colleagues [3]. This algorithm computes approximate discretized maps of the dust extinction and molecular column densities surrounding each mesh cell with the help of information stored in an oct-tree structure. These maps then allow us to calculate the amount by which the ISRF is attenuated in each mesh cell, and hence also the amount by which the $H_2$ and CO photodissociation rates are reduced compared to their values in optically thin gas. At the same time as modelling the chemistry, we also model the thermal evolution of the gas due to radiative and chemical heating and cooling, using a simplified but accurate cooling function [6, 5].

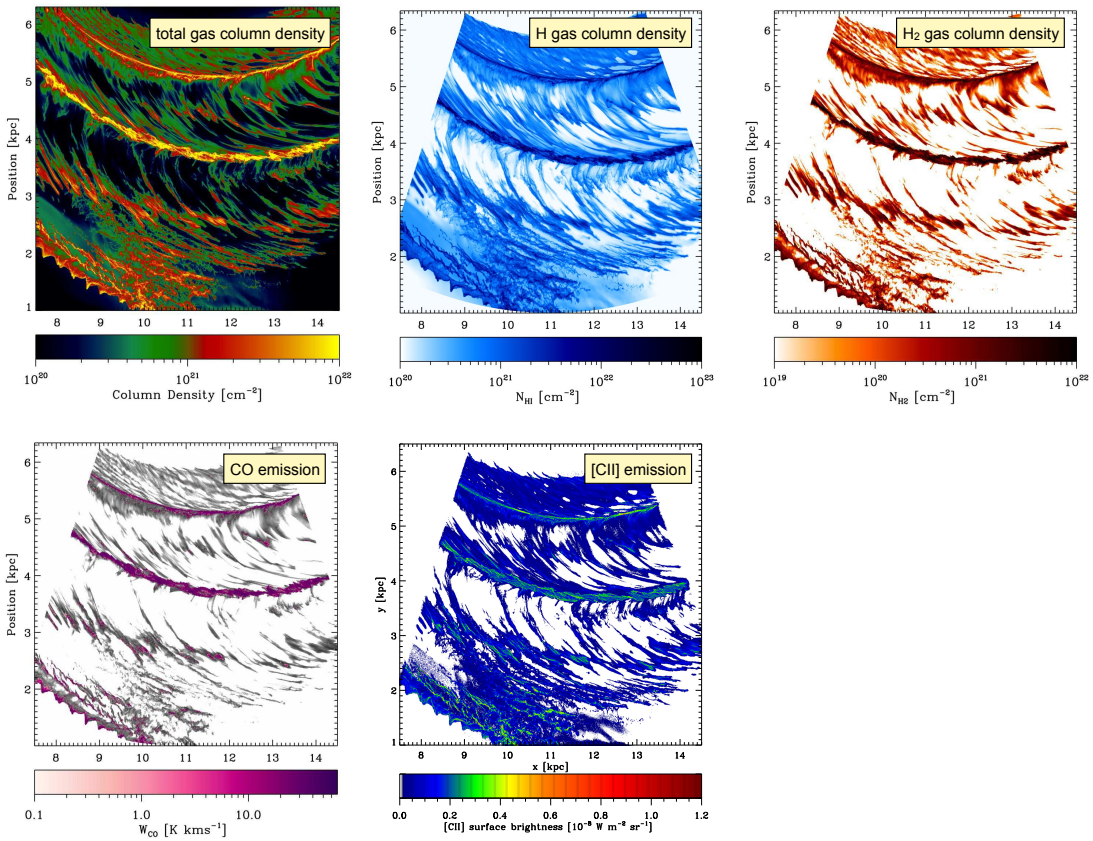


Figure 1: Map of the column densities and emission from various important chemical species in a selected region of the disk of a Milky Way type galaxy from the simulation of Smith et al. [13]. The *top left* shows the total column density of the gas. The *top middle* depicts the column density of atomic hydrogen, and the *top right* illustrates the distribution of molecular hydrogen. As molecular hydrogen itself does not emit under typical Milky Way conditions, observers often resort to studying the emission of carbon bearing species. At the *bottom left* we therefore show the emission of carbon monoxide (purple) superimposed on the column density of molecular hydrogen (in grey). The *bottom middle* image provides an impression of the fine structure emission of singly ionized carbon, the [CII] line; for more details, see Glover & Smith [9]. Note that all maps exhibit a wide range of morphologies, including dense spiral arms, filamentary spurs, and diffuse inter-arm regions.

## 3 Selected Results

By mass, the ISM consists of around 70% hydrogen, 28% helium, and 2% heavier elements (referred to generically as "metals"). However, because helium is chemically inert, it is common to distinguish the different phases of the ISM by the chemical state of hydrogen in each phase. For example, ionized bubbles are called HII regions, while atomic gas is often termed HI gas, in both cases referring to the spectroscopic notation. Dark clouds are sufficiently dense and well-shielded against the dissociating effects of interstellar ultraviolet radiation to allow $H_2$ and CO to survive for millions of years. They are therefore called molecular clouds. These are the regions that give birth to new generations of stars, and so they are the focus of most current studies of the star formation process.

One would like to observe molecular clouds by observing the emission from the $H_2$ molecules, since $H_2$ is the main constituent of the clouds. Unfortunately, $H_2$ is a very light molecule with widely-spaced energy levels, and its first accessible radiative transition lies around 500 K above its ground state. Since most of the molecular gas has a temperature of less than 50 K, the result is that transitions in $H_2$ are rarely excited. For this reason, observers focus instead on emission at radio and sub-millimeter wavelengths from dust grains or from heavy molecules such as CO that tend to be found in the same locations as $H_2$. The outer layers of molecular clouds are also often studied using the fine structure line of singly ionized carbon ($C^+$).

Because we employ a time-dependent chemical network that runs alongside the hydrodynamics in every computational cell and that is updated at every timestep in the simulation, we can produce synthetic maps of various chemical species. Figure 1 provides examples of this approach. In the top row we show the column densities of the total gas, of atomic hydrogen, and of molecular hydrogen. The bottom row illustrates the emission from CO and $C^+$. Further details of these emission maps can be found in [13] and [9], respectively.

Figure 2 focuses on the most important tracer of molecular gas, the emission from CO, and provides zoom-ins into different regions. Visual inspection of the images reveals that a significant fraction of molecular hydrogen is not well traced by CO. This is the so-called CO-dark $H_2$ gas. One obvious hiding place of this gas is in dark envelopes surrounding CO-bright molecular clouds. This has been investigated in the past [15] using static one-dimensional radiative transfer calculations with highly detailed chemical networks (PDR codes, where PDR stands for photo-dissociation region). In the three-dimensional simulations of ISM dynamics presented here we also find CO-dark $H_2$ in the immediate vicinity of CO-bright clouds. But in addition, these calculations show that a significant amount of CO-dark $H_2$ is located in extended filaments with lengths of tens to hundreds of parsecs. They are typically located in the inter-arm regions of the disk and inclined to the main spiral arms.

These filaments are created when denser gas clumps are sheared out by the differential rotation of the disk following their passage through the spiral arm [2]. Their highly elongated geometry makes the filaments more susceptible to photodissociation since it is easier for radiation to penetrate the cloud along the short axes of the filament. Compared to a spherical cloud a filamentary one has a greater surface to volume ratio which increases the difficulty of achieving a sufficient column density of gas to shield the CO. Many of the longer filaments in our calculation do have CO-bright regions close to their centers, but some remain CO-dark throughout. Measurements of the ends of these structures using UV line absorption would characterize them as diffuse molecular clouds with high $H_2$ fractions but little or no CO, whereas the central regions would be easily visible in CO emission and would be characterized as dense molecular clouds. However, in reality, both "clouds" are part of the same extended structure.

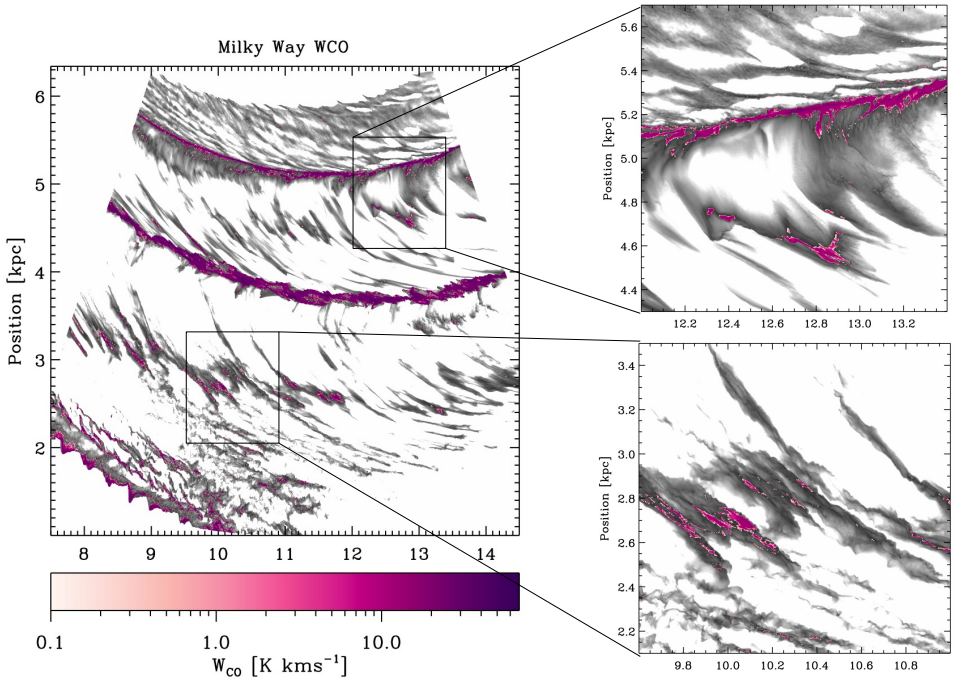


Figure 2: Comparison of $H_2$ column density and CO integrated intensity for selected regions. The images demonstrate that a significant fraction of molecular hydrogen is not well traced by CO. This is the so-called CO-dark $H_2$ gas.

## 4 Summary

In this contribution, we have discussed numerical simulations of Smith and collaborators [13], in which we model a significant portion of the disk of a Milky Way like galaxy with a version of the Arepo moving mesh code [14] that includes a self-consistent treatment of the chemistry of the interstellar medium. In the most highly refined portion of our simulation we reach a mass resolution of only four solar masses. This approach enables us to resolve substructure within the disk sufficiently accurately to match the observed transition from atomic to molecular hydrogen gas without having to resort to some ad-hoc subgrid-scale model to represent unresolved density fluctuations. We can, for example, determine the fraction of CO-dark $H_2$ gas with unprecedented precision and compare the simulation value with the results from current measurements. Other applications include the prediction of [CII] emission for observational campaigns with SOFIA[1], which is a high-altitude airplane equipped with a 2.5 meter telescope, or the calculations of synthetic HI emission maps that help improve our astrophysical interpretation of data from 21 cm surveys of the plane of our Milky Way or of external galaxies (such as THOR and THINGS, lead by researchers at the Max Planck Institute for Astronomy in Heidelberg)[2].

[1]SOFIA – Stratospheric Observatory for Infrared Astronomy: `https://www.nasa.gov/mission_pages/SOFIA/index.html`

[2]THOR – The HI/OH/Recombination Line Survey of the Inner Milky Way: http://www2.mpia-hd.mpg.de/thor/Overview.html, THINGS – The HI Nearby Galaxy Survey: http://www.mpia.de/THINGS/Overview.html

## Acknowledgements

The publication by Smith and collaborators has been supported by the following grants: DFG Priority Program SPP 1573 *Physics of the Interstellar Medium*, DFG Collaborative Research Center SFB 881 *The Milky Way System* (sub-projects B1, B2, B5 and B8), ERC Advanced Grant *STARLIGHT* (project number 339177), ERC Starting Grant *EXAGAL* (project number 308037). The calculations have been performed in part at the Leibniz Supercomputing Center in Garching, at the SFB Cluster maintained by the Jülich Supercomputing Center, and at the HPC Facilities in the State of Baden-Württemberg.

## References

[1] Bauer A., Springel V., 2012, MNRAS, 423, 2558

[2] Bonnell I. A., Dobbs C. L., Smith R. J., 2013, MNRAS, 430, 1790

[3] Clark P. C., Glover S. C. O., Klessen R. S., 2012, MNRAS, 420, 745

[4] Draine B. T., 1978, ApJS, 36, 595

[5] Glover S. C. O., Clark P. C., 2012, MNRAS, 421, 116

[6] Glover S. C. O., Federrath C., Mac Low M.-M., Klessen, R. S., 2010, MNRAS, 404, 2

[7] Glover S. C. O., Mac Low M.-M., 2007a, ApJS, 169, 239

[8] Glover S. C. O., Mac Low M.-M., 2007b, ApJ, 659, 1317

[9] Glover S. C. O., Smith R. J., 2016, MNRAS, 462, 3011

[10] Klessen R. S., Glover S. C. O., 2016, Saas-Fee Advanced Course 43 (Springer-Verlag Berlin Heidelberg), 85

[11] Nelson R. P., Langer W. D., 1997, ApJ, 482, 796

[12] Sijacki D., Vogelsberger M., Kereš D., Springel V., Hernquist L., 2012, MNRAS, 424, 2999

[13] Smith R. J., Glover S. C. O., Clark P. C., Klessen R. S., Springel V., 2014, MNRAS, 441, 1628

[14] Springel V., 2010, MNRAS, 401, 791

[15] Wolfire M. G., Hollenbach D., McKee C. F., 2010, ApJ, 716, 1191

# NEMO's part in investigating the Higgs boson

Ulrike Schnoor and Felix Bührer

Physikalisches Institut, Albert-Ludwigs-Universität Freiburg

After the discovery of a particle compatible with a Higgs boson in 2012, one of the main efforts at the Large Hadron Collider (LHC) at the European Center for Nuclear Research (CERN) has been the investigation of the new particle's properties. This talk describes some of the related studies as well as the general workflow of LHC data analysis as it is carried out at computing centers around the world. Some of this work is performed at the `NEMO` computing cluster at the University of Freiburg, a resource of the *bwHPC-C5* project. It offers additional computing power to the existing Tier-2 and Tier-3 site of the World-wide LHC Computing Grid (WLCG) in Freiburg, the Black Forest Grid (`BFG`), through the deployment of virtual research environments.

## 1 Introduction

The High-Performance Computing (HPC) cluster `NEMO` [1] at the University of Freiburg is one of the Tier-3 centers within the *bwHPC-C5* project [2]. It provides the communities of elementary particle physics, neuroscience, and microsystems engineering in the state of Baden-Württemberg with a hybrid of cloud computing and HPC resources.

The particle physics community has been driving developments of data-intense research from the start [3], with the most well-known contribution being the 1989 proposal of the World-Wide Web [4]. Even in the era of Big Data, it ranks among the occupants with the largest needs of computing storage [5]. Most of the data production, storage, and analysis is carried out using the World-wide LHC Computing Grid (WLCG) [6].

One of the most important results so far at the Large Hadron Collider has been the observation of a new particle compatible with a Higgs boson in 2012 [7]. This discovery has started the pursuit of a variety of Higgs-related measurements: From the couplings to the particles of the Standard Model to spin and parity properties of the Higgs boson, a large amount of follow-up measurements has already been published, e.g. [8]. So far, all results are in agreement with the Standard Model predictions. However, in many cases, the statistical and systematic uncertainties are rather large, allowing for a range of deviations from the Standard Model which could still be realized in nature. Section 2 briefly outlines the basic theory and current research in particle physics.

The Black Forest Grid (`BFG`) at the University of Freiburg has been a part of the WLCG since 2005. The ATLAS production and analysis jobs for which the `BFG` has provided resources have been and continue to be a part of the discoveries and measurements of ATLAS. Section 3

describes the LHC and the WLCG projects. New approaches to extend the resources for local user jobs and, in an opportunistic way, the Tier-2 resources, are being tested at the `NEMO` HPC cluster and will be described in Sec. 4.

# 2 The Standard Model of Particle Physics

## 2.1 Fundamental forces and elementary particles

The Standard Model of Particle Physics (SM) is the most complete theory describing three of the four fundamental forces. It has been developed in the 1960s [9, 10] and has proven to be a very successful theory, accurately describing all observed particle interactions in the currently accessible energy range. The only known exceptions are the gravitational force, which is not included in the SM, and the masses of neutrinos.

The SM is a quantum field theory based on local gauge symmetries which generate the forces between the elementary particles. Each force is mediated by the corresponding gauge bosons: For the electroweak force, which unifies the electromagnetic and weak forces, these are the photon, $W^{\pm}$, and $Z^0$ bosons. The strong force describing interactions of quarks within nuclei and hadronic bound states is mediated by gluons.

The known fundamental particles can be grouped according to their properties and the interactions in which they take part. Particles with spin 1/2, the fermions, are divided in two groups: Leptons, which interact via the electroweak force, and quarks, which interact via the electroweak and the strong forces. In the lepton sector, doublets of electrically charged leptons and zero electric charge neutrinos can be arranged in three so-called families ordered by mass of the charged lepton (electron, muon, or $\tau$ lepton). Similarly, the six quark flavors are ordered in three families where the quarks within one family form a doublet under the weak symmetry.

For each particle of the SM, one antiparticle exists which carries the same mass, same spin, and the exact opposite charges.

## 2.2 The Higgs mechanism and its discovery at the LHC

In the SM, the fundamental fermions and bosons are described as massless. However, experimental evidence has shown that the weak bosons, charged leptons and the quarks, and even neutrinos, are massive with masses ranging from less than 1 eV (neutrinos) up to 172 GeV (top quark). Introducing a mass for these particles breaks the electroweak symmetry. The Higgs mechanism provides a description to break this symmetry spontaneously, while the underlying Lagrangian still fulfills the symmetries. According to this mechanism, particles gain their mass through the interaction with a scalar field. The excitations of this field generate the Higgs boson, which is massive itself.

The postulation of the Higgs mechanism in 1964 [11, 12, 13] started the hunt for a signal of the Higgs boson. At the predecessors of the LHC, no sign for this boson had been found. Finally, in 2012, the two largest experiments ATLAS and CMS have presented the discovery of a new gauge boson based on data analysis in different decay channels at a mass of 125 GeV [14].

## 2.3 Scrutinizing the Higgs boson and open questions

Several theories beyond the SM incorporate a Higgs-like boson generated through electroweak symmetry breaking. However, if the Higgs sector contains physics beyond the SM, certain properties of the 125 GeV boson should deviate from the values predicted by the SM.

Several open questions imply the need for physics beyond the SM. The Higgs mechanism does not give a reason for the values of the masses of the elementary particles, which range over many orders of magnitude. Also, several observations have lead to the conclusion, that a new kind of matter called "dark matter" must exist [15, 16]. However, none of the known elementary particles accounts for its effects.

Furthermore, the imbalance of matter and anti-matter in the universe can not be explained within the SM. Today's universe consists mostly of matter, and no large amounts of anti-matter have been found, even though during the Big Bang, equal amounts of anti-matter and matter should have been produced according to the so-called CP symmetry [17]. The SM contains a small asymmetry between matter and anti-matter [18], which is not sufficient to explain the observed ratio of matter to anti-matter though. Hence, searches for new sources of violation of the CP symmetry are being investigated. One such possibility is that the Higgs sector introduces CP violation. Investigations of CP violation in the Higgs sector, using the weak gauge boson fusion production of Higgs bosons, have been carried out at the ATLAS experiment using computing resources in Freiburg [19]. A follow-up study with data from 2015 and 2016 will be using the `NEMO` cluster for parts of the data analysis.

# 3 The Large Hadron Collider and the World-wide LHC Computing Grid

## 3.1 The ATLAS experiment at the Large Hadron Collider

The ATLAS experiment is a large multipurpose particle detector measuring proton-proton collisions provided by the Large Hadron Collider (LHC). It is located near Geneva, Switzerland and has been taking data since 2009.

The LHC is situated in a circular tunnel of 27 km circumference. It accelerates two oppositely directed proton beams to an energy of 6.5 TeV each (in 2015 and 2016). The two beams collide at four interaction points, each occupied by a large particle detector. The largest detector is the ATLAS experiment with a length of 45 m and a height of 25 m. It consists of several subdetectors as depicted in Fig. 1.

In the years 2012-2016, the ATLAS data acquisition has produced an output of raw data of 10-15 petabytes per year [20, Fig. 3.7].

## 3.2 The World-wide LHC Computing Grid

The World-wide LHC Computing Grid (WLCG) is a distributed computing system consisting of more than 170 sites in 42 countries contributing computing power as well as storage to the LHC experiments [6]. The WLCG is organized in a hierarchical way, with the Tier-0 centers at CERN and Wigner Research Center for Physics, Budapest, Hungary in the center (Fig. 1). The Tier-1 level comprises 13 large computing facilities, and 140 centers make up the Tier-2 level.

## 3.3 The ATLAS computing model

The distributed data management (DDM) and distributed computing services must deal with the vast amounts of collision data that the ATLAS experiment produces when the LHC is running as well as simulated data gained from computational resources. Sufficient backup and fast access to datasets for analyzers must be ensured. Processes of interest usually account for only very small fractions of the collected events. After thorough calibration procedures, data

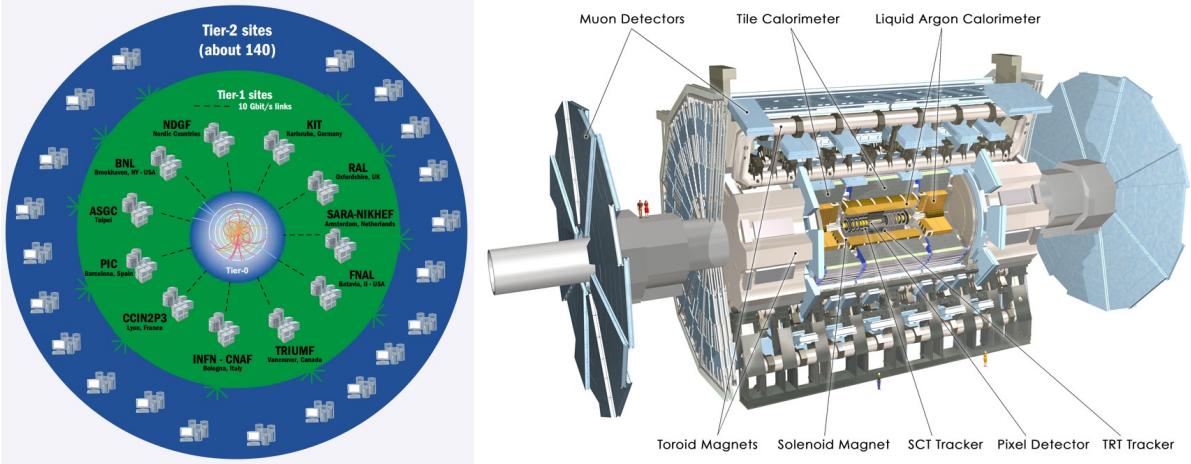


Figure 1: Left: Structure of the WLCG[1]. Right: Schematic of the ATLAS experiment[2].

samples are subsequently reduced through the application of filters optimized for the selection of interesting events.

The ATLAS computing model [21] incorporates all steps from the raw data to the completed statistical analysis of signal events. It is divided in several steps, each reflected in a specific data format described by the ATLAS Event Data Model (EDM) [22].

The primary processing of collision data from the detector is handled at the Tier-0 center. The resulting raw data is archived at the Tier-0 as well as at Tier-1 centers, where it is also reprocessed. The Tier-1 centers provide capacities to store and to analyze the reprocessed data. Derivation algorithms are run on the reconstructed data, providing analysis-specific reduction of the content saved per event. Derived datasets are then copied to Tier-2 facilities where they can be analyzed. Each Analysis Object Data (AOD) dataset is replicated once at a Tier-1 and once at a Tier-2 disk. In addition to data processing capacities, the Tier-2 centers provide capacities for simulation and for calibration of processed raw data. Simulated data is stored at the Tier-1 centers analogously to detector data. Tier-3 facilities provide additional computing resources.

The final element of the chain is the scrutinizing data analysis performed by the researchers [23]. This requires the optimization of selection criteria, simulation of specific event samples, evaluation of systematic uncertainties; furthermore the application of fits and the generation of so-called toy Monte Carlo events for the statistical analysis [23]. These tasks are carried out on Tier-2 and Tier-3 resources or on additional resources provided by institutes and universities around the world.

## 3.4 The Black Forest Grid in Freiburg

The Black Forest Grid (`BFG`) is a shared Tier-2 and Tier-3 site of the WLCG. It comprises 220 worker nodes providing a total of 3000 cores (hyperthreaded). For distributed WLCG storage, a `dCache` instance provides a total of 1.35 PB. The space provided to ATLAS users corresponds to 1/60 of the total storage of ATLAS in the WLCG. In addition, a parallel storage based on the `lustre` [24] file system is deployed, providing 145 TB of storage to local (Tier-3) users.

The site has been in operation since 2005. It is currently shared with local users from the

[1]Source: http://wlcg-public.web.cern.ch/tier-centres
[2]Source: http://kjende.web.cern.ch/kjende/zpath_files/img/highslide/ATLAS_detector_alles_mittel_EN.png

communities of physics, biodynamics, and other groups. In the imminent future, these local users are moving to the resources of the *bwHPC-C5* centers.

# 4 Virtualizing the ATLAS research environment

## 4.1 The NEMO HPC cluster in Freiburg

The *bwForCluster* NEMO is a High-Performance Computing resource at the Rechenzentrum at Universität Freiburg. It comprises 756 worker nodes, each with 40 cores (hyperthreaded) and a RAM of 128 GB. The nodes are interconnected with a 100 Gbit/s OmniPath [25] system. Each node is supplied with a local 240 GB SSD.

After its installation in July 2016, the NEMO cluster has been ranked 214 in the TOP 500 list [26]. It uses a novel approach for a hybrid of HPC and cloud computing [27] and serves the communities of elementary particle physics, microsystems engineering, and neuroscience in the state of Baden-Württemberg.

## 4.2 ATLAS software on NEMO

ATLAS data analysis programs currently mainly run on Scientific Linux 6 (SL6) operating systems, which is based on RedHat Enterprise Linux 6. Most of the software environment is provided by the CERN VM File System (cvmfs). Hence, ATLAS data analysis is run ideally on machines with a SL6 operating system providing cvmfs infrastructure.

The *bwForCluster* NEMO runs CentOS7 as operating system and does not provide cvmfs. Therefore, in order to run ATLAS software on NEMO, the virtualization and containerization of the environment is investigated as a means to emulate the ATLAS environment on NEMO as the host system. It can then be used for local (WLCG Tier-3) and grid jobs (WLCG Tier-2).

## 4.3 Virtualization of the ATLAS infrastructure

The virtualization of ATLAS software on NEMO makes use of its already established hybrid cluster approach. An instance of OpenStack [28] is deployed allowing to run both bare metal jobs and virtual machines (VMs). The latter are using kvm [29] as the hypervisor.

In order to start virtual machines on NEMO on demand for jobs submitted at the BFG, the challenge lies in the connection of the batch schedulers of the two systems, which is illustrated in Fig. 2. The BFG login nodes serve as user interfaces. The scheduler deployed at the BFG, a slurm [30] instance, is used to allow users to schedule jobs running on VMs, while the VMs themselves are scheduled by the Moab [31] instance running at NEMO.

The *elastic computing* feature of the slurm scheduler [32] is used to request the start-up of new VMs on demand.

The VM is based on an SL6 image contextualized using packer [33] and running a dedicated puppet [34] role similar to the one used for setup of regular BFG worker nodes. Using packer and puppet allows to automatize and versionize the generation of a new image whenever an update should be propagated to the VMs.

## 4.4 NEMO's part in investigating the Higgs boson

With the setup for virtualized research environments described above, NEMO can be used by researchers from the connected institutions for data analysis of ATLAS data. Groups from

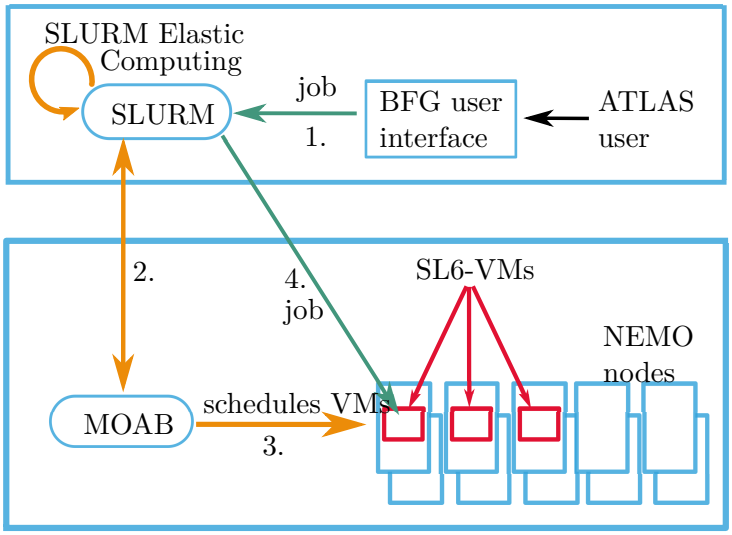


Figure 2: Virtualization environment for ATLAS on `NEMO`.

Freiburg are taking advantage of this resource. The same setup can potentially be exploited for opportunistic use of `NEMO` for standalone CPU-intensive tasks such as event generation campaigns [35].

## 5 Conclusions and Outlook

The ATLAS experiment at the LHC is investigating the nature of the Higgs boson, a particle connected to the mechanism of electroweak symmetry breaking which constitutes an important part of the Standard Model of particle physics. At the same time, it can offer insights into physics beyond the Standard Model, which is investigated through the measurement of its properties, such as its behavior with respect to the CP symmetry.

The ATLAS computing model relies on distributed computing to handle the up to 15 PB of data output from the experiment deploying the World-wide LHC Computing grid.

One of the Tier-2 sites of the WLCG is the `BFG` at Universität Freiburg. Efforts to virtualize the ATLAS research environment are currently on-going, with the aim of allowing jobs using Tier-3 resources of the `BFG` to run on the *bwHPC-C5* `NEMO` center at Universität Freiburg. Main challenges include the integration into the schedulers of `NEMO` and `BFG` to start virtual machines on demand, providing access to the local user environment, as well as the automatic generation of a fully functional, versionized virtual machine image.

## Acknowledgements

The *bwHPC-C5* project has been funded by the Ministry of Science, Research and the Arts of the state of Baden-Wuerttemberg, Germany.

The authors thank Konrad Meier (Computing Center Universität Freiburg) for collaboration on the virtualization setup. Many sincere thanks to Anton J. Gamel and Michael Böhler for successful operation of the Black Forest Grid and to Markus Schumacher for the project leadership. Cooperation with the HPC team (Michael Janczyk, Konrad Meier, Dirk von Suchodoletz, Bernd Wiebelt) at the Computing Center at Universität Freiburg is gratefully acknowledged.

## References

[1] "bwForCluster NEMO at Universität Freiburg." https://www.hpc.uni-freiburg.de/nemo, accessed 2017-01-05

[2] "bwHPC-C5 Project." https://www.bwhpc-c5.de/, accessed 2017-01-05

[3] Paolo Zanella. "30 Years of Computing at CERN." http://ref.web.cern.ch/ref/CERN/CNL/2001/002/cern-computing/, accessed 2017-01-05

[4] https://www.w3.org/History/1989/proposal.html, accessed 2017-01-13

[5] https://www.wired.com/2013/04/bigdata/, accessed 2017-01-13

[6] The LCG TDR Editorial Board. "LHC Computing Grid: Technical Design Report." LCG-TDR-001, CERN-LHCC-2005-024. 20 June 2005. http://cds.cern.ch/record/840543/files/lhcc-2005-024.pdf accessed 2017-01-09

[7] ATLAS Collaboration. "Observation of a new particle in the search for the Standard Model Higgs boson with the ATLAS detector at the LHC." Phys. Lett. B 716 (2012) 1-29; CMS collaboration. "Observation of a new boson at a mass of 125 GeV with the CMS experiment at the LHC." Phys. Lett. B 716 (2012) 30

[8] ATLAS and CMS Collaborations. "Measurements of the Higgs boson production and decay rates and constraints on its couplings from a combined ATLAS and CMS analysis of the LHC $pp$ collision data at $\sqrt{s} = 7$ and 8 TeV." JHEP 08 (2016) 045

[9] S.L. Glashow. "Partial-symmetries of weak interactions." Nuclear Physics. 22 (4): 579–588.

[10] S. Weinberg. "A Model of Leptons." Phys. Rev. Lett. 19 (21): 1264–1266.

[11] F. Englert, R. Brout. "Broken Symmetry and the Mass of Gauge Vector Mesons." Physical Review Letters. 13 (9): 321–323.

[12] P.W. Higgs. "Broken Symmetries and the Masses of Gauge Bosons." Physical Review Letters. 13 (16): 508–509.

[13] G.S. Guralnik; C.R. Hagen; T.W.B. Kibble. "Global Conservation Laws and Massless Particles." Physical Review Letters. 13 (20): 585–587.

[14] ATLAS and CMS Collaborations. "Combined Measurement of the Higgs Boson Mass in $pp$ Collisions at $\sqrt{s} = 7$ and 8 TeV with the ATLAS and CMS Experiments." Phys. Rev. Lett. 114, 191803 (2015)

[15] Jacobus Cornelius Kapteyn. "First attempt at a theory of the arrangement and motion of the sidereal system." Astrophysical Journal. 55: 302–327 (1922)

[16] J.H. Oort. "The force exerted by the stellar system in the direction perpendicular to the galactic plane and some related problems." Bulletin of the Astronomical Institutes of the Netherlands, 6 : 249-287 (1932)

[17] L. Landau. "On the conservation laws of weak interactions, Nuclear Physics." Band 3, 127–131 (1957)

[18] J. H. Christenson, J. W. Cronin, V. L. Fitch, R. Turlay. "Evidence for the $2\pi$ Decay of the $K_2^0$ Meson System." Physical Review Letters. 13: 138 (1964)

[19] ATLAS Collaboration. "Test of CP Invariance in vector-boson fusion production of the Higgs boson using the Optimal Observable method in the ditau decay channel with the ATLAS detector." Eur. Phys. J. C76 (2016) 658

[20] "Update of the Computing Models of the WLCG and the LHC Experiments." WLCG-ComputingModel-LS1-001, http://cds.cern.ch/record/1695401/files/LCG-TDR-002.pdf, accessed 2017-01-09

[21] ATLAS Collaboration. "ATLAS Computing Technical Design Report." https://cdsweb.cern.ch/record/837738/files/lhcc-2005-022.pdf, accessed 2017-01-09

[22] A. Buckley, T. Eifert M. Elsing, D. Gillberg, K. Koeneke, A. Krasznahorkay, E. Moyse, M. Nowak, S. Snyder, P. van Gemmeren. "Implementation of the ATLAS Run 2 event data model." 2015 J. Phys.: Conf. Ser. 664 072045 (http://iopscience.iop.org/1742-6596/664/7/072045)

[23] O. Behnke, K. Kroninger, G. Schott, T. Schorner-Sadenius. "Data Analysis in High Energy Physics: A Practical Guide to Statistical Methods." Wiley-VCH 2013. ISBN:3527410589

[24] "Lustre File System." http://lustre.org/, accessed 2017-01-09

[25] "OmniPath." http://www.intel.de/content/www/de/de/high-performance-computing-fabrics/omni-path-architecture-fabric-overview.html, accessed 2017-01-10

[26] NEMO on the TOP500 Supercomputer Statistics List https://www.top500.org/system/178839, accessed 2017-01-10

[27] https://www.bwhpc-c5.de/wiki/index.php/Category:BwForCluster_NEMO, accessed 2017-01-10

[28] OpenStack Open Source Cloud Computing Software https://www.openstack.org/, accessed 2017-01-10

[29] KVM (Kernel-based Virtual Machine) www.linux-kvm.org/, accessed 2017-01-10

[30] https://slurm.schedmd.com/overview.html, accessed 2017-01-13

[31] http://www.adaptivecomputing.com/products/hpc-products/moab-hpc-basic-edition/, accessed 2017-01-10

[32] https://slurm.schedmd.com/elastic_computing.html, accessed 2017-01-13

[33] Packer: tool for creating machine and container images for multiple platforms from a single source configuration. https://www.packer.io/, accessed 2017-01-13

[34] Puppet Enterprise. "IT automation for cloud, security, and DevOps." https://puppet.com/, accessed 2017-01-10

[35] B. Wiebelt, M. Janczyk, D. v. Suchodoletz, A. Aertsen, S. Rotter, G. Quast, M. Schumacher, A. Greiner. "Strukturvorschlag für eine bwHPC-Governance der ENM-Community." in "Kooperation von Rechenzentren: Governance und Steuerung – Organisation, Rechtsgrundlagen, Politik." De Gruyter, Oldenburg, 2016

# Multiscale Modelling with Accelerated Algorithms

Wolfgang Wenzel

Institute of Nanotechnology, Karlsruhe Institute of Technology

Multiscale Materials Modelling Simulation becomes increasingly important to understand phenomena at the nanoscale and develop novel materials. In recent years, we have developed multiscale simulation approaches for de-novo characterization and optimization of materials and device properties on the basis of their nanoscale constituents. Here we discuss development of the atomic molecular switches [1, 2], the electronic and structural properties of nanocarbon materials [3, 4, 5] and organic semiconductor devices [5, 6]. Small-molecule organic semiconductors are used in a wide spectrum of applications, ranging from organic light emitting diodes to organic photovoltaics. However, the low carrier mobility severely limits their potential, e.g. for large area devices. As an example of our methodology, we present a parameter-free model, which provides an accurate prediction of experimental data over ten orders of magnitude in mobility, and allows for the decomposition of the carrier mobility into molecule-specific quantities. We also demonstrate that a single molecular property, i.e. the dependence of the orbital energy on conformation, is the key factor defining mobility for hole transport materials. The availability of first-principles models to compute key performance characteristics of organic semiconductors may enable in-silico screening of numerous chemical compounds for the development of highly efficient opto-electronic devices.

## References

[1] Xie, F.Q., Maul, R., Obermair, C., Wenzel, W., Schon, G. & Schimmel, T. "Multilevel Atomic-Scale Transistors Based on Metallic Quantum Point Contacts." Advanced Materials 22, 2033-+ (2010).

[2] Branchi, B., Karipidou, Z., Sarpasan, M., Knorr, N., Rodin, V., Friederich, P., Neumann, T., Meded, V., Rosselli, S., Nelles, G., Wenzel, W., Rampi, M.A. & Von Wrochem, F. "Self-Assembled Metal-Terpyridine Wires for Robust Large Area Molecular Devices." Adv. Materials (in press) (2016).

[3] Lukas, M., Meded, V., Vijayaraghavan, A., Song, L., Ajayan, P.M., Fink, K., Wenzel, W. & Krupke, R. "Catalytic subsurface etching of nanoscale channels in graphite." Nat Commun 4, 1379 (2013).

[4] Beljakov, I., Meded, V., Symalla, F., Fink, K., Shallcross, S., Ruben, M. & Wenzel, W. "Spin-Crossover and Massive Anisotropy Switching of 5d Transition Metal Atoms on Graphene Nanoflakes." Nano Letters 14, 3364-3368 (2014).

[5] Moench, T., Friederich, P., Holzmueller, F., Rutkowski, B., Benduhn, J., Strunk, T., Koerner, C., Vandewal, K., Czyrska-Filemonowicz, A., Wenzel, W. & Leo, K. "Influence of Meso and Nanoscale Structure on the Properties of Highly Efficient Small Molecule Solar Cells." Advanced Energy Materials 6 (2016).

[6] Friederich, P., Symalla, F., Meded, V., Neumann, T. & Wenzel, W. "Ab-initio Treatment of Disorder Effects in Amorphous Organic Materials: Towards Parameter Free Materials Simulation." Journal of Chemical Theory and Computation (2014).

# The genetic population structure of multiple species of *Daphnia* waterfleas

Robert H.S. Kraus[1], Anne Thielsch[2], Bruno Streit[3], and Klaus Schwenk[4]

[1]Department of Biology, University of Konstanz
[1]Department of Migration and Immuno-Ecology, Max Planck Institute for Ornithology
[2,4]Institute for Environmental Science, University of Koblenz-Landau
[3]Institute of Ecology, Diversity and Evolution, Goethe-University Frankfurt am Main

We studied the genetic population structure of European *Daphnia* waterfleas of 46 ponds and lakes and 1626 individuals across the whole of Europe. By using a genetic marker system of 12 so-called microsatellites we were able to divide these individuals into genetically similar groups without prior information on their sampling locations and to infer assignment to one of three species, and within species to one of several populations. This task required a computationally intensive sequence of independent but repeated analyses. The HPC infrastructure of the Baden-Württemberg bwHPC-C5 initiative provided us with the resources to parallelise these otherwise serial analyses and arrive at a useful solution both faster and more accurate as otherwise possible. Specifically, we used the Bayesian clustering algorithms implemented in the software Structure 2.3.4 on the bwUniCluster by using bash scripts and the command 'parallel'. The three *Daphnia* species, *D. longispina*, *D. cucullata* and *D. galeata*, displayed distinct population structures which lead to the inference of differences in the reaction to anthropogenic pressure to which they are exposed, depending on, for example, level of eutrophication or stocking of fish for industrial food production. These were linked to known ecological and life history traits and were discussed in the framework of global environmental change and its potential influence on natural food webs in fresh water habitats.

# CFD Study of the Blood Flow in Cerebral Aneurysms Treated with Flow Diverter Stents

Augusto F. Sanches and Eva Gutheil

Interdisciplinary Center for Scientific Computing, Heidelberg University

Flow diverters are high-density meshed stents designed to reduce the flow into the aneurysm and enhance the potential of aneurysmal thrombosis formation, which presents a condition expected to reduce the risk of growth and rupture of residual aneurysms. In this study, the blood flow in cerebral aneurysms with implanted stents is modeled and analyzed taking into account the design and porosity of the flow diverter, where the focus is the flow reduction through the cerebral aneurysm. For a high-density mesh flow diverter, the reduction in the flow through the aneurysm was higher compared to the low-density mesh regular stent. Thus, a regular stent may not provide enough efficiency in flow reduction inside the aneurysm, possibly causing treatment failure, and the flow diverter is a more efficient invasive treatment to reduce the risk of rupture in cerebral aneurysm. Computational fluid dynamics (CFD) simulations of intracranial aneurysm hemodynamics usually assume a Newtonian blood rheology model. The present study shows that this assumption may overestimate the wall shear stress in intracranial aneurysm domes and underestimate the risk of rupture.

## 1 Introduction

Cerebral aneurysm is a vascular disease characterized by the local dilatation of arterial walls in the intracranial space. The prevalence of intracranial aneurysms in the general population is approximately 2%-3% [1]. Rupture of an aneurysm can cause subarachnoid hemorrhage, associated with a high risk of mortality and morbidity [2]. Due to widely used imaging methods in clinical surgery, the detection of unruptured aneurysms becomes more and more frequent. While patient-specific (e.g. family history, smoking) and aneurysm-specific (e.g. size, location) factors increase the risk of rupture, they are not very specific. In order to reduce the risk of rupture and hemorrhage and to identify highly effective treatment options, the understanding of the hemodynamic mechanisms involved is of great importance, and numerical tools may provide excellent support of the medical treatment of cerebral aneurysms.

There are two effective approaches for the treatment of intracranial aneurysms: Clipping of the aneurysmal neck, and endovascular intervention. The latter one is the treatment of choice for cerebral aneurysms because of both its safety and efficacy. The major advantage of this

treatment is the fact that there is no need to do a craniotomy, avoiding the exposure of the surface of the brain vessel.

The flow diverter stent is a promising method of endovascular reconstruction for large and complex intracranial aneurysms, with an overall porosity metallic mesh placed in the parent artery to reduce blood flow in the aneurysm to the point of stagnation and gradual aneurysmal thrombosis [3].

Computational techniques offer new capabilities in the healthcare provision for intracranial aneurysms. The availability of a simulation tool for a virtual flow diverter is extremely useful to support the decisions of treatment options by medical experts and to develop and optimize new implant designs [4]. In the present project, the development of a computational tool for the modeling and simulation of the hemodynamic effects of the endovascular stents with different porosities are developed. Both a flow diverter and a regular stent are modeled and analyzed taking into account their design, porosity, and the flow reduction through a giant sidewall cerebral aneurysm. A workflow which is able to connect the clinical data and a numerical software package to carry out CFD simulations based on patient-specific computational tomography (CT) medical images, and patient-specific boundary conditions is demonstrated. A model based on geometrical properties of braided flow diverter stents that includes the wires' location as well the length and local porosity of the stent in a patient specific vasculature is used.

The study includes the influence of the blood rheology assumption of a Newtonian versus non-Newtonian viscosity model to investigate the wall shear stress in the dome of the cerebral aneurysm, which is considered to be associated with the risk of rupture.

The simulation intends to provide realistic insight into the pathological vessel parameters and better evaluation of the risk of rupture for a given patient.

## 2 Computational Grid, Mathematical and Numerical Methods

An idealized giant sidewall cerebral aneurysm, cf. Fig. 1, with a diameter of 33 mm is modeled based on a three-dimensional cerebral rotational angiography image provided by the Neuroradiology Department of Heidelberg Medical School. The spherical aneurysm is located at distance 2.0 mm above a straight cylindrical artery of diameter 4.5 mm. The length of the artery inlet to the aneurysm proximal is 52 mm and the length of the aneurysm distal to the artery outlet is also 52 mm.

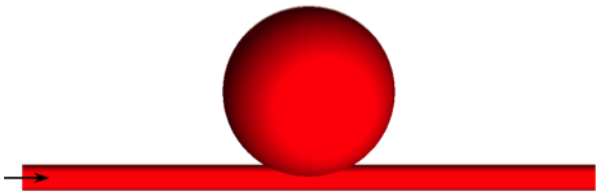

Figure 1: Geometry of the giant cerebral aneurysm

Two stents with meshes made of cylindrical wires are considered which fit the shape of the parent artery. Their geometrical configuration and properties are summarized in Fig. 2 in terms of a stent unit cell [5]. The stent with a low metal coverage proportion and high porosity is called regular stent (RS) and that with a high metal coverage proportion and low porosity is known as flow diverter stent (FD).

Patient-specific geometries for CFD are created from 3D rotational angiogram (3DRA) for

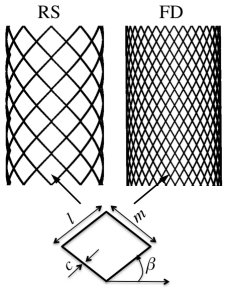


| Dimension | RS | FD |
|---|---|---|
| $l$ [mm] | 0.96 | 0.30 |
| $m$ [mm] | 0.94 | 0.30 |
| $c$ [µm] | 60 | 42 |
| $\beta$ [°] | 49 | 55 |
| $\epsilon$ (porosity) [-] | 0.88 | 0.73 |

Figure 2: Left: geometrical configuration; Right: properties of the regular stent (RS) and flow diverter (FD)

every patient. The CT images are imported into the software ImageLab to repair and delete artifacts, segmentation and smoothing of the region of interest, as shown by the Fig. 3, left and center parts. A terminal middle cerebral aneurysm with a diameter of 9.0 mm, was provided by the Heidelberg Medical School, and an internal carotid artery (ICA) aneurysm shown in Fig. 4 (left) with a diameter of 4.25 mm was obtained from the Toronto Western Hospital, Canada.

The computational grids for the simulations were generated using the software ICEM-CFD v.11 (Ansys Inc.). The tetrahedral mesh number is increased until the flow field independent of the number of grid cells is guaranteed. For the untreated aneurysm (UA) model, 6.14 million grid

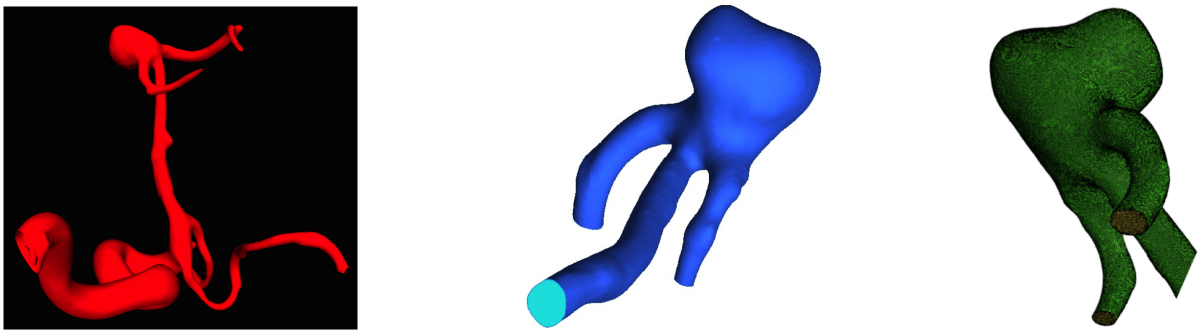

Figure 3: Terminal middle cerebral aneurysm: segmentation (left), geometry (center) and mesh (right)

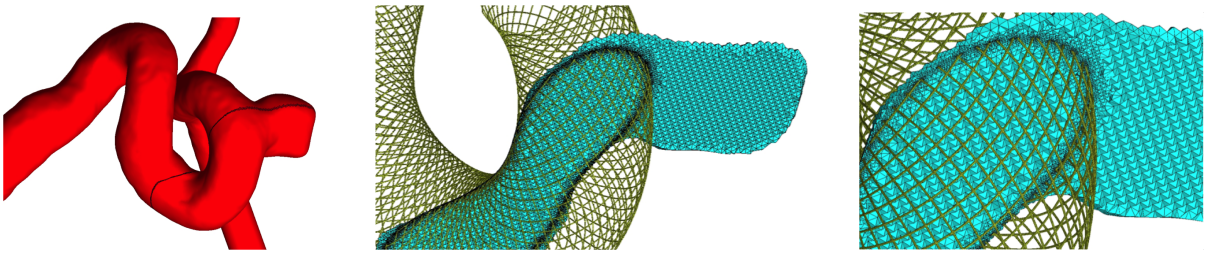

Figure 4: ICA aneurysm with flow diverter: geometry (left), meshing cut plane (center), and image zoom of the meshing cut plane (right)

cells are used, and for the aneurysm merged with the RS, 11.39 million cells are used, whereas for the aneurysm combined with the FD, 11.93 million grid cells are necessary.

Considering the patient-specific aneurysms, 8.3 million grid cells for terminal aneurysm as shown by the Fig. 3 (right), and 31 million grid cells for the ICA aneurysm deployed with the flow diverter as shown in Fig. 4 center and right parts.

The laminar flow is described by three-dimensional incompressible transport equations, which are solved using the finite volume based software platform OpenFoam v3.1. A uniform velocity profile of 0.56 m/s for the peak systole is prescribed at the inlet [6], and the pressure gradient at the outlet is zero. All the vascular walls are assumed rigid with a no-slip boundary condition, and the elasticity of the stent is neglected.

The blood flow is not homogeneous and its rheological properties are mainly dependent on the hematocrit or the volume fraction of red blood cells in the blood, cholesterol, fibrinogen, for instance. In the present study, the most commonly used power-law model of Carreau-Yasuda [7] is used for the non-Newtonian fluid.

For the UA, the high performance computing resource used was 64 processors during 36 hours clock time. For the RS and FD, 256 processors were used with 4 and 7 days clock time, respectively. In the patient-specific flow diverter situation, the simulation was performed during two weeks clock time using 256 processors.

## 3 Results and Discussion

The terminal aneurysm shows a slowly recirculating secondary vortex near the dome. The non-Newtonian and Newtonian models predict similar velocity and wall shear stress (WSS) distributions in the parent vessels of the aneurysm. However, as shown in the Fig. 5, large discrepancies in the WSS between the predictions of the different rheology models are found in the dome area of the terminal aneurysm, where the flow is relatively stagnant. In this region, the non-Newtonian model predicts lower shear rates and WSS values as well as a higher blood viscosity compared to the Newtonian model. Thus, the assumption of a Newtonian blood flow may underestimate the risk of rupture in the aneurysms.

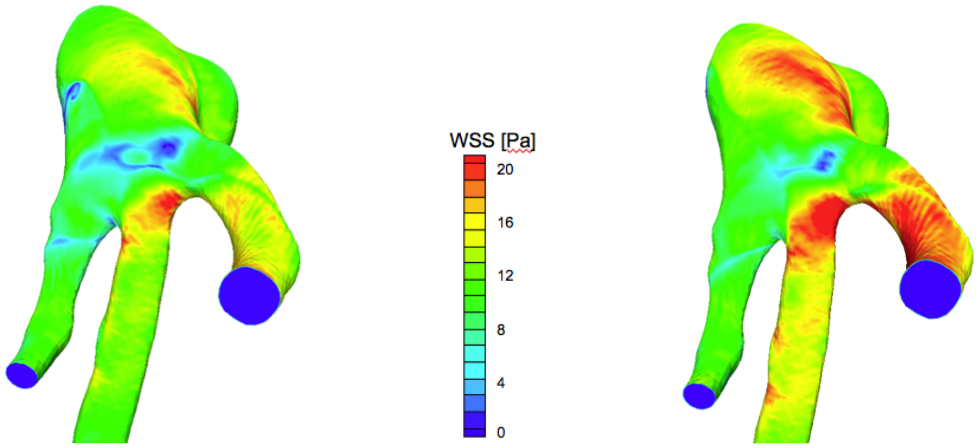


Figure 5: Wall shear stress distribution in front view: non-Newtonian (left) and Newtonian (right) blood flow

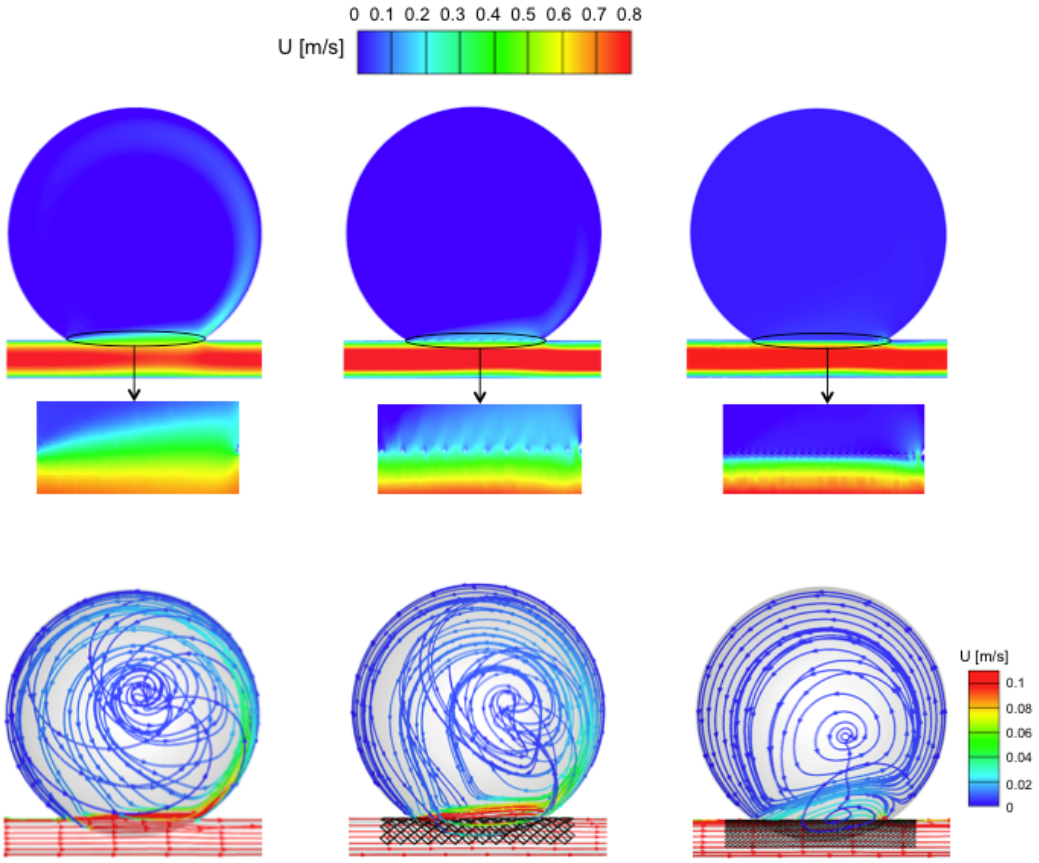


Figure 6: Velocity contour at the mid plane (top) and velocity streamlines (bottom) of the untreated aneurysm (left), regular stent (center) and flow diverter (right) during the peak systole

The magnitude of the flow velocity inside the aneurysm is strongly reduced due to the use of the RS and even more due to the FD, as shown in Fig. 6. The reduction of the aneurysm inflow and the flow activity after the implantation of a stent or flow diverter is a key factor for thrombus formation inside the aneurysm.

In both the pure aneurysm and the aneurysm treated with the regular stent, the flow pattern at the neck of the cerebral aneurysm consists of a main clockwise distal inflow jet. A possible physical mechanism to describe this phenomenon involves both shear stress and pressure [8]. The shear stress transmitted at the cerebral aneurysmal neck, induced by a strong velocity gradient in the parent artery, drives a counter-clockwise intra-aneurysmal flow. The use of the flow diverter causes the flow to transfer into a clockwise streamline from the proximal to distal side of the neck, driving a low motion swirl to the aneurysm's dome. The implantation of the FD impedes the flow at the aneurysm's neck, resulting in both a lower shear stress transmission and an increase of pressure gradient along the parent artery. The latter pushes the circulating fluid inward and outward the cerebral aneurysm at the proximal and distal sides of the neck, respectively.

## 4 Conclusions

The flow diverter effectively reduces the blood flow velocity into cerebral aneurysms and provides a structure to support endothelialization and reconstruction of the parent artery. The use of the flow diverter is superior compared to the regular stent, and flow separation at the distal side of the neck is observed, promoting aneurysmal thrombosis. The Newtonian fluid assumption may underestimate the flow viscosity and overestimate the WSS in regions of stasis or slow recirculation typically found in the dome in complex-shaped aneurysms as well as in aneurysms following endovascular treatment.

## Acknowledgements

The authors thank Prof. Dr. M. Bendszus and Dr. M. Möhlenbruch from Neuroradiology Department of Heidelberg Medical School and Dr. P. Bouillot, Dr. O. Brina and Prof. Dr. V. Pereira, from Toronto Western Hospital, Canada, for providing the medical images and data. They gratefully acknowledge the high-performance computing at bwUniCluster funded by the Ministry of Science, Research and the Arts Baden-Württemberg, and the financial support of the Graduate School "MathComp".

## References

[1] Rinkel, G.J., M. Djibuti, A. Algra, and J. van Gijn. Prevalence and risk of rupture of intracranial aneurysms: a systematic review. Stroke (1998) 29:251-256.

[2] Kaminogo, M., M. Yonekura, and S. Shibata. Incidence and outcome of multiple intracranial aneurysms in a defined population. Stroke (2003) 34:16-21

[3] Möhlenbruch, M.A., C. Herweh, L. Jestaedt, S. Stampfl, S. Schönenberger, P.A. Ringleb, M. Bendszus, and M. Pham. The FRED flow-diverter stent for intracranial aneurysms: clinical study to asses safety and efficacy. Am J Neuroradiol (2015) 36:1155-1161

[4] Bouillot, P., O. Brina, R. Ouared, K.O. Lovblad, M. Farhat, V.M. Pereira. Particle imaging velocimetry evaluation of intracranial stents in sidewall aneurysm: hemodynamic transition related to the stent design. PLoS ONE (2014) 9:1-17

[5] Bouillot, P., O. Brina, R. Ouared, K.O. Lovblad, M. Farhat, V.M. Pereira. Hemodynamic transition driven by stent porosity in sidewall aneurysms. J Biomech (2015) 48:1300-1309

[6] Reymond, P., F. Merenda, F. Perren, D. Rüfenacht, N. Stergiopulos (2009) Validation of one-dimensional model of the systemic arterial tree. Am J Physiol Heart Circ Physiol 297:H208-H222

[7] Gambaruto, A., J. Janela, A. Moura, A. Sequeira. Shear-thinning effects of hemodynamics in patient-specific cerebral aneurysms. Math Biosc Eng (2013) 10:649-665

[8] Meng, H., Z. Wang, M. Kim, R.D. Ecker, L.N. Hopkins. Saccular aneurysms on straight and curved vessels are subject to different hemodynamics: implications of intravascular stenting. Am J Neuroradiol (2006) 27:1861-1865

# Estimation of cerebral network structure

Jonathan Schiefer and Stefan Rotter

Bernstein Center Freiburg & Faculty of Biology, University of Freiburg

Our goal is to design and test new methods to reconstruct causal interactions between local populations of neurons based on population signals measured at multiple sites. This involves a number of challenges for which the usage of high performance computing is essential. These challenges occur in both the data analysis itself, as well as in large-scale network simulations to validate the data analysis.

## 1 Introduction

Inference of brain connectivity is of great importance both in basic research and for clinical applications. To this end, we have devised a new method for inferring effective connectivity from a complete set of covariances of neuronal activity measured at multiple sites. In other words, we are looking for causal relations reflected by measured brain signals. Our method exploits the covariance structure of the activity very efficiently. This makes our method robust with regard to temporal resolution and renders it applicable to various data types occurring in clinical practice, including electrocortigograms (ECoG) and functional magnetic resonance imaging (fMRI).

Our inference method uses statistical data analysis and machine learning. Since in the analysis of real data the ground truth is unknown, we employ biophysically informed large-scale numerical simulations to validate the results of data analysis. For both fields of application high performance computing is essential.

## 2 Data analysis

Inspired by [4], which focused on estimating effective connectivity among single neurons using spike train covariances, we extended the method to continuous population signals recorded from the brain.

As model we use a linear system with a vector of continuous signals $Y(t)$ given by

$$\begin{aligned} Y(t) &= X(t) + \int G(\tau) Y(t-\tau) d\tau \\ &= X(t) + (G * Y)(t) \end{aligned} \tag{1}$$

where $X(t)$ is the external input, and $G(\tau)$ is a matrix of kernels describing the pairwise interaction between nodes. Fourier transformation and rearranging equation (1) yields

$$\hat{Y}(\omega) = (\mathbb{1} - \hat{G}(\omega))^{-1} \hat{X}(\omega).$$

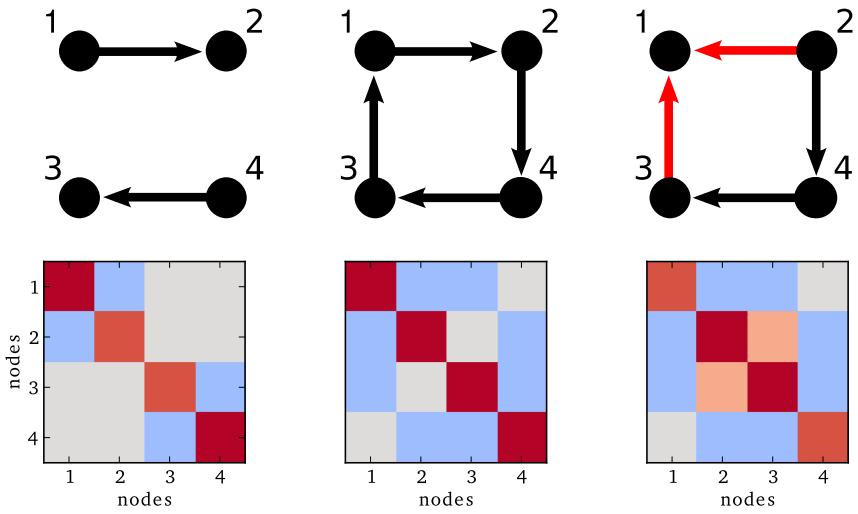


Figure 1: Small networks with 4 nodes each and different connectivity between them (top). They exhibit different activity dynamics, which is also reflected in the associated covariance matrix (bottom). In general, many different networks can lead to the same covariance matrix, and inferring connectivity from covariance is not possible; the inverse problem is ill-defined. However, assuming that the network is sparse (only a small fraction of links are actually present), the method of $L^1$-minimization (using gradient descent) helps to disambiguate the solution. The second order statistics of activity is particularly sensitive to collider structures (red arrows) in a network, and our method is able to exploit exactly these entries in the inverse covariance matrix ("precision matrix") to infer both the existence and the direction of connections [3] (image source: Schiefer et al, arXiv:1708.02423 [q-bio.NC], 2017).

The covariance matrix $C$ for $Y$ is then given by

$$\hat{C}(\omega) = \mathbb{E}[\hat{Y}(\omega)\hat{Y}^*(\omega)] = (\mathbb{1} - \hat{G}(\omega))^{-1}\hat{D}(\omega)(\mathbb{1} - \hat{G}^*(\omega))^{-1}, \tag{2}$$

where the matrix

$$\hat{D}(\omega) = \mathbb{E}[\hat{X}(\omega)\hat{X}^*(\omega)],$$

is diagonal, provided the components of external input are pairwise uncorrelated.

We can now reconstruct $\hat{G}(\omega)$ from equation (2)

$$\tilde{C}^{-1} = B^*B = B^*U^*UB \tag{3}$$

with $B = \sqrt{\hat{D}^{-1}}(\mathbb{1} - \hat{G})$ and a unitary matrix $U \in \mathrm{Mat}_n(\mathbb{C})$. We are looking for the sparsest matrix $G$ with this property. This means that starting with an initial matrix $B_0$, we have to minimize the (modified) $L^1$-Norm of

$$\|UB_0\|_1 = \sum_{i \neq j} |(UB_0)_{ij}|$$

with respect to $U$. For the optimization procedure, we use a gradient descent algorithm described in [3]. The number of times this optimization has to be executed depends on the required frequency resolution. Additionally, the estimation of the connectivity can be improved using bootstrapping. This introduces the additional cost that the number of boots necessary to achieve significant results is quite high.

The optimization via gradient descent is a procedure where no parallelization is possible. In total, with a frequency resolution of 256 DFT points and 10 000 boots, the optimization has to be performed $129 \times 10\,000 = 1\,290\,000$ times. This task is split up by calculating the bootstrap covariance matrices and then performing the optimization for each boot separately, for all frequency bands. This results in single core jobs where each job takes approximately 20 minutes.

## 3 Simulation

For validation of the estimation of effective connectivity, we use biophysically informed numerical simulations of very large networks. These simulations are supposed to generate the same data types as the ones we use for the network inference. For simulation ECoG data we set up a simulation scheme using NEST (Neural simulation tool [2]).

As shown in [1], downscaling the size of networks has limitations regarding effective connectivity and covariances. This means that reducing the number of neurons in a network can either keep the effective connectivity of the network or the covariance structure of the resulting activity unchanged, but not both at the same time. In our project we are studying the relation of these measures, so we have a strong interest in avoiding any downscaling as far as possible. This means the networks we simulate in terms of size should be as biologically realistic as possible.

Since the commonly used ECoG electrode grids have 64 macro-contacts each, we also simulated a network of 64 mesoscopic sub-networks, consisting of 1 000 LIF-neurons each. Each of the 64 sub-networks represents the neural population recorded by one ECoG electrode. Within each sub-network the neurons are randomly connected with a connection probability of 10%. These subnetworks are connected by excitatory neurons, which form additional long-range connections to neurons in other populations. The extracellular fields that are induced by synaptic activity in every individual neuron are then accumulated over each population and recorded. These 64 signals are then used for estimating the meso-scale connectivity among the 64 populations. In our approach, the relevant aspects for the estimation of effective connectivity are the first and second order signal statistics. Therefore, our simulation should be consistent with measured data regarding these properties. To achieve this, we developed a new model of ongoing activity projecting to the recorded populations from other parts of the brain.

For the simulation we use the parallelization methods provided by NEST including MPI and multi-threading. These make the simulation of 64 000 neurons plus external input and measuring devices feasible.

## 4 Conclusion

As described above the availability of high performance computing (here, the HPC cluster NEMO with high speed interconnect) is essential for our project In both data analysis and simulation, HPC is a key factor to achieve results in a biologically realistic setting. In data analysis, NEMO enables us to apply bootstrap methods which would not be feasible without HPC. In the case of numerical simulations we are able to treat bigger networks, which reduce the unwanted scaling effects that are detrimental to our method. Even with up-to-date high-end HPC facilities it is currently not possible to simulate networks of the same sizes as they occur in human brains, but the new possibilities offered by NEMO represent an important step in the right direction.

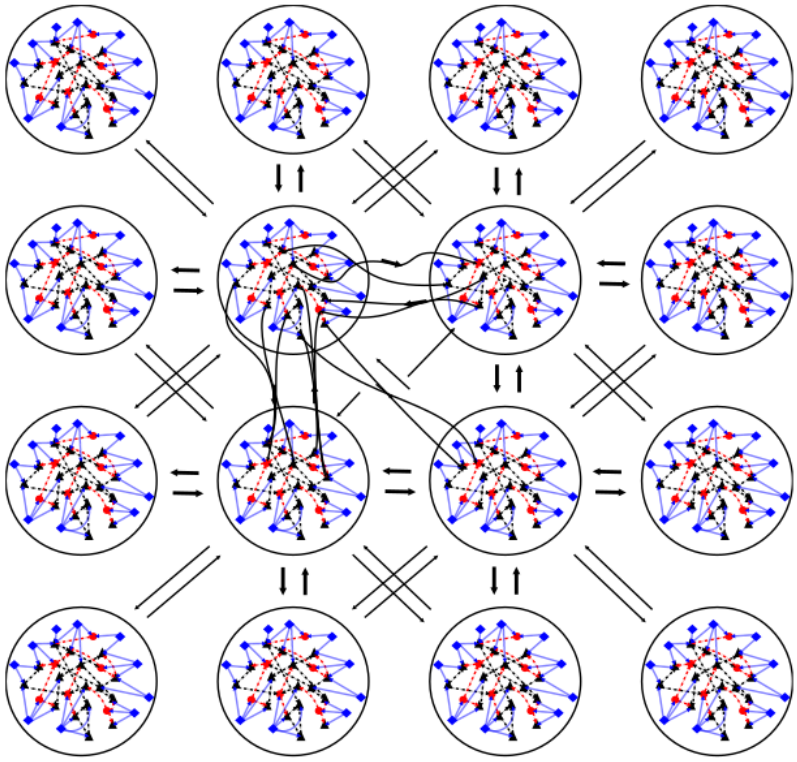

Figure 2: Scheme of the simulated network. Each circle represents the neural population underneath one ECoG electrode. Within each population neurons are randomly connected with 10% probability, but excitatory neurons form additional long-range connections to neurons in other populations according to a pre-defined connectivity scheme on a mesoscopic scale. The goal now is to reconstruct this mesoscopic long-range connectivity from the recorded accumulated extracellular fields (induced by synaptic activity) of all neurons in each population [5].

## Acknowledgements

Funded by the German Research Foundation (DFG, grant EXC 1086). Supported by the state of Baden-Württemberg through bwHPC and the German Research Foundation (DFG, grant INST 39/963-1 FUGG). We thank V. Pernice, A. Niederbühl and L.M. Schäfer for providing their software for data analysis and numerical simulations to us.

## References

[1] Sacha Jennifer Van Albada, Moritz Helias, and Markus Diesmann. Scalability of Asynchronous Networks Is Limited by One-to-One Mapping between Effective Connectivity and Correlations. *PLoS Computational Biology*, 2015.

[2] Hannah Bos, Abigail Morrison, Alexander Peyser, Jan Hahne, Moritz Helias, Susanne Kunkel, Tammo Ippen, Jochen Martin Eppler, Maximilian Schmidt, Alex Seeholzer, Mikael Djurfeldt, Sandra Diaz, Janne Morén, Rajalekshmi Deepu, Teo Stocco, Moritz Deger, Frank Michler, and Hans Ekkehard Plesser. Nest 2.10.0, December 2015.

[3] Alexander Niederbühl. Inferring network structure from covarying neural activity. Diploma Thesis in Biology, 2014.

[4] Volker Pernice and Stefan Rotter. Reconstruction of sparse connectivity in neural networks from spike train covariances. *Journal of Statistical Mechanics: Theory and Experiment*, 2013(03):P03008, 2013.

[5] Lisa Schäfer. Modelling neuronal population signals in networks of spiking networks. Master Thesis in Biology, 2015.

# The Virtue of High Performance Computing for the Statistical Analysis of Social Networks

Lars Leszczensky and Sebastian Pink

Mannheim Centre for European Social Research, University of Mannheim

We illustrate the potential of the bwHPC for sociological research. After briefly explaining why modern sociological research requires more computational time, we outline a recently developed computationally intense statistical model for the analysis of relational data. We close by summarizing an empirical study in which we applied this model to answer a substantive question and greatly benefited from the bwHPC with regard to computation time.

## 1 Introduction

Most sociological statistical analyses are conveniently estimable on single-core office computers. Examples for typical analyses are linear or logistic regression models that are estimated based on a survey of not more than 5,000 individuals, which take only a few minutes to run. However, a growing number of sociologists uses simulation techniques to answer substantive questions and this tremendously increases the computational resources needed. The reason is that simulation incorporates randomness and, consequentially, one run of a model is not sufficient. Instead, multiple runs of the same model specification are carried out and averaged afterwards to condense information. For such computationally intense simulations the distributed bwHPC cluster resources are of great use as they save lots of computation time.

Within a project funded by the German Research Foundation, we are interested in friendship formation among around 2,000 adolescents, which we observed in schools in North Rhine-Westphalia. We surveyed multiple grade-level networks in which we collected data on friendship nominations of all students within an entire grade (i.e., students of different classrooms within the same academic year could nominate one another). Furthermore, we repeated these surveys several times after roughly nine months each, so that we are able to follow the evolution of these friendship networks over time [4].

An appropriate statistical model to analyze such network panel data is the so-called stochastic actor-oriented model for the co-evolution of networks and behavior (SAOM) [7]. In essence, this model traces the evolution of the friendship nominations over time by simulating individual friendship-making decisions of the students of one network according to theoretically important elements of this decision (e.g., friends having the same sex as oneself or friends of friends becoming friends).

On a conventional office computer these models take about four hours to run. However, the number of estimated models equals the number of the individual networks that were surveyed, in our case typically 13. This makes this kind of statistical analysis suitable for parallel computation. We distribute the estimation of each SAOM to one core of one bwHPC node. This means a thirteenfold increase, or in other words, we are able to retrieve the results after four hours instead of 52 hours. Importantly, for an scientific article many model specifications have to be tested so that this computational advantage is even further multiplied by the amount of these different specifications. After the individual results of the SAOM are retrieved, they are averaged over by means of meta-analysis [1, 2].

## 2 Stochastic Actor-Oriented Models for the Co-Evolution of Networks and Behavior

SAOM can be regarded as empirically calibrated agent-based simulation models [8]. The process of network evolution leading from an initial state of an empirically observed network to subsequent network states observed at later points in time is modeled as the outcome of a stochastic process that is based on a sequence of actors' decisions. Each actor repeatedly decides myopically whether to change (i.e., create or dissolve) one of his outgoing ties or to retain the status quo. The choice of one particular network state $x$ for one actor $i$ is determined by his so-called evaluation function,

$$f_i(\beta, x) = \sum_k \beta_k s_{ki}(x). \tag{1}$$

The evaluation function is a linear combination of $k$ effects $s_{ki}(x)$ (e.g., structural, actor, and dyadic effects) and their respective statistical parameters $\beta_k$ [7, p. 47]. The set of statistical parameters $\beta$ is estimated by means of simulation. Based on raw estimates, parameters are subsequently iteratively adjusted [6]. After a set of statistical parameters has been identified and fixed, their covariance is estimated by simulating a rather large number of networks [5]. As a result, a SAOM for a single network yields a vector of parameter estimates $\beta$ as well as a $k \times k$ covariance matrix. Afterwards, in a meta-analysis [1] the input data are a $n \times k$ matrix $\hat{\theta}$ of $k$ parameter estimates for $n$ networks as well as a set $S$ of $n$ $k \times k$ matrices representing the within-study covariance matrices of the parameter estimates.

## 3 Exemplary Research

We outline the application of such SAOM to answer a substantive research question. The statistical models were run on the bwHPC, more precisely on 13 processors of one node. This research effort, which was published the journal Social Networks [3], sheds light on differences in ethnic segregation with regard to the structural embeddedness of students in classrooms and the respective grades.

It is well-established that adolescents' school-based friendship networks tend to be segregated along ethnic lines. But few studies have examined whether variation in network boundaries affects the degree of ethnic friendship segregation. We argue that ethnic homophily (i.e., those with the same ethnicity, e.g., Turkish, Polish, or German, befriend each other) is more pronounced in grade-level than in classroom-level networks. We consider classrooms to be low-cost situations for students to initiate and maintain friendship ties, because access to and daily interaction with classmates are very easy. Students not only attend daily lessons together but are also

exposed to the same obligations, have to tackle the same tasks (e.g., do the same homework), and share experiences related to class trips or other joint activities. Grade-level networks, by contrast, constitute a high-cost situation for the formation of friendships within school. Students in the same grade, who do not share a classroom, have fewer opportunities to meet, and share fewer common experiences than those who are bound together by a joint classroom. Within school they can meet during breaks, but while classmates can be contacted quite easily before and after lessons, contact with schoolmates in other classrooms requires more of an active effort (e.g., walking to other classrooms, waiting for students, or encountering other students who one barely knows). As a consequence, a student may only invest in a relatively costly cross-classroom friendship if he or she perceives this friendship to be particularly beneficial. Ethnic homophily may thus result in a higher percentage of same-ethnic friendships at the grade level than at the classroom level.

We empirically tested this hypothesis using two repeated observations of 13 grade-level networks. In line with our theoretical argument, the tendency to form same-ethnic friendships was indeed stronger at the grade level, which translated into stronger ethnic segregation in friendship networks at the grade level than at the classroom level. Technically, four preferences are of interest: creating same-classroom-same-ethnicity ties, same-classroom-different-ethnicity ties, different-classroom-same-ethnicity ties, and different-classroom-different-ethnicity ties. We identified the joint contribution of the respective effects by inserting their estimated mean parameters into the evaluation function. The resulting contributions to the evaluation function are 0.07 for same-classroom-same-ethnicity ties, 0.0 for same-classroom-different-ethnicity ties, -0.46 for different-classroom-same-ethnicity ties, and -0.82 for different-classroom-different-ethnicity ties. Accordingly, the difference in preferences for same-ethnic friendships compared to interethnic friendships at the grade level was, at 0.36 (-0.46-(-0.82)), more pronounced than the respective preferential difference at the classroom level at 0.07 (0.07-0.0). This means that having the same ethnic background was more important for friendship selection if two students were not in the same classroom. This finding confirmed our hypothesis of a higher ethnic segregation of grade-level friendships.

## Acknowledgements

This research was supported by a grant from the German Research Foundation (DFG/KA 1602/6-1; 6-2).

## References

[1] An, W. “Multilevel meta network analysis with application to studying network dynamics of network interventions.” Social Networks (2015): 48-56.

[2] Gasparrini, A., Armstrong, B., and M. G. Kenward. “Multivariate Meta-Analysis for Non-Linear and other Multi-Parameter Associations.” Statistics in Medicine, 31, (2012): 3821-3839.

[3] Leszczensky, L. and S. Pink. “Ethnic Segregation of Friendship Networks in School: Testing a Rational-Choice Argument of Differences in Ethnic Homophily Between Classroom- and Grade-Level Networks.” Social Networks, 42, (2015): 18–26.

[4] Leszczensky, L., Pink, S. and F. Kalter. “Friendship and Identity in School: Field Report on

Wave 1, Wave 2, and Wave 3 (Technical Report)." Working Paper 161. Mannheim, Germany: Mannheimer Zentrum für Europäische Sozialforschung. (2015).

[5] Ripley, R. M., Snijders, T. A. B., Boda, Z., Vörös, A., and P. Preciado, P. "Manual for RSIENA (Version September 21, 2015)." University of Oxford, Nuffield College, Oxford, UK. (2015).

[6] Snijders, T. A. B. "The Statistical Evaluation of Social Network Dynamics." Sociological Methodology, 31, (2001): 361-395.

[7] Snijders, T. A. B., van de Bunt, G. G., and C. E. G. Steglich. "Introduction to Stochastic Actor-Based Models for Network Dynamics." Social Networks, 32, (2010): 44-60.

[8] Snijders, T. A., and C. E. G. Steglich. "Representing Micro–Macro Linkages by Actor-Based Dynamic Network Models." Sociological Methods & Research, 44, (2015): 222-271.

# Distributed optimisation of decentralised energy systems under uncertainty on HPC systems

Hannes Schwarz

Institute for Industrial Production (IIP), Chair of Energy Economics,
Karlsruhe Institute of Technology (KIT), Germany

Nowadays, there is a decentralisation of the German energy sector driven by fluctuating renewable energy sources (RES) that are subject to non-negligible uncertainties. Stochastic modelling techniques enable an adequate consideration of manifold uncertainties in the investment and operation process of decentralised energy systems. However, their mathematical formulations lead to large-scale programs that are not feasible on one computer. The program is therefore decoupled and distributively optimised on high-performance computing (HPC) systems. Thus, robust-sufficient setup decisions for decentralised energy systems can be provided that are expected to be optimal.

## 1 Introduction

In the German energy sector, we are nowadays faced with the trend from a centralised to a decentralised energy supply (see e.g. [1, 2, 3, 4]). The decentralisation is mainly driven by fluctuating renewable energy sources (RES) which requires a high temporal resolution when real energy systems are considered. Moreover, RES are subject to weather-related uncertainties that cannot be neglected in the modelling process to achieve optimal decisions. Stochastic modelling techniques enable the optimisation of decentralised energy systems with an adequate consideration of these uncertainties (see e.g. [5, 6, 7, 8] for details), but typically lead to large-scale programs that are not feasible on one computer. The program is therefore decoupled into many smaller sub-programs that are distributively optimised on high-performance computing (HPC) systems.

This paper is structured as follows. The problem and its mathematical formulation are described in Section 2. The distributed optimisation process on HPC systems is presented in Section 3 and computational results are shown in Section 4. Finally, Section 5 gives a conclusion of the work and indicates needs for further research.

## 2 Problem description

The economic profitability of decentralised energy systems mainly depends on the investments at the first stage and their operation at the second stage. While the investments at the first stage can be considered as here-and-now decisions without uncertainty, the operation at the second stage is subject to uncertain conditions: such as energy supply and demand or electricity prices, which can occur in scenarios with different probabilities. Stochastic programming considers uncertainties by optimising the investment and operation decisions not for one specific, but for all possible scenarios with respect to their stochastic nature.

In [9], stochastic programming is used to optimise heat storages of a residential quarter in combination with a photovoltaic (PV) system and heat pumps. The quarter is modelled as a so-called two-stage stochastic mixed-integer linear program (S-MILP).[1] The objective function of the program is:

$$\min_{c_{g,i},e^{grid}_{n,t},e^{fi}_{n,t}} ANF \sum_{g}\sum_{i} cost_i \cdot c_{g,i} + \sum_{n}\pi_n \sum_{t} p^{grid} \cdot e^{grid}_{n,t} - p^{fi} \cdot e^{fi}_{n,t}, \tag{1}$$

where the capital cost of investment $i$ of building group $g$ is converted into equivalent series of uniform amounts per period at the first stage. Thereby, the annuity factor $ANF$ takes into account the lifetime of the investment and an alternative investment at a certain interest rate of the fixed capital. At the second stage, the sum of energy obtained from the external grid $e^{grid}_{n,t}$ at price $p^{grid}$ minus the energy fed into the grid $e^{fi}_{n,t}$ at tariff $p^{fi}$ over all time steps $t = \{1, ..., T\}$ results in energy cost of each scenario $n = \{1, ..., N\}$ that occurs with probability $\pi_n$.

In the case study, storage units for space heating and for domestic hot water are optimised assuming a technical lifetime of 20 years related to an interest rate of 10%. The period $t = \{1, ..., 35040\}$ includes one year with a temporal resolution of 15 minutes. Essential constraints are that the electrical supply and demand as well as the thermal supply and demand are balanced at any time. Furthermore, the storage possibility and the heat supply are limited. Uncertain parameters are the supply of the PV system and heat pumps as well as the electrical and thermal demand of the households. These uncertainties are represented by different scenarios generated on the basis of a Markov process which have proven suitable to this kind of problem. The whole program and further information are presented in [9].

## 3 Distributed optimisation process on HPC systems

In order to keep the program feasible, it is decoupled and distributively optimised on HPC systems. In principle, every stochastic program can be decoupled by losing intra- and inter-scenario connections. In the case study, a scenario is internally connected by the storage capacities and the storage levels over the time steps. The storage capacities connect the scenarios among each other. The intra- and inter-scenario-connected variables are fixed and optimised by an outer derivative-free optimisation (DFO): a steepest-ascent hill-climbing approach [11].[2] As a consequence, the program can be decoupled in $M$x$N$ sub-programs which are optimised by *CPLEX*, a commercial MILP solver, on C computing nodes. As soon as all sub-programs are optimised, they are coupled to compute the minimal cost of the fixed variables which is needed for the DFO. Fig. 1 shows the distributed optimisation process of the stochastic program.

[1] Further information about two-stage stochastic programming can be found, for instance, in [10].

[2] Note that the used hill-climbing approach is a local search approach that can only guarantee local optimality. It can be replaced by any other DFO algorithm, even by a global search approach, if enough computing resources are available.

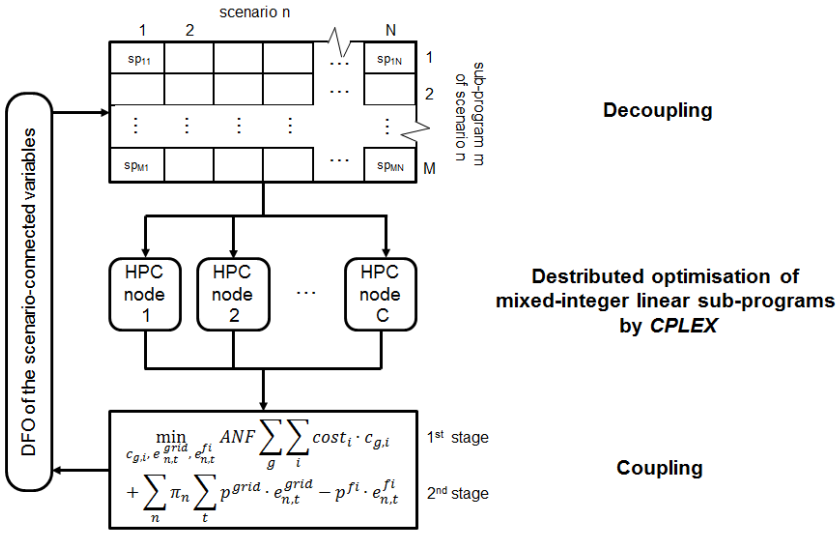


Figure 1: Distributed optimisation process of the stochastic program.

The decoupling in combination with the DFO and the distribution of the sub-programs to HPC clusters are implemented by a visual basic application (VBA) on a Windows master machine. In this setup, the Windows master machine communicates to Windows- or Linux-based machines by the tool *PuTTY* or *PsExec*, respectively. Thus, computing nodes of different HPC systems can be used. For the optimisation of the residential quarter, computing nodes of the *bwUniCluster* and the *bwForCluster* (Linux-based) as well as some computing nodes of the Institute of Industrial Production (IIP) (Windows-based) were in use: Nodes with 4-16 GB RAM and 1-16 cores are required for 15-30 minutes to ensure a solution of the sub-programs with a sufficient quality that is needed for the DFO.

## 4 Computational results

For the case study, $M = 100$ scenarios are generated and decoupled. Additionally, the one-year period of each scenario is decoupled into $N = 27$ periods of two weeks leading to $M$x$N = 2700$ sub-programs per scenario-connected variable for the outer DFO. About 20 steps of the outer optimisation are needed to find the optimal storage sizes.

The optimisation of one complete scenario for one building group is still feasible within 2 days on one computing node (see Table 1). However, the optimisation of one scenario for the entire residential quarter is not feasible. Therefore, a decoupling of the stochastic program is required. If this decoupled program of one scenario for one building group was sequentially optimised on one computing node, the computing wallclock time would amount to 6 days. Due to the distributed optimisation on HPC systems, the same problem is solved within 5 hours assuming exclusive access to 512 computing nodes for this time period. The full program, i.e. 100 scenarios for the quarter (=4 building groups), takes approximately 7 days.

The computing wallclock time of 7 days of the full program can be further reduced by up to 75% using scenario reduction techniques and automated algorithm configuration of the used

| | Constraints | Decision variables (thereof integer) | Computing wallclock time | | |
|---|---|---|---|---|---|
| | | | 1 node* using *CPLEX* | 1 node** using *CPLEX* + decoupled | 512 nodes** using *CPLEX* + decoupled |
| 1 building group | 946 080 | 490 572 (70 086) | up to 2 days | ~6days | ~5h |
| Quarter (4 building groups) | 3 048 480 | 1 962 285 (280 344) | ∅ | ~90days | ~1day |
| 100 scenarios of 1 building group | 9,E+07 | 5,E+07 (7,E+06) | ∅ | ~1,6years | ~28h |
| 100 scenarios of the quarter | 3,E+08 | 2,E+08 (3,E+07) | ∅ | ~25years | ~7days |

*with up to 1 TB RAM, 32 Cores@2.4-2.6Ghz, max. 72h, rel. Gap=2%

**with up to 16 GB RAM, 16 Cores@2.4-2.6Ghz, max. 0.5h, rel. Gap=0.5%

Table 1: Computing wallclock time of different program variants sequentially or distributively optimised on 1 computing node or 512 computing nodes of a HPC system.

*CPLEX* solver (see [12]). Practically, however, due to time restrictions per job of the HPC queuing systems, the computation still takes almost a week.

A comprehensive analysis of the results with regard to energy economic aspects of the residential quarter is done in [9]. The main findings are:

- Thermal storage units generally prove beneficial.
- Storage units for domestic hot water are more profitable than for space heating due to the more constantly provided demand side flexibility throughout a year.
- The optimal storage capacity for space heating is generally larger when uncertainties are considered in comparison to the deterministic optimisation.

## 5 Conclusions

The centralised German energy structure is changing towards decentralised energy systems that are subjected to manifold uncertainties. Stochastic modelling techniques help to avoid bad investment decisions, but lead to very large-scale programs that require a decoupling to keep it computationally feasible. However, the optimisation of the full program would take about 25 years computing wallclock time on one computing node. The distributed optimisation on HPC systems with, e.g., 512 nodes achieves a solution within 7 days or, if scenario reduction techniques and automated algorithm configuration are employed, within two days.

Nevertheless, the optimisation of decentralised energy systems is still challenging considering the fact that such computer resources are hardly available for those time periods of one day and more. In practice, the computation takes much more time due to resource restrictions of HPC systems. Consequently, model changes and more complex energy system models are still time and cost-intensive. Therefore, the computational effort needs to be reduced by improving the computational interaction between the size and complexity of the employed programs and the used HPC resources. One way would be to optimise the amount of memory required for the inner optimisation of the sub-programs. Reduced memory requirements would allow more runs on a single node or cheaper nodes with less RAM. Another way would be a heuristic solution

approach for the sub-programs (e.g. machine learning methods) instead of the resource-intensive optimisation by *CPLEX*. Besides, the outer hill-climbing approach could be replaced by a DFO algorithm that needs fewer steps to find optimal solutions. If enough computing resources are available, it could also be extended by a DFO guaranteeing global optimality.

## Acknowledgements

The authors acknowledge support by the state of Baden-Württemberg through bwHPC and the Germany Research Foundation (DFG) through grant no INST 35/1134-1 FUGG.

## References

[1] Altmann, M., A. Brenninkmeijer, J.-C. Lanoix, D. Ellison, A. Crisan, A. Hugyecz, G. Koreneff und S. Hänninen. 2010. Decentralized energy systems. Tech. rep. European Parliament's Committee (ITRE). Accessed: 29. September 2016. http://www.europarl.europa.eu/document/activities/cont/201106/20110629ATT22897/20110629ATT22897EN.pdf.

[2] Owens, B. 2014. The rise of distributed power. General Electric (ecomagination). Accessed: 30. September 2016. https://www.ge.com/sites/default/files/2014%2002%20Rise%20of%20Distributed%20Power.pdf.

[3] Yazdanie, M., M. Densing und A. Wokaun. 2016. "The role of decentralized generation and storage technologies in future energy systems planning for a rural agglomeration in Switzerland." Energy Policy 96:432–45.

[4] Kobayakawa, T. und T. C. Kandpal. 2016. "Optimal resource integration in a decentralized renewable energy system: Assessment of the existing system and simulation for its expansion." Energy for Sustainable Development 34:20–29.

[5] Dantzig, G. B. 1955. "Linear programming under uncertainty." Management Science 1: 197–206.

[6] Wallace, S. W. und S.-E. Fleten. 2003. "Stochastic programming models in energy." In Stochastic Programming. Bd. 10, 637–77. Handbooks in Operations Research and Management Science: Elsevier.

[7] Shapiro, A., D. Dentcheva und A. P. Ruszczynski. 2009. Lectures on stochastic programming: modeling and theory. MPS-SIAM series on optimization 9. Philadelphia Pa. SIAM.

[8] King, Alan J. und Stein W. Wallace. 2012. Modeling with Stochastic Programming. Springer series in operations research and financial engineering. New York: Springer. http://dx.doi.org/10.1007/978-0-387-87817-1.

[9] Schwarz, H., V. Bertsch und W. Fichtner. 2015. "Two-stage stochastic, large-scale optimization of a decentralized energy system – a residential quarter as case study." Working Paper Series in Production and Energy 10. Karlsruhe: KIT. https://publikationen.bibliothek.kit.edu/1000049862.

[10] Ahmed, S. 2010. "Two-stage stochastic integer programming: a brief introduction." In Wiley Encyclopedia of Operations Research and Management Science, hg. v. James J. Cochran, Louis A. Cox, Pinar Keskinocak, Jeffrey P. Kharoufeh und J. C. Smith. Hoboken, NJ, USA: John Wiley & Sons, Inc.

[11] Taborda, D.M.G. und L. Zdravkovic. 2012. "Application of a hill-climbing technique to the formulation of a new cyclic nonlinear elastic constitutive model." Computers and Geotechnics 43:80–91.

[12] Schwarz, H., L. Kothoff, H. H. Hoos, V. Bertsch und W. Fichtner. "Using automated algorithm configuration to improve the optimization of decentralized energy systems modeled as large-scale, two-stage stochastic programs." Working Paper Series in Production and Energy 24. Karlsruhe: KIT. https://publikationen.bibliothek.kit.edu/1000072492.

# Quantum Chemical Simulations for Astrochemistry

Jan Meisner

Institute for Theoretical Chemistry, University of Stuttgart

The tunnel effect is a quantum mechanical phenomenon which allows quantum objects to pass potential energy barriers bigger than the total energy of the object. Following Newton's classical equations of motion the object is forbidden to pass the barrier but following the wave nature of quantum mechanics, the particle can tunnel through this barrier. The tunneling of atoms in molecules leads to surprising observations. In symmetric reactions, tunneling causes a splitting of the vibrational energy levels. In asymmetric reactions, the tunnel effect can increase the reaction rates and also enable chemical reactions which would not be observed classically. This is especially true when the temperature is very low as it is the case in the interstellar medium. Therefore, in astrochemistry in particular this quantum effect can play a significant role.

## 1 Atom Tunneling

On the microscopic scale of quantum physics, objects can be described either as particles or as waves. This is called wave-particle dualism and is one of the fundamental quantum mechanical principles. The wave nature of an object is mathematically described by a wave function $\Psi$ which follows the Schrödinger equation

$$i\hbar\frac{\partial}{\partial t}\Psi = \hat{H}\,\Psi \tag{1}$$

Here, $\hbar$ is the so-called reduced Planck's constant and $\hat{H}$ is the Hamilton operator corresponding to the total energy – the sum of kinetic energy $T$ and potential energy $V$ – of a system:

$$\hat{H}\,\Psi = \left(\hat{T} + \hat{V}\right)\Psi = E\,\Psi \tag{2}$$

The wave function $\Psi$ describes the physical quantum state of a system and the square of the absolute value can be interpreted as the probability density $\rho(x,t)$ to find the quantum object at the position $x$ at the time $t$.

$$\rho(x,t) = |\Psi(x,t)|^2 \tag{3}$$

In classical physics, the total energy of a particle needs to be at least as high as the potential energy to overcome the barrier. In quantum mechanics, the wave function – and thus the

probability of finding a particle – on the other side of a barrier is not zero when the potential energy is bigger than the kinetic energy of the quantum object. For a rectangular barrier, as shown in figure 1, the wave function can be easily analyzed. In the classically forbidden region, the amplitude of the wave function decays exponentially. The analytical solution shows that exponential decay of the wave amplitude depends on the mass of the particle $m$, on the energy barrier $E_A$, and on the width of the barrier $x$.

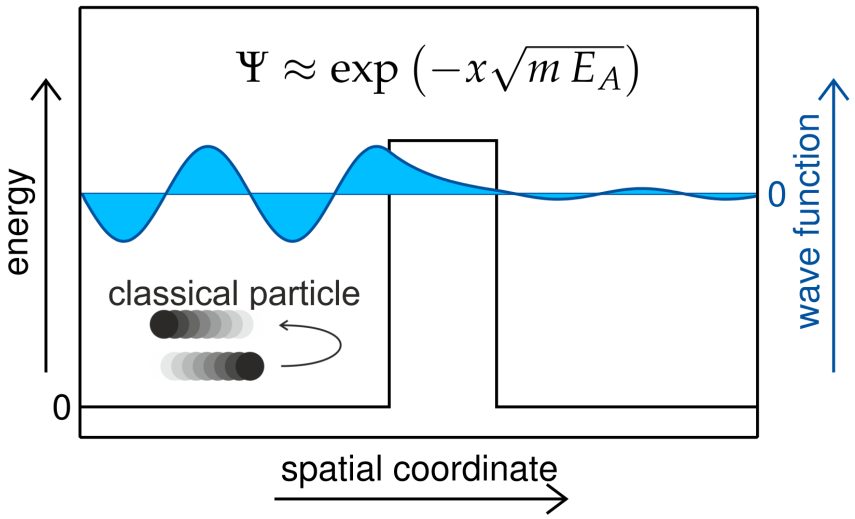


Figure 1: Wave function during the tunneling through a rectangular barrier. The equation above the barrier shows the analytical behaviour of the wave function within a rectangular barrier. The picture is taken and modified from reference [1].

Atoms and molecules are small enough to be labelled as quantum objects and activation barriers of chemical reactions can be tunnelled though if

- the atoms mainly involved in the motion are light, i.e. first or second period elements like hydrogen,
- the distances the atoms have to cover during the reaction is small, and
- the energy barrier is not extremely high.

At room temperature atom tunneling is nearly restricted to hydrogen atoms. Because of the mass dependence of the tunnel effect, deuterium (heavy hydrogen) atoms are less likely to undergo tunneling through the barrier. This leads to high kinetic isotope effects (KIEs) which are defined as the ratio of the reaction rate constant of the light system $k_H$ and the reaction rate constant of the heavy system $k_D$:

$$KIE = \frac{k_H}{k_D} \tag{4}$$

The KIE is a suitable probe to examine the atom tunneling experimentally because it can be directly measured.

At lower temperatures atom tunneling enables chemical reactions, which would otherwise be impossible, and heavier atoms such as carbon or oxygen contribute to the tunneling motion. As the field of atom tunneling in chemical reactions is of increasing scientific interest and can not be covered in full detail, here we want to refer to a review which shows the progresses of the last years [1].

## 2 Astrochemistry

There are more than 170 different molecules observed in the interstellar medium. Astrochemistry describes the distribution, formation, destruction, and all other interactions of chemical species. The most important differences to the familiar reaction conditions in a lab are a low particle density, a particularly high photon density, and low temperatures. Hydrogen atoms and molecular hydrogen are comparably abundant species, thus, tunneling is a suitable mechanism for most reactions involving potential energy barriers.

Apart from the small gaseous molecules, there are also dust particles coated with water ice. These can work as catalysts *e.g.* in the hydrogen addition reaction to CO, which is a key step in the formation of formaldehyde and methanol in space [2, 3]. In general, there are different possible reaction mechanisms on a surface. Two of them, the Eley-Rideal mechanism and the Langmuir-Hinshelwood mechanism are discussed here, see Figure 2. In the former case, one atom or molecule is adsorbed on the surface and another one approaches from the gas phase and they directly form a transition state which then reacts to the products. In the Langmuir-Hinshelwood mechanism, both reactants are adsorbed prior to the reaction. After that, both of them can diffuse on the surface which proceeds either thermally or through atom tunneling. When both particles meet, they can form a transition state and react to the products.

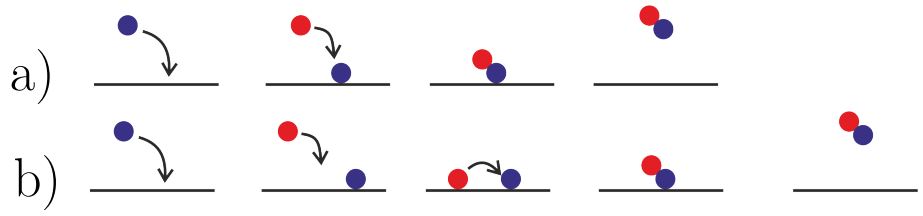


Figure 2: a) Eley-Rideal reaction mechanism. One particle is first adsorbed on a surface and a second one meets it directly forming the products. b) Langmuir-Hinshelwood mechanism. Both particles are adsorbed separately. Diffusion allows reaction to the products.

## 3 Results

Different chemical reactions which possess potential energy barriers were investigated [4, 5, 6, 7, 8]. A few of them are shown in Table 1. All of them are neutral-radical reactions with a potential energy barrier of a small to medium height. The potential is obtained by means of density functional theory (DFT) or, if possible, highly correlated wave function methods.

### 3.1 $H_2$ + OH

One prototype reaction for four-atomic systems is the reaction

$$H_2 + OH \rightarrow H_2O + H. \tag{5}$$

This reaction is assumed to be one of the main routes of $H_2O$ formation in the interstellar medium and is therefore of high interest. The potential energy barrier and the imaginary frequency at the transition structure are calculated at CCSD(T)-F12 level to be 22.5 kJ/mol and 1199i $cm^{-1}$. For the low temperatures occurring in the interstellar medium this barrier would be too high to overcome. Nevertheless, the barrier is particularly thin as can be seen by the high imaginary

| Reaction | | | Lit. |
|---|---|---|---|
| $H_2 + OH$ | $\rightarrow$ | $H_2O + H$ | [4] |
| $H_2 + NH_3^+$ | $\rightarrow$ | $NH_4^+ + H$ | [5] |
| $H_2O_2 + H$ | $\rightarrow$ | $H_2 + HO_2$ | [6] |
| $H_2O_2 + H$ | $\rightarrow$ | $H_2O + OH$ | [6] |
| $HNCO + H$ | $\rightarrow$ | $H_2NCO$ | [7] |
| $CH_4 + OH$ | $\rightarrow$ | $CH_3 + H_2O$ | [8] |
| $H_2CO + H$ | $\rightarrow$ | $H_2 + HCO$ | |
| $H_2CO + H$ | $\rightarrow$ | $H_3CO$ | |
| $H_2CO + H$ | $\rightarrow$ | $H_2COH$ | |
| $H_2 + O$ | $\rightarrow$ | $H + OH$ | |

Table 1: Reactions studied in our group.

frequency and therefore, the tunneling effect is assumed to be distinct. We calculated reaction rate constants in the gas phase using the semiclassical instanton theory [4]. The reaction rates of all possible isotopologues were also calculated, see Figure 3. The strong impact of atom tunneling leads to high KIEs of 100-500 for the deuteration of the transferred hydrogen atom. The other two hydrogen atoms do not contribute significantly to the tunneling motion as is shown by the comparably low KIE of 1-10 for deuteration of these atoms.

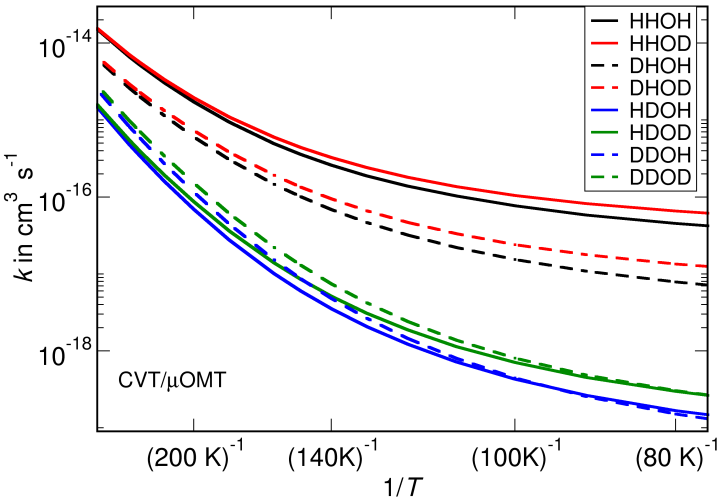


Figure 3: Temperature dependence of the reaction rate constants of all possible isotopologues (so called Arrhenius plots). Here, *e.g.* DHOD denotes the reaction of DH and OD to a D atom and HOD, as it is shown by the order of the letters. The picture is taken from reference [4] with kind permission of the American Institute of Physics (AIP).

We also simulated the reaction on a water ice surface as shown in figure 4 by means of a QM/MM framework. In this case, the four atoms directly involved in the reaction and 19 water molecules of the crystalline surface were included in the QM part and the MM part simulates an ice surface of 50 x 50 Å.

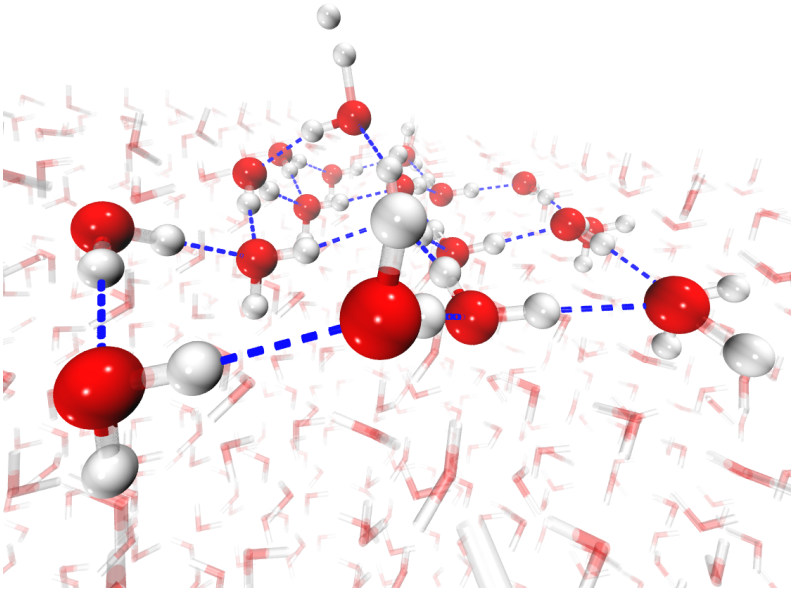

Figure 4: Transition state structure of the reaction of $H_2$ + OH on a crystalline ice surface. The water ice molecules in the QM part are shown as transparent ball and stick model while the MM molecules are shown as thin lines.

## 4 Conclusion

The study of the tunnel effect of atoms is an evolving field in experimental and theoretical chemistry. In particular at cryogenic temperatures atom tunneling leads to surprising results and can change stability and chemical reactivity qualitatively. Due to the large mass-dependence, high KIEs arise what makes atom tunneling detectable experimentally. Atom tunneling is found to occur in organic chemistry, biochemistry, as well as inorganic chemistry and it determines the reactivity at the cryogenic temperatures prevalent in e.g. the interstellar medium. Therefore, it is necessary to include atom tunneling in considerations and calculations of astrochemical reactions where potential energy barriers can only be passed if tunneling plays a dominant role.

In the case of the reaction of molecular hydrogen with OH radicals, the Arrhenius plot is curved because of the atoms – mainly the transferred hydrogen – tunneling through the potential energy barrier. This increases the reaction rate at the prevalent temperatures significantly and affirms that this reaction is a possible step in the formation of water in the interstellar medium.

## Acknowledgements

This research was supported in part by the bwHPC initiative and the bwHPC-C5 project provided through associated compute services of the JUSTUS HPC facility at the University of Ulm. The author would like to thank the German Research Foundation (DFG) for financial support of the project within the Cluster of Excellence in Simulation Technology (EXC 310/2) at the University of Stuttgart.

## References

[1] Jan Meisner and Johannes Kästner. "Atom Tunneling in Chemistry" , *Angew. Chem. Int. Ed.* **55**, 5400 – 5413 (2016) "Der Tunneleffekt von Atomen in der Chemie" , *Angew. Chem.* **128**, 5488 – 5502 (2016)

[2] K. Hiraoka, T. Sato, S. Sato, N. Sogoshi, T. Yokoyama, H. Takashima, S. Kitagawa. "Formation of Formaldehyde by the Tunneling Reaction of H with Solid CO at 10 K Revisited", *Astrophys. J.*, **577**, 265. (2002)

[3] H. Hidaka, M. Watanabe, A. Kouchi, N. Watanabe. "Reaction Routes in the CO-$H_2CO$-$d_n$-$CH_3OH$-$d_m$ System clarified from H(D) Exposure of Solid Formaldehyd at low Temperatures", *Astrophys J.,* **702**, 291 (2009)

[4] Jan Meisner and Johannes Kästner. "Reaction rates and kinetic isotope effects of $H_2 + OH \rightarrow H_2O + H$" *J. Chem. Phys.* **144**, 174303 (2016) ArXiv: http://arxiv.org/abs/1605.08776

[5] Sonia Álvarez-Barcia, Marie-Sophie Russ, Jan Meisner and Johannes Kästner "Atom tunnelling in the reaction $NH_3^+ + H_2 \rightarrow NH_4^+ + H$ and its astrochemical relevance", accepted at *Faraday Discuss.*, DOI: 10.1039/C6FD00096G

[6] Thanja Lamberts, Pradipta K. Samanta, Andreas Köhn, and Johannes Kästner. "Quantum tunneling during interstellar surface-catalyzed formation of water: the reaction $H + H_2O_2 \rightarrow H_2O + OH$" *Phys. Chem. Chem. Phys.* **18**, 33021-33030 (2016)

[7] Lei Song and Johannes Kästner. "Formation of the prebiotic molecule $NH_2CHO$ on astronomical amorphous solid water surfaces: accurate tunneling rate calculations" *Phys. Chem. Chem. Phys.,* **18**, 29278–29285 (2016) Arxiv: https://arxiv.org/abs/1610.01007

[8] Thanja Lamberts, Gleb Fedoseev, Johannes Kästner, Sergio Ioppolo, Harold Linnartz. "Importance of tunneling in H-abstraction reactions by OH radicals. The case of $CH_4$ + OH studied through isotope-substituted analogues", accepted at *Astronomy & Astrophysics*, DOI: 10.1051/0004-6361/201629845

# From experimentel chemistry to in-silico chemistry

## Selected topics of computational NMR spectroscopy of carbocations

Hans-Ullrich Siehl

Institute of Organic Chemistry I, Ulm University

Carbocations are important reactive intermediates in Organic Chemistry. Many chemical reactions in polar media as well as biochemical transformations proceed via positively charged ionic intermediates, i.e. carbocations. These are only local (not global) minima on the energy surface with very short lifetimes (may be a millionth of a second or less).

We elucidate structure and electronic stabilization modes of new and unusual carbocations which some have been discussed controversially for many years. Using matrix co-condensation techniques we prepare long-lived carbocations with the aid of superacids at low temperatures in solution. These are characterized experimentally using high field $^{1}$H, $^{13}$C and $^{29}$Si NMR spectroscopy. The experiments are accompanied by high level ab initio molecular orbital calculation of the molecular geometry and charge distribution as well as magnetic properties such as NMR chemical shifts and spin-spin coupling constants.

We describe here the experimental and computational characterization of the first $\beta$-silyl-stabilized simple alkyl cation and the first characterization of a static $\gamma$-silyl-substituted bicyclobutonium ion.

## 1 The $\beta$-silyl effect in tert.-butyl cation

The low temperature $^{13}$C NMR spectrum of the $\beta$-triisopropylsilyl substituted t-butyl cation prepared from the corresponding silyl substituted Alkene precursor under very carefully controlled experimental conditions is shown in Fig. 1.

Quantum chemical calculations with wave function methods including electron correlation were performed for $\beta$-silyl substituted tert.-butyl cations with various silyl groups. The calculations reveal the geometrical distortions accompanying $\beta$-silyl hyperconjugative stabilization (Fig. 2). Visualization of NBO calculations show the formation of a 2-electron 3-center bond thus confirm the stabilization by the $\beta$-silyl group (Fig. 3). MP2 ab initio calculation of NMR chemical shifts for a $Si(CH_3)_3$-substituted model structure are in accord with the experimental chemical shifts for the $Si(ipr)_3$ substituted cation (Fig. 4).

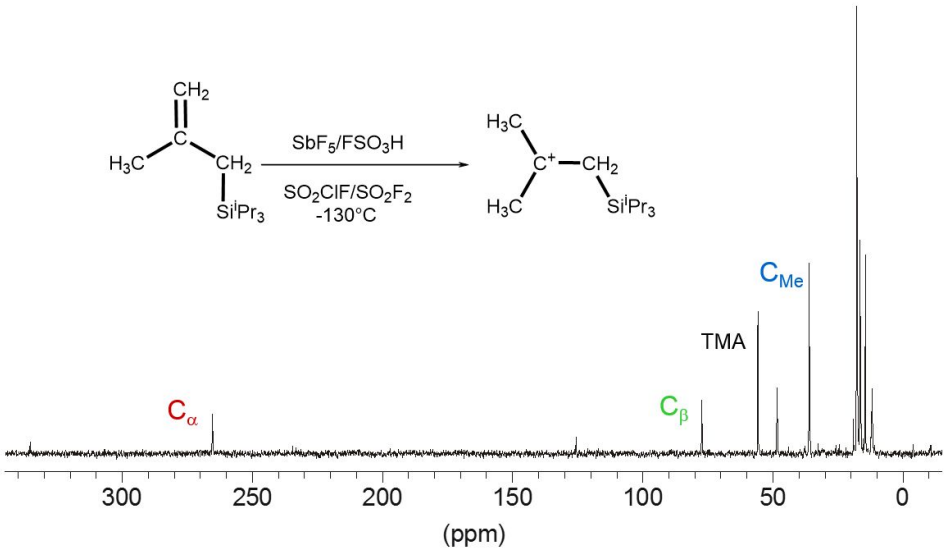


Figure 1: 100 MHz $^{13}$C NMR, $SO_2ClF/SO_2F_2$, -130° , ref. TMA= 55.65 ppm.

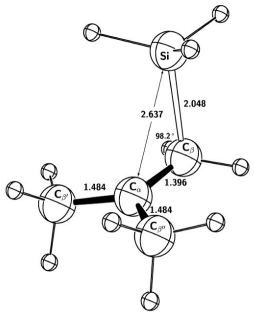


Figure 2: Hyperconjugational distortion of $\beta$-$SiH_3$ substituted t-butyl cation.

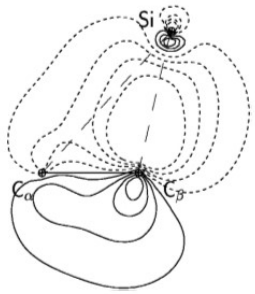


Figure 3: NBO-Analysis showing the natural localized molecular orbital (NLMO) of the 2e3c bond.

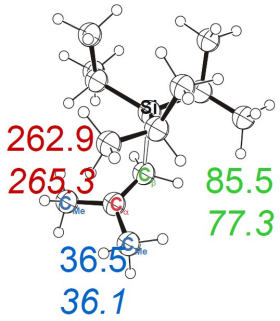


Figure 4: Experimental (italic) $^{13}$C NMR chemical shifts of Si(ipr)$_3$-substituted t-butyl cation and calculated (regular) chemical shifts of $Si(CH_3)_3$-substituted t-butyl cation.

## 2 From hyperconjugational distortion to hypercoordination (bridging)

The $C_4H_7^+$ system has been investigated for many years. The flat potential energy surface leads to a fast threefold degenerate interconversion of the bicyclobutonium ion with the isomeric cyclopropylmethyl cation (Fig. 5). Only averaged chemical shifts could be observed even at the lowest temperatures in solution. Early quantum chemical calculations were not decisive.

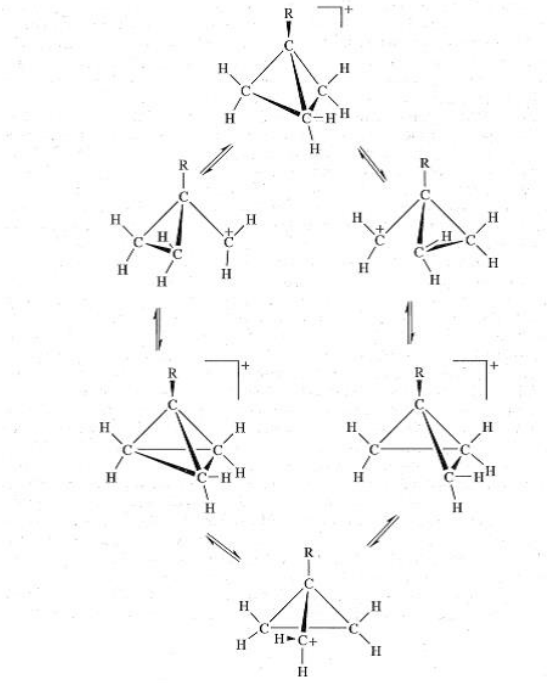

Figure 5: Threefold degenerate rearrangement of $C_4H_7^+$ cations.

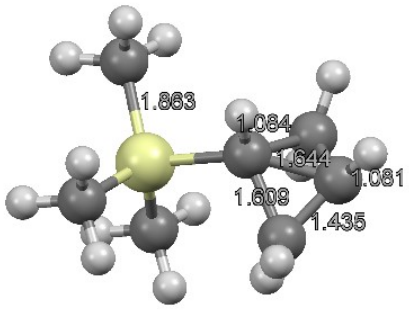


Figure 6: $\gamma$-silyl substituted bicyclobutonium ion.

We have applied the silyl effect to generate the first static bicyclobutonium ion in solution. Fig. 6 shows the preferred bridged bicyclobutonium structure of the $\gamma$-silyl substituted $C_4H_6R^+$ (R= $Si(CH_3)_3$) cation. A comparison of experimental and calculated $^{13}C$ NMR chemical shifts shows excellent agreement (Fig. 7).

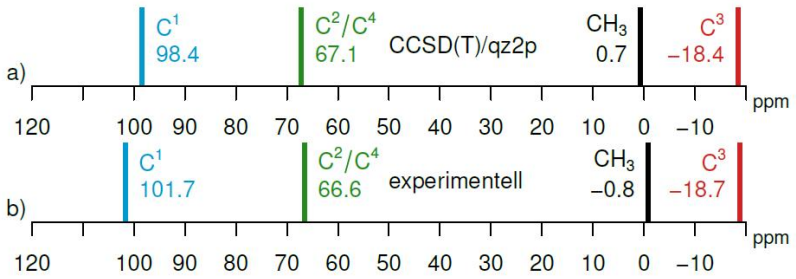


Figure 7: Comparison of experimental and calculated NMR chemical shifts of $\gamma$-silyl substituted bicyclobutonium ion

The experimental (J = 5,5 Hz) and calculated (5,9 Hz) vicinal $J_{H1H3}$ spin spin coupling constant (Fig. 8) as well as the calculated $J_{C1C3}$ spin spin coupling constant and coupling deformation density calculations are in accord with bridged structure of the silyl substituted bicyclobutonium ion. NBO calculations indicate an occupied NLMO for the bridging bond (Fig. 9) and a vacant orbital at Silicon in accord with the VB-description of the $\gamma$silyl effect.

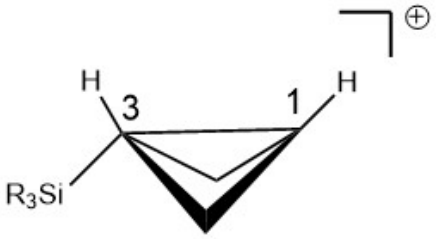


Figure 8: Transannular $^{3}J_{H,H}$ spin spin coupling in silyl substituted bicyclobutonium ion.

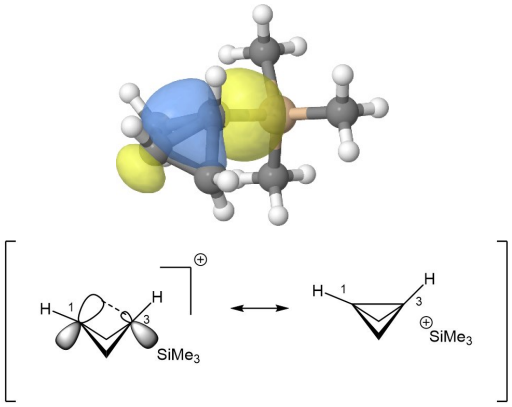


Figure 9: NLMO of the bridging bond in 3-$SiCH_3)_3$ substituted bicyclobutonium ion.

## Acknowledgements

Access to the computational resources of bwHPC with project bw14L006 is gratefully acknowledged.

## References

[1] H.-U-Siehl, Martin Fuß. Martin Holzschuh, manuscript submitted. Martin Holzschuh, PhD thesis, Ulm University 2016.

[2] H.-U. Siehl, Calculation of NMR-Parameters in Carbocation Chemistry, in Calculation of NMR and EPR Parameters, Eds., M. Kaupp, M. Bühl, V.G. Malkin, Wiley VCH, 2004.

[3] H.-U. Siehl, Experimental and Computational NMR Spectroscopic Investigations of Silyl-Substituted Carbocations, in Recent Developments in Carbocation and Onium Ion Chemistry, Ed. K.K. Laali, ACS Symp. Series 965, 2007.

[4] H.-U. Siehl, The Interplay between experiment and theory: Computational NMR Spectroscopy of Carbocations, in Adv. Phys. Org. Chem., Vol. 42, Ed. J.P. Richard, Academic Press, 2008.

# Multi-scale WRF simulations for atmospheric process understanding and boundary layer research

Hans-Stefan Bauer, Thomas Schwitalla, Volker Wulfmeyer, Oliver Branch, Andreas Behrendt, Shravan Muppa, Florian Späth, Eva Hammann, Andrea Riede, and Simon Metzendorf

Institute of Physics and Meteorology
University of Hohenheim

A multi-scale configuration of the Weather Research and Forecasting (WRF) model, containing 4 nests from 2.7 km down to 100 m horizontal resolution, is applied to investigate the evolution of turbulence on a sunny spring day in Western Germany. The simulations are driven by realistic lower boundary conditions for orography, land use and soil characteristics. The initial and lateral forcing of the meteorology is done with the operational analysis of the European Centre for Medium-range Weather Forecasting (ECMWF). The selected case is an intensive observation period during the HD(CP)2 Observation Prototype Experiment (HOPE) where also lidar systems of the Institute of Physics and Meteorology were operated. The evolution of turbulence during the day in the fine-scale 100 m domain is presented on the Symposium.

## 1 Introduction

Numerical models are excellent tools for process studies, since they provide a full 4D representation of the atmosphere. Having said that, commonly-used mesoscale models do not permit the explicit simulation of smaller-scale processes such as large turbulent eddies ( 100-2000 m) since the whole turbulence spectrum is parameterized (or inferred non-explicitly). In order to 'see' smaller circulations, so-called "Large-Eddy-Simulation" (LES) models can be used. Through application of extremely high resolution and low-pass filtering, we directly simulate larger eddies – the dominant spectra for turbulent transport of heat and moisture.

For a long time, LES models were applied to investigate turbulence under 'idealized' land surface (homogeneous) and lateral boundary (periodic) conditions (e.g. [2],[1]). The natural progression is to apply LES models within 'real' conditions. Then we can simulate the diurnal evolution of turbulence above actual landscapes and under different meteorological conditions. Such representations are crucial given the 2-way coupling between the land surface and the atmosphere, known as land surface-atmosphere (LSA) feedbacks. Real-case simulations also allow us to make comparisons against field observations to assess the model performance.

## 2 Methodology

For all tasks, the Weather Research and Forecasting advanced research model (WRF-ARW) (in the following abbreviated as WRF) [4] is applied. WRF is a state-of-the-art numerical weather prediction model designed for both research and operational applications. It is suitable for a broad span of applications across scales ranging from global down to fine large-eddy scales as used in this presentation. WRF is applied in a multi-domain configuration starting with a resolution of 2.7 km in the outer domain. Three more nests were inserted with resolutions of 900 m, 300 m and finally 100 m. Figure 1 shows the domain configuration of the experiment.

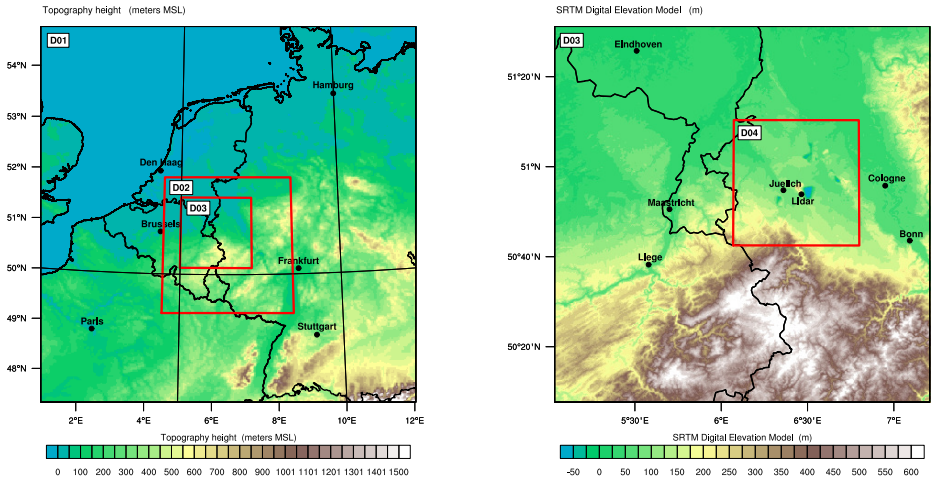


Figure 1: Domain configuration of the WRF model chain. Left: Outer three domains with 2700 m resolution (D01), 900 m resolution (D02) and 300 m resolution (D03). Right: Location of the innermost domain with 100 m resolution (D04) within D03.

All domains are simulated simultaneously in a one-way nested mode. The outer domain was driven by the ECMWF operational analysis to initialize the meteorology for the case study as well as possible.

The model physics is represented by a well-tested set of parameterizations capable to represent atmospheric processes over the range of the selected scales. It is furthermore coupled with the NOAH-MP land surface model [3] to realistically simulate the land surface and its interaction with the lowermost atmosphere. Operating WRF in LES mode requires both a high horizontal and vertical grid resolution. Both need to be of the same size over the vertical range of the investigated processes. Since we investigate processes from the boundary layer up to the full troposphere, more than 100 vertical levels are necessary.

Important first task was the optimization of the setup. For this purpose, a series of sensitivity experiments for a fair weather spring day in 2013 was carried out. In the following, the results of the final configuration for this case are discussed.

## 3 Preliminary Results

With the optimal setup, the evolution of the convective boundary layer at that day was investigated. Figure 2 shows four time steps during the evolution of the boundary layer. Shown is the turbulent kinetic energy, illustrating the intensity of turbulence, at model level 19 (approx. 1000 m above ground).

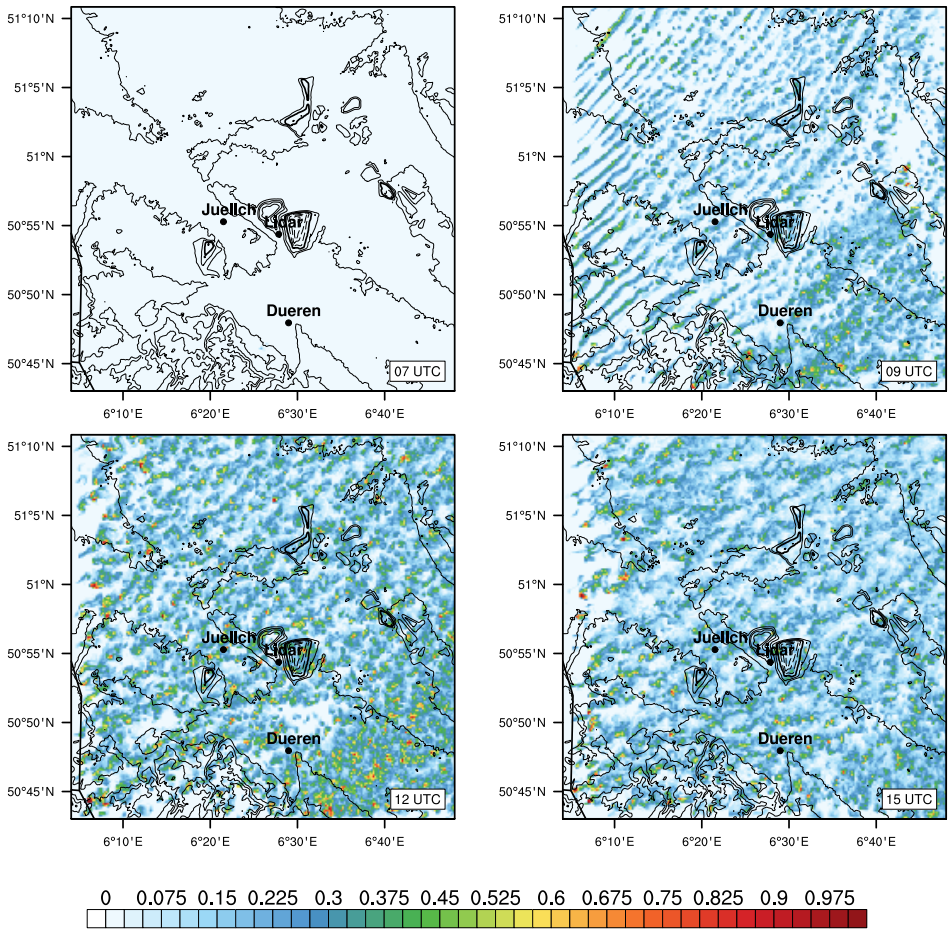


Figure 2: Turbulent kinetic energy ($cm^2/s^2$) for model level 19 (approx. 1000 m above ground) simulated by WRF with 100 m horizontal resolution at 07 UTC, 09 UTC, 12 UTC and 15 UTC, 24 April 2013.

At 7 UTC, before the onset of turbulence, the values are small. At 9 UTC, turbulence slowly starts to develop. Since the turbulent eddies are still weak and small, the strip-like structure influences a large part of the model domain. Such role-like structures are typical for environments with weak turbulence , as shown by [5]. Strongest turbulence occurs in the southeastern part of the domain where the break-up into turbulent eddies already occurred supported by the westerly flow over the higher terrain to the west. At 12 UTC, the convective boundary layer is fully evolved. Only a narrow region on the windward side of the domain is seen where the adjustment from the coarser outer domain takes place. At 15 UTC, turbulence already weakened. Interestingly, the horizontal dimension of the turbulence elements seems to

be larger comparing 12 and 15 UTC. This is consistent with the daytime growth of the turbulent eddies. The narrow region of weak turbulence along the windward boundary indicates that the transition from the coarser 300 m domain to the inner 100 m domain works smoothly and no artificial circulations are induced.

Furthermore, time-height cross sections of different variables, demonstrating the temporal evolution of the boundary layer, were investigated and shown in Figure 3. It covers the time period from 10 UTC to 16 UTC and nicely illustrates the evolution of the boundary layer. The temporal resolution of the data is 5 minutes.

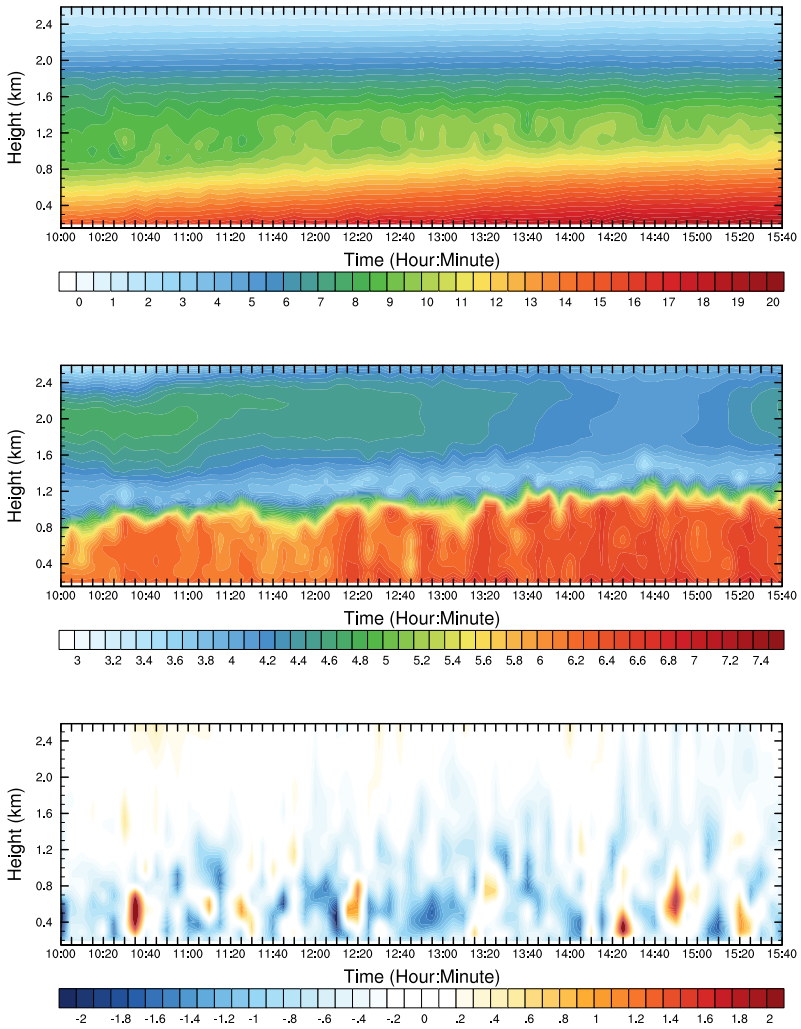


Figure 3: Time-height cross sections of the lower 2.6 km of the model atmosphere at the location of the Hohenheim lidar systems for 24 April 2013. Top: Temperature (°C). Middle: Water vapor mixing ratio (g/kg). Bottom: Vertical velocity (m/s). Output interval of WRF was 5 minutes.

In the temperature panel (top), the rise of the boundary layer top height during the development is nicely seen. Furthermore, the iterating upward transports of warm air and downward intrusions of colder air into the boundary layer are seen. The boundary layer top and the vertical

transports are even better seen in the water vapor cross section. The sharp gradient in the water vapor field marks the boundary layer top. The dry layer directly above the boundary layer top and an elevated moister layer above, a precursor of an approaching low pressure system from the west that lead to cloudy and rainy conditions during the following two days are well represented. Iterating moist and dry regions mark rising moist bubbles and the downward intrusion of dry air from above the boundary layer top. The vertical velocity panel (bottom) shows active turbulence by iterating upward and downward motion. As expected from observations, narrow and strong updrafts iterated with broader and weaker compensating downdrafts.

## 4 Conclusions and outlook

The first results are very promising. Turbulence evolves as expected from literature and no obvious problems caused by the downscaling from mesoscale to LES are seen. This indicates that the applied setup is a feasible tool for the investigation of turbulence under realistic case-study-based conditions. The system will be further optimized in future applications during upcoming field campaigns and the investigations of the process evolution during high-impact weather events (e.g. severe convection).

## References

[1] Mirocha, J. D., Lundquist, J. K. and Kosovic, B., 2010. Implementation of a non-linear subfilter turbulence stress model for large-eddy simulation in the advanced research WRF model. Mon. Wea. Rev. 138, 4212–4228.

[2] Moeng, C. H., 1984. A large-eddy-simulation model for the study of the planetary boundary layer turbulence. J. Atmos. Sci. 41, 2052-2062.

[3] Niu, G.-Y., Yang, Z.-L., Mitchell, K. E., Chen, F., Ek, M. B., Barlage, M., Kumar, A., Manning, K., Niyogi, D., Rosero, E., Tewari, M. and Xia, Y., 2011. The community Noah land surface model with multiparameterization (Noah-MP): Model description and evaluation with local-scale measurements. J. Geophys. Res. 116, D12109, DOI: 10.1029/2010JD015139.

[4] Skamarock, W. C., Klemp, J. B., Dudhia, J., Gill, D. O., Barker, D. M., Duda, M., Huang, X.-Y., Wang, W. and Powers, J.-G., 2008. A Description of the Advanced Research WRF Version 3. NCAR Technical Note TN-475+STR, 113pp.

[5] Weckwerth, T. M., Horst, T. W. and Wilson, J. W., 1998: An observational study of the evolution horizontal convective rolls. Mon. Wea. Rev. 127, 2160-2179.

# bwUniCluster: Baden-Württemberg's University Cluster

Robert Barthel and Simon Raffeiner

Steinbuch Centre for Computing, Karlsruhe Institute of Technology

"bwUniCluster" is a tier-3 High Performance Computing cluster co-financed by Baden-Württemberg's Ministry of Science, Research and the Arts, and the shareholders: Universities of Freiburg, Tübingen, Ulm, Heidelberg, Hohenheim, Konstanz, Mannheim, Stuttgart, the KIT and the HAW Baden-Württemberg e.V. (an association of universities of applied sciences in Baden-Württemberg). Together with the bwForClusters JUSTUS, MLS&WISO, NEMO and BinAC it constitutes the multi-cluster entry level of Baden-Württemberg's High Performance Computing (bwHPC).

## 1 Introduction

Baden-Württembergs's current initiative on high-performance computing (HPC), officially labelled **bwHPC** [1], has been evolving the traditional HPC entry level, i.e., tier 3, to a federated, heterogeneous HPC cluster infrastructure (cf. figure 1) and state-wide HPC support base. The

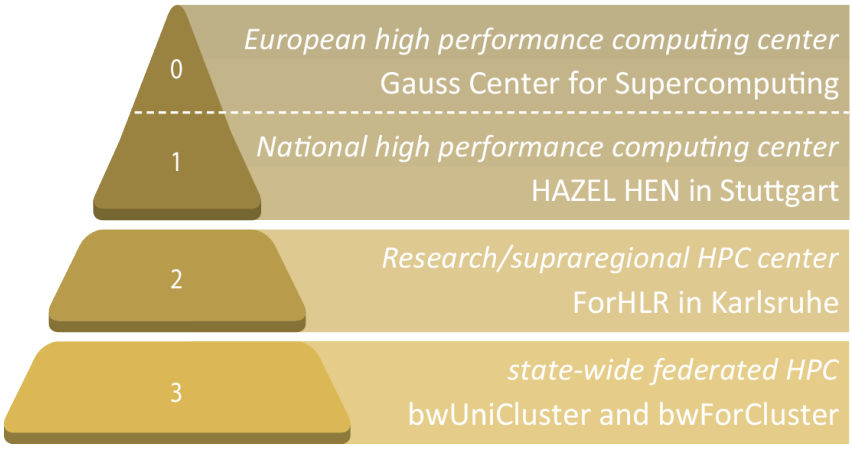


Figure 1: HPC performance pyramid in the state of Baden-Württemberg, Germany: from top (tier 0) to bottom (tier 3) with decreasing scalability and performance level.

initiative bwHPC, recommended for funding by the German Research Foundation (DFG) and considered a model concept for Germany, covers the promotion of HPC with different performance classes and competence centers at all levels.

The bwUniCluster system constitutes within bwHPC one of the five clusters of the HPC entry level. Complementary to the four HPC research clusters (bwForClusters), which are tailored to the needs of specific scientific communities, bwUniCluster provides the resources of Baden-Württemberg's universities for general purpose computing covering teaching and all science communities without a dedicated bwForCluster.

bwUniCluster has been been co-financed by Baden-Württemberg's Ministry of Science, Research and the Arts, and university shareholders[1], hence the derived name "bwUniCluster" from *B*aden-*W*uerttemberg's *uni*veral or university *cluster*.

bwUniCluster is located at the Karlsruhe Institute of Technology and has been operating since January 2014. In March 2017, bwUniCluster will be expanded by a second partition, more than doubling the initial computing capacity.

## 2 Hardware architecture

The first partition consists of 532 compute nodes with two 8-core Intel Xeon E5-2670 ("Sandy Bridge") processors and 64 gigabytes of main memory each, plus eight compute nodes with four 8-core Intel Xeon E5-4640 processors and 1 Terabyte of main memory each [2]. The second partition will consists of 352 compute nodes with two 14-core Intel Xeon E5-2660v4 ("Broadwell") processors and 128 gigabytes of main memory each. Together with the second partition total peak performance for the system will be 440 TeraFLOPS as well as providing in total 86 Terabyte of main memory.

On bwUniCluster two parallel file system based on Lustre are used for globally (i.e., on all nodes) accessible user data. Both file systems differ in usability lifetime, redundancy and total capacity. While `$HOME` is permanent and under backup, its 469 Terabyte is not primarily for computing activities. Globally available data scratch is provided by the workspace file system with a total capacity of 938 Terabyte. However workspaces have a limited lifetime and no redundance.

For providing an extremely fast and high data throughput network with very low latency all nodes are connected to a central InfiniBand fabric at 56 GBit/s per node (4x FDR).

## 3 Support

User support for bwUniCluster is provided mainly by members of the project bwHPC-C5 [3] including:

- maintaining a comprehensive HPC software stack (currently with over 200 software modules) extensible upon user requests,
- HPC teaching courses,
- second level support for any HPC related issues and high-level support teams (aka bwHPC tiger teams), and
- elaborated online best practice and user guides [4].

[1] Universities of Freiburg, Tübingen, Ulm, Heidelberg, Hohenheim, Konstanz, Mannheim, Stuttgart, the KIT and the HAW Baden-Württemberg e.V. (an association of universities of applied sciences in Baden-Württemberg)

## 4 Access & Registration

The use of bwUniCluster is free of charge for all academic members of the shareholders[1]. After issued a bwUniCluster entitlement by the home organisation one can register online for the service, while access to the cluster can be established via SSH. Further details are covered in the Best Practices Wiki [5].

## 5 Citation

As every funded work, the use of bwUniCluster system has to be cited in any work related publication as follows:

> "The authors acknowledge support by the state of Baden-Württemberg through bwHPC."

## References

[1] Hartenstein, H., T. Walter, and P. Castellaz. "Aktuelle Umsetzungskonzepte der Universitäten des Landes Baden-Württemberg für Hochleistungsrechnen und datenintensive Dienste." Praxis der Informationsverarbeitung und Kommunikation, Band 36, Heft 2 (2013): 99-108. http://dx.doi.org/10.1515/pik-2013-0007

[2] Scheller, U.: "KIT betreibt zentralen Hochleistungsrechner der Landesuniversitäten". SCC-News, 01-2014, pp 6–7.

[3] http://www.bwhpc-c5.de

[4] http://www.bwhpc.de/wiki

[5] http://www.bwhpc.de/wiki/index.php/bwUniCluster_User_Access

# ForHLR: a New Tier-2 High-Performance Computing System for Research

Robert Barthel and Simon Raffeiner

Steinbuch Centre for Computing, Karlsruhe Institute of Technology

ForHLR (short for German "Forschungshochleistungsrechner") is a new petaflop high-performance computing (HPC) system dedicated to multiparallel, i.e., 100 – 1000 core, applications and consists of two installation phases: ForHLR Phase I and ForHLR Phase II. The former has already been in operation since September 2014, while the latter was inaugurated on March 4, 2016. Both systems are available to the entire German scientific community. All compute proposals are to be peer-reviewed by the HLRS steering committee.

## 1 Introduction

ForHLR, short for German "Forschungshochleistungsrechner", is the current installation of the tier-2 high-performance computing (HPC) system in the state of Baden-Württemberg, Germany [1]. This HPC system gaps the currently fastest European supercomputer, i.e., Hazel Han, (tier-1 system) and the HPC enabling (tier-3) infrastructure, i.e., bwUniCluster and the bwForCluster JUSTUS, MLS&WISO, NEMO and BinAC, in the state of Baden-Württemberg, Germany. The ForHLR system consists of two cluster: ForHLR Phase I and ForHLR Phase II.

## 2 Hardware Architecture

### 2.1 ForHLR Phase I

The ForHLR I system marks the first phase of the ForHLR installation and has been cofunded by the Ministry of Science, Research and the Arts Baden-Württemberg, Germany and DFG (German Research Foundation).

The ForHLR Phase I infrastructure [2] consists of 512 compute nodes with two 10-core Intel Xeon E5-2670v2 ("Ivy Bridge") processors and 64 gigabytes of main memory each, plus 16 compute nodes with four 8-core Intel Xeon E5-4620v2 processors and 512 gigabytes of main memory each. Total peak performance for the system is 216 TeraFLOPS, the total amount of main memory is 41.1 Terabytes. All nodes are connected to a central InfiniBand fabric at 56 GBit/s per node (4x FDR).

On ForHLR Phase I two parallel file system based on Lustre are used for globally (i.e., on all nodes) accessible user data. Both file systems differ in usability lifetime, redundancy and total

capacity. While `$HOME` is permanent and under backup, its 469 Terabyte is not primarily for computing activities. Globally available data scratch is provided by the workspace file system with a total capacity of 938 Terabyte. However workspaces have a limited lifetime and no redundance.

### 2.2 ForHLR Phase II

The ForHLR Phase II system [3] marks the second phase of the ForHLR installation and has also been cofunded by the Ministry of Science, Research and the Arts Baden-Württemberg, Germany and DFG (German Research Foundation).

It consists of 1152 compute nodes with two 10-core Intel Xeon E5-2660v3 ("Haswell") processors and 64 gigabytes of main memory each, plus 21 compute nodes with four 12-core Intel Xeon E7-4830v3 processors and 1 Terabyte of main memory each. Total peak performance for the system is one PetaFLOPS, the total amount of main memory is 95 Terabytes. Similar to ForHLR Phase I, a permanent (`$HOME`) as well as a workspace parallel filesystems are available for data storage with 670 Terabyte and 4.8 Petabyte, respectively.

All nodes are connected to a central InfiniBand fabric at 56 GBit/s per node (4x FDR), while the InfiniBand Backbone uses 100 GBit/s connections (4x EDR). The ForHLR II system is located at KIT's Campus North and is coupled to the existing Lustre parallel filesystems through a 320 Gbps long-range InfiniBand link bridging the 11 kilometers to SCC's second data center at Campus South.

A novelty of this installation is the highly efficient hot-water cooling system, which reuses the waste heat for the heating of the nearby office building.

## 3 Access & Registration

The ForHLR system is available to all research areas and has been customized, in particular, to energy science, environmental science, materials science and engineering technology. Moreover both systems are dedicated to solving highly complex scientific scenarios using highly scalable and multiparallel application codes, i.e., utilizing 100 – 1000 CPU cores. Smaller compute projects ought to be for ForHLR Phase I while the most resource demanding ones are preferably assigned to ForHLR Phase II.

Although academic use is free of charge, preliminary accounts are given only for a short term to test ForHLR architecture and the software stack while accounts of long term compute projects are bound to approved CPU hours.

Compute projects are peer-reviewed in terms of application scalability/usability and CPU hour feasibility for the ForHLR systems. To be proper reviewed applicants must submit a 3 to 5 page long project description elsewhere [4].

## 4 Citation

As every funded work, the use of the ForHLR systems have to be cited in any work related publication as follows:

"This work was performed on the computational resource ForHLR Phase I (ForHLR Phase II) funded by the Ministry of Science, Research and the Arts Baden-Württemberg and DFG (German Research Foundation)."

## References

[1] Hartenstein, H., T. Walter, and P. Castellaz. "Aktuelle Umsetzungskonzepte der Universitäten des Landes Baden-Württemberg für Hochleistungsrechnen und datenintensive Dienste." Praxis der Informationsverarbeitung und Kommunikation, Band 36, Heft 2 (2013): 99-108. http://dx.doi.org/10.1515/pik-2013-0007

[2] Häfner, H.: "ForHLR – ein Hochleistungsrechner für die Forschung". SCC-News, 02-2014, pp 4–5.

[3] Gernert, H., R. Lohner and R. Mayer: "ForHLR – Der neue Forschungshochleistungsrechner am KIT". SCC-News, 01-2016, pp 8–12.

[4] http://www.scc.kit.edu/dienste/proposals.php

# Towards a temperature monitoring system for HPC systems

Martin Baumann, Sotirios Nikas, and Fabian Gehbart

Computing Centre, Heidelberg University

In the context of high-performance computing (HPC), the removal of released heat is one challenging topic due to the continuously increasing density of computing power. A temperature monitoring system provides insight into the heat development of an HPC cluster which is important to investigate the efficiency of the cooling system and allows for defect detection. We present a scalable and flexible monitoring solution based on low-cost components with a Raspberry Pi as a monitoring client and propose a set-up for monitoring the temperature of an HPC cluster.

## 1 Introduction

In the IT rooms of the Heidelberg University Computing Centre, a highly efficient cooling technology is realized where the outdoor air temperature is used for water chilling (free cooling). The racks are equipped with water-cooled heat exchanger back doors to cool the exhausting air to ambient air temperature (details can be found in [1]). To gain a deeper understanding of the heat situation surrounding or inside the computer racks, a high number of temperature sensors is required. We describe what sensors we are using, how we connect these to a big bus system, and how we read and manage the temperature values.

## 2 Sensor technology and flexible bus-cabling

For this project, we use the *Dallas DS18B20* temperature sensor, cf. [2], which is a digital thermometer with three pins (ground, voltage, data), see Fig. 1 (a). This sensor can measure temperature values between -55 °C and +125 °C with an accuracy of ±0.5 °C from -10 °C to +85 °C. Its resolution can be chosen between 9 and 12 bit leading to a precision from 0.5 °C to 0.0625 °C. Due to its low price of about €1 per sensor, the simplicity of the 1-Wire protocol, and the relatively high precision and temperature range the *DS18B20* is well suited for building up a temperature monitoring system for an HPC cluster.

Several vendors are offering *DS18B20* sensors pre-assembled on cables. However, we are assembling the sensors by ourselves to be able to use standard network patch cables, since those cables have good shielding and for the RJ-45 connectors many adapters exist. Only three of the eight wires of a patch cable are used for the sensor, five wires remain available for other purposes (e.g. other sensors). The assembling process consists of bisecting a patch cable and soldering

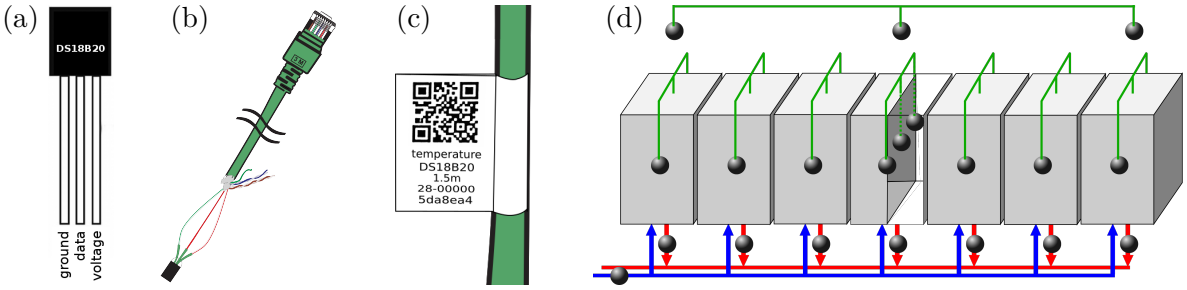


Figure 1: (a) Illustration of the sensor *DS18B20*, (b) the assembled sensor cable with RJ-45 connector without heat-shrinking tubes, (c) label containing information about the sensor and the cable length, and (d) the sensor positioning in the environment of a server rack row (sensors indicated by black circles).

the three pins of a sensor to three specified wires of a patch cable, see Fig. 1 (b). Heat-shrinking tubes of different diameters are used to avoid any short circuit between the three sensor pins and hold together the wires for higher resilience.

Since we are using RJ-45 connectors, a big bus system comprising a large number of sensors can be built using standard patch cables and RJ-45 bus boards which are offered by various vendors. In the end, the bus system is connected to the general purpose input output (GPIO) pins of a Raspberry Pi. By reading the sensors separately (see next section), each sensor's unique ID can be determined. This ID will be exploited for the identification of each single sensor in a bus system of many connected sensors. For practical reasons, we equip each assembled cable with a label containing the sensor's model name, ID, and cable length. To support automated reading, the information is additionally encoded in a QR code which is placed on the label, see Fig. 1 (c).

## 3 Reading sensor values within a monitoring system

For reading the sensor values, we have written a short Python program that makes use of the 1-Wire protocol. This tool is executed on a Raspberry Pi allowing to read the values of all sensors in the bus system. Before the sensors are installed in the IT room for production operation, their functional capability and precision are evaluated. To do so, all sensors are positioned alongside and simultaneous temperature measurements are conducted. Additionally, the response time of the sensors, i.e. the time the sensors need to follow changing temperatures, can be considered for the validation process. Thus, the outliers can be identified and sorted out.

There are several influence factors that can limit the maximum number of sensors that can be connected. These include the cabling (e.g. the length of the cables) and the ohmic resistance of the pull up resistor (we used a resistor with 270 Ω). It turns out that even the Linux Kernel of the Raspberry Pi's operating system has some influence (later versions seem to be better; we used the kernel version 4.4.14-v7+). In our set-up, the maximum number of sensors that could be read out by the Raspberry Pi in one single bus was 161 sensors.

For the realization of a monitoring system for a high number of temperature sensors existing monitoring tools such as Zabbix or Nagios can be employed. For that purpose, a Simple Network Management Protocol (SNMP) agent was developed to run on the Raspberry Pi that allows communication using the SNMP, cf. [3], which is a standard protocol for information management in IP networks. The client sends temperature values to the monitoring server on

a regular basis where the data is stored for a long time. The server can have powerful visualization and analysis features and can also be extended by custom features. Additionally, the client can observe the temperature values with a higher temporal resolution (e.g. to recognize outliers within seconds) and can send *traps* to the monitoring server in case of overheating or other noticeable situations.

## 4 On-site installation

As mentioned before, the cooling technology employed in the IT rooms of the Heidelberg University Computing Centre is based on passively cooled back doors. In this technology, the heat development of the environment of an HPC system primarily depends on the heat balance of the air flowing into and leaving the server racks. The outflowing air temperature again is determined by the temperature within the server rack and the effect of cooling by passing through the back door. The back door serves as heat exchanger which increases the water temperature flowing through the back door while cooling the air.

For an overall picture of the spatial temperature distribution, several temperature values must be known: the air temperature in front, inside and behind of each server rack and the water temperature before and after flowing through each server's back door. In contrast to the warm water (depending on the rack's energy consumption), the cool water temperature is approximately the same for each rack, for which reason it is sufficient to use only one sensor. For the determination of the HPC cluster's surrounding temperature climate, some sensors are positioned above the rack row. Overall, there are four sensors installed at each rack, plus one additional sensor per rack row for the cool water temperature, plus few sensors for the air temperature above the rack row, see Fig. 1 (d).

In the next phase of the project, additional sensors for measuring the energy consumption will be integrated to the bus system and will be included in the monitoring. The relation between the energy consumption of the HPC system while running different applications and the associated heat development will then be analysed.

## Acknowledgements

The authors acknowledge support by the Ministry of Science, Research and the Arts of the State of Baden-Württemberg (MWK) through the project bwHPC-C5.

## References

[1] e3computing: eCube cooling technology for data centers, http://www.e3c.eu, March 2015.

[2] Dallas Semiconductor: Data sheet for DS18B20 programmable resolution 1-Wire® digital thermometer, http://www.dalsemi.com/.

[3] T. Hochstrasser: Konzeption und Entwicklung eines verteilten Systems zum Sensor-Monitoring, Bachelor thesis, Ruprecht-Karls-Universität Heidelberg, Institut für Informatik, 08-2016.

# Numerical Analysis of the Temperature Distribution in a Subway Tunnel

Anders Berg

Institute for Building Energetics, University of Stuttgart

Only a few technical modifications are required to use a tunnel as a geothermal source or sink for heating and cooling purposes. This idea is realized in the GeoTU6 project with a geothermal test section inside the Fasanenhof subway tunnel in Stuttgart, Germany. Two tunnel sections are equipped with absorber pipes along a length of 10 meters. The pipes are linked with a heat pump situated in a control room nearby. The tunnel is equipped with measuring devices to determine the temperature fields in the ground, the tunnel lining and the tunnel air. In addition, the tunnel air velocity is measured. The research priority is to investigate how the tunnel air influences the amount of extracted energy of the absorber system.

## 1 Introduction

Computational fluid dynamics (CFD) is performed to investigate the influence of the tunnel air temperature in dependence on various parameters. Steady state simulation results are compared with experimental data from the on-site measurements. Based on simulation and measurement results, an approximation equation is to be deduced for the tunnel air temperature in dependence of the above mentioned parameters. A 3D representation, containing tunnel air, tunnel lining and surrounding ground is created. The tunnel has a length close to 360 meters. The geometry can be seen in Figure 1. A mesh is generated which contains about 30 million cells. The simulations are performed with OpenFOAM version 2.4. The boundary conditions for the CFD simulations are taken from on-site measurements.

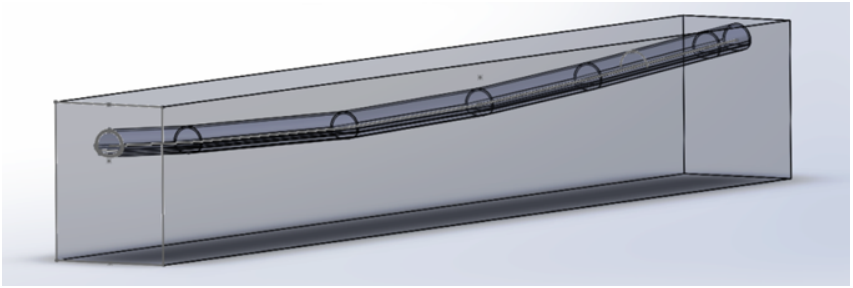

Figure 1: Computational domain of the model

## 2 Resources

The simulations are performed on the parallel cluster ForHLR I which is situated at the Karlsruhe Institute of Technology in Germany. It is a distributed memory parallel computer and the simulation cases are run on 20-way Intel Xeon compute nodes. Each node has 64 GB of main memory. In order to investigate the appropriate number of compute cores to be used for the numerical investigations a scalability analysis is performed. During this analysis several simulations with a varying number of compute cores are performed. 200 compute cores are selected for the performed simulations, which is equal to 10 nodes. This means that the 30 million mesh cells will be distributed on these cores, leading to approximately 150,000 cells per compute core. The simulations have an approximate simulation time of 21 hours. This leads to a total of 4200 core hours per simulation.

## 3 Results and Discussion

Qualitative simulation results of the tunnel air temperature distribution and the temperature field of its surroundings can be seen in Figure 2 for the cases November 2014 to March 2015. The temperatures are displayed on a plane going through the middle of the tunnel. It can be seen how the difference in tunnel and soil temperature varies during the year.

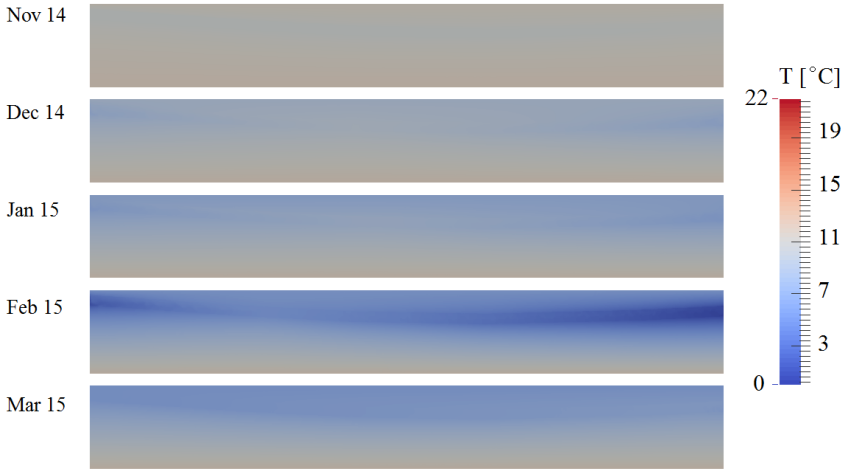


Figure 2: Temperature distribution of tunnel air and surroundings (November 2014 - March 2015)

## 4 Conclusions

Further simulations and validation will give a closer insight on how well the temperature distribution inside the tunnel is captured by the numerical model.

## Acknowledgements

The project is supported by the Federal Ministry for Economic Affairs and Energy and the Stuttgarter Straßenbahnen.

# Bio-economic simulation on bwUniCluster: The assessment of sustainable agricultural systems in Southern Amazon, Brazil

Marcelo Carauta and Thomas Berger

Department of Land Use Economics in the Tropics and Subtropics, Hohenheim University

The aims of this project is assess the trade-offs between different agricultural practices and production systems in Southern Amazon, Brazil.

## 1 Introduction

The focus of Brazilian Land Use policy has changed over the last decade towards sustainable agriculture. The country pledged to take domestic actions to substantially decrease its greenhouse gas (GHG) emissions, in order to balance agricultural production and environmental protection. According to this pledge, national GHG emissions shall be reduced by 36.1–38.9% until 2020. Agriculture alone is expected to reduce 166 million tons of CO2eq, or 43% of the national mitigation efforts by 2020.

## 2 Study Area

Mato Grosso is the third largest state of Brazil extending over 903,000 sq. km, which amounts to the area of France and Germany taken together. Favorable climatic conditions allowing for two growing seasons per year, together with the introduction of improved seeds and techniques for dealing with soil acidity transformed Mato Grosso into a major player in soybean, maize and cotton production. The state is also known for its biodiversity, holding three different biomes: Cerrado (Brazilian Savannas), Pantanal and Amazon Rainforest. Despite being a large agricultural producer, the state still preserves approximately 60% of its native forest.

## 3 Objective

We conducted a quantitative analysis with a farm level approach on farm systems in Mato Grosso and developed a region specific bio-economic micro-simulation model which is able to capture the interregional differences between farms, farm-based economic behavior and human-environment interactions in agriculture. The simulation results provide detailed information on how the decision variables affect the production systems.

## 4 Model Coupling

Its main element consists of an economic component which simulates farm-level decision making problems and is implemented in the Mathematical Programming-based Multi-Agent Systems (MPMAS), a multi-agent software for simulating land use change in agriculture. In order to link the simulated farm-based economic behavior with human-environmental interactions we implemented a second component, a dynamic, process-based biophysical simulator, which was implemented in the simulation model for nitrogen and carbon dynamics in agro-ecosystems (MONICA). The third component is a simulation model which describes the carbon and nitrogen dynamics in arable soils. This component was implemented in Carbon-Nitrogen-Dynamics (CANDY) model, a software that provides information about C stocks in soils, organic matter turnover, N uptake by crops, leaching and water quality. Further details on modeling approach, methodology and data can be accessed from Carauta et al. [1, 2].

## 5 Conclusions

Our simulations can provide realistic results and important insights to the problem's comprehension because: (1) it simulates farmers behavior under site-specific conditions; (2) captures real-world heterogeneity; (3) captures bio-economic conditions; (4) captures economic incentives; (5) allows farm-level as well as regional level assessments; (6) takes into consideration several agricultural practices; (7) captures key determinants on crop yield and (8) allows assessment of different policies set-ups.

## Acknowledgements

This research was funded by Brazilian Coordination for the Improvement of Higher Education Personnel (CAPES, BEX Number 10421/14-9). This work was performed on the computational resource bwUniCluster funded by the Ministry of Science, Research and the Arts Baden-Württemberg and the Universities of the State of Baden-Württemberg, Germany, within the framework program bwHPC.

## References

[1] Carauta, Marcelo, Affonso Amaral Dalla Libera, Rafael Felice Fan Chen, Anna Hampf, Ianna Raissa Moreira Dantas, José Maria F J Silveira, and Thomas Berger. "On-Farm Trade-Offs for Optimal Agricultural Practices in Mato Grosso, Brazil." In 54o Congresso da Sociedade Brasileira de Economia, Administração e Sociologia Rural, (2016) doi:10.13140/RG.2.2.22655.00169.

[2] Carauta, Marcelo, Affonso Amaral Dalla Libera, Evgeny Latynskiy, Anna Hampf, José Maria F J Silveira, and Thomas Berger. "Integrated Assessment of Novel Two-Season Production Systems in Mato Grosso, Brazil." In Proceedings of the 8th International Congress on Environmental Modelling and Software, edited by S Sauvage, J M Sanchez-Perez, and A E Rizzoli, 430–37, (2016) doi:10.13140/RG.2.1.3824.4088.

# Theoretical investigation of the demethylation of acetic acid

Dieter Johann Peter Faltermeier

Institute of Inorganic Chemistry, Heidelberg University

## 1 Introduction

The DFG Research Unit 763 "Natural Halogenation Processes in the Environment- Atmosphere and Soil" has been carrying out research projects in the field of halogenated organic compounds. Recent soil samples from Australia point to a natural production of chloromethane in salt lakes. The iron-catalyzed oxidation reactions of organic material was investigated. For this purpose, various analytical methods (GC-FID, GC-MS, IC) were used. Furthermore, quantum mechanical calculations were performed to find reaction intermediates and to investigate the reaction mechanism.[1]

## 2 Computational Methods

In this project, complexes of $Fe^{IV}$ and bispidine[2,3] based ligands $L^{1\text{-}4}$ were investigated as catalysts for the reaction with acetic acid (Fig. 1). The DFT calculations (Functional B3LYP[4]; Basisset def2-tzvp[5,6]; PCM-Model (solvent = Water)) were performed with Gaussian09[7].

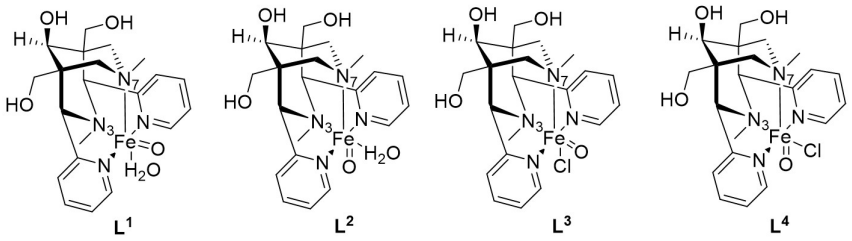


Figure 1: $Fe^{IV}$ complexes of ligands $L^1$, $L^2$, $L^3$ and $L^4$.

## 3 Results

The $Fe^{IV}$ complexes have two important spin states (Fig 2.). Therefore the complexes were optimized in S=1 and S=2 multiplets to find the estimated ground state. The iron(IV)-oxo bispidine complexes were analyzed by their energy, bond lengths, charges and spin densities.

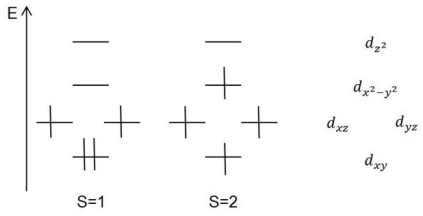


Figure 2: Spin states of the investigated iron$^{IV}$ complexes.

$L^1$ and $L^3$ have the lowest ground state energies. The difference in the bond length is significant. Every coordination bond in the chloro complex is longer than in the water complex. Furthermore, experimental results show, that the water-complex plays the important role in the reaction mechanism. Therefore the transition states and products were analyzed for the reaction of $L^1$ with acetic acid. Two different types of reactions were examined. One is the C-H activation of the methyl group of the acetic acid and the other one is the oxidation of the carboxylic group. When comparing the two different spin states on the reaction coordinate (Scheme 1), it is remarkable that the energy barrier of the high spin complex is almost half of the low spin complex. Therefore it is likely that the S=1 state switches to the S=2 state and then activates the C-H bond.

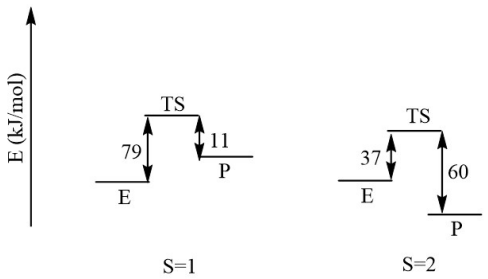


Figure 3: Reaction coordinate of the H-Atom abstraction by $L^1$. (E = educts, TS = transition state, P = products)

The attack of the carbonyl group is very energetically unfavorable. When comparing the energy barrier between the C-H activation (Scheme 1) and the attack of the C1-Atom (Scheme 2), one can see a large difference in the activation barriers.

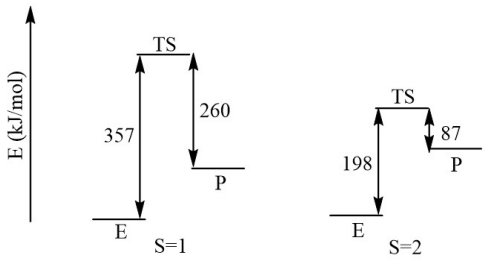


Figure 4: Reaction coordinate of the C-Atom abstraction by $L^1$. (E = educts, TS = transition state, P = products)

## 4 Conclusions

In this work $Fe^{IV}$ bispidine complexes have been examined for their activity in the reaction with acetic acid. The iron(IV)-oxo complex $L^1$ acts as a catalyst in the activation of the C-H bond and possibly as an oxidant for the carbonxylic group. So far, there is no experimental proof of the intermediates. Further spectroscopic studies (EPR, stopped-flow of the intermediates) are inevitable for a deeper insight into the mechanism. This will be supported by further (DFT) quantum chemical calculations.

## Acknowledgements

We are grateful for computational resources provided by the bwForCluster JUSTUS, funded by the Ministry of Science, Research and Arts and the Universities of the State of Baden-Württemberg, Germany, within the framework program bwHPC-C5.

## References

[1] Faltermeier D.; Masterarbeit 2016; Universität Heidelberg.

[2] P. Comba, M. Kerscher, W. Schiek, Prog. Inorg. Chem. 2007, 55 613-704.

[3] C. Mannich, P. Mohs, Chem. Ber. 1930, 63, 608-612.

[4] S. F.Sousa, P. A. Fernandes, M. J. Ramos, J. Phys. Chem. A, 2007, 111, 10439-10452.

[5] A. Schafer, C. Huber, R. Ahlrichs, J Chem Phys., 1994, 100, 5829-5835.

[6] F. Weigend, R. Ahlrichs, Phys Chem Chem Phys., 2005, 7, 3297-3305.

[7] M. J. Frisch, G. W. Trucks, H. B. Schlegel, G. E. Scuseria, M. A. Robb, J. R. Cheeseman, G. Scalmani, V. Barone, B. Mennucci, G. A. Petersson, H. Nakatsuji, M.Caricato, X. Li, H. P. Hratchian, A. F. Izmaylov, J. Bloino, G. Zheng, J. L. Sonnenberg, M. Hada, M. Ehara, K. Toyota, R. Fukuda, J. Hasegawa, M. Ishida, T. Nakajima, Y. Honda, O. Kitao, H. Nakai, T. Vreven, J. A. Montgomery Jr., J. E. Peralta, F. Ogliaro, M. J. Bearpark, J. Heyd, E. N. Brothers, K. N. Kudin, V. N. Staroverov, R. Kobayashi, J. Normand, K. Raghavachari, A. P. Rendell, J. C. Burant, S. S. Iyengar, J. Tomasi, M. Cossi, N. Rega, N. J. Millam, M. Klene, J. E. Knox, J. B. Cross, V. Bakken, C. Adamo, J. Jaramillo, R. Gomperts, R. E. Stratmann, O. Yazyev, A. J. Austin, R. Cammi, C. Pomelli, J. W. Ochterski, R. L. Martin, K. Morokuma, V. G. Zakrzewski, G. A. Voth, P. Salvador, J. J. Dannenberg, S. Dapprich, A. D. Daniels, Ö. Farkas, J. B. Foresman, J. V. Ortiz, J. Cioslowski, D. J. Fox, Gaussian, Inc., Wallingford, CT, USA, 2009.

# Numerical Analysis of the Flow and Particle Pattern in a Realistic Human Nasal Cavity

Ali Farnoud[1], Ingo Baumann[2], and Eva Gutheil[1]

[1]Interdisciplinary Center for Scientific Computing, Heidelberg University
[2]Department of Otorhinolaryngology, Head and Neck Surgery, Medical Center of the Heidelberg University

A numerical study of the dispersion and deposition of liquid drugs sprayed into the nasal airway is presented. A realistic three-dimensional model of the human nasal airway is constructed from computed tomography (CT) scans. Unsteady Eulerian-Lagrangian equations are used to simulate the transitional laminar-turbulent airflow and the micro-particle dispersion and deposition in a realistic human nasal airway. The results of two different numerical volume grids show that the coarse mesh is not suitable to capture the flow characteristics. The simulation shows that most of the particles deposit in the anterior and posterior regions of the nasal cavity, which is due to the changes in flow direction in this area.

## 1 Introduction

The study of the aerosol dispersion and deposition in the human nasal passage is relevant in controlling the inhalation of toxic particles in the air and administration of therapeutic aerosols for patients suffering chronic rhinosinusitis, asthma, allergies, diabetes, or migraine headaches. Recently, drug delivery via the nasal passage has become an alternative approach to oral drug administration since this approach has advantages such as quick effect, local administration, and minimal side effects. In the present study, the airflow and particle dispersion and deposition in a realistic human nasal cavity is studied numerically.

## 2 Methodology and Numerical Methods

The CT images in .DICOM format are obtained with a slice thickness of 1 mm. Subsequently, identification of the region of interest, artifacts removal, segmentation, extraction of the .STL file and generation of the triangulated surface are preformed by using the software packages of ImageJ, meshLab, NeuRA2 [1]. The software ICEM-CFD Ansys 11.0 is used to generate the tetrahedral volume grid.

A large eddy simulation (LES) using the solver "pimpleFoam" of OpenFOAM 4.0 with the Smagorinsky sub-grid scale model is coupled to the Lagrangian parcel library in order to solve the

incompressible gas-phase equations and the Lagrangian particle equations. The simulations are performed for two volume grids with 0.5 [2] and 15 million tetrahedral grid cells using a moderate steady inhalation rate of 7.5 L/min over 2 s. 10,000 mono-disperse particles with a diameter of 10 µm are injected uniformly at the nostrils with the corresponding gas initial velocity over the first time step. The computations are performed on bwUniCluster using 256 processors with a time step of $10^{-5}$ s for both gas and particle phases to simulate a real process of two seconds. For the simulations with 0.5 and 15 million grid cells, the clock times are approximately 11 and 60 hours, respectively.

## 3 Results and Discussion

The study shows that 15 million grid cells resolve the flow characteristics such as vortices and gas velocity which are not captured by the coarser mesh. Figure 1 depicts the contour plots of the gas velocity at different coronal planes between the nasal valve (slice 1) and the nasopharynx (slice 8) for the finer grid. Figure 2 illustrates the right view of the particle deposition pattern. The particle concentration is high in the nasal valve, the nasopharynx, and in parts of the nasal septum.

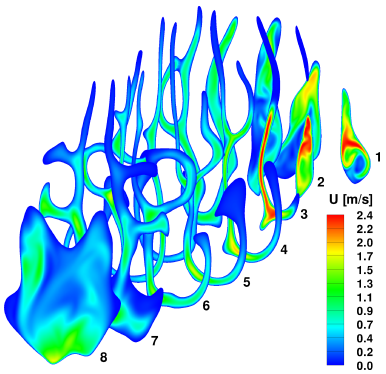


Figure 1: Gas velocity at different cross sections.

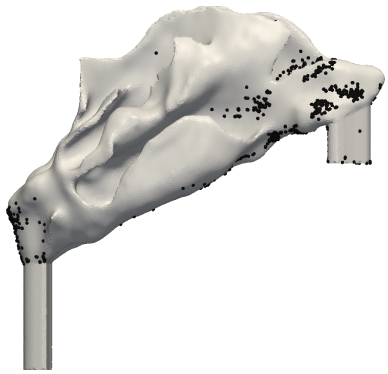

Figure 2: Particle deposition pattern.

## Acknowledgements

This project is supported by the German Research Foundation (DFG) through a research fellowship of the HGS MathComp. Moreover, high-performance computing time at the bwUniCluster which is funded by the ministry of science, research and arts of the state of Baden-Württemberg, Germany is gratefully acknowledged.

## References

[1] Cui, X.G.. "CFD Study of the Flow Field and Particle Dispersion and Deposition in the Upper Human Respiratory System" PhD Dissertation, Heidelberg University (2012).

[2] Farnoud, A., X.G. Cui, I. Baumann, and E. Gutheil. "Numerical Analysis of the Flow and Particle Pattern in the Human Nasal Cavity" 9th International Conference of Multiphase Flow, Florence, Italy (May 2016).

# (TD-)DFT-Supported Analysis of Triarylamine Vinyl Ruthenium Conjugates: Spin- and Charge-Delocalization

Christopher Hassenrück and Rainer F. Winter

Department of Chemistry, University of Konstanz

Density Functional (DFT) and Time-Dependent Theory (TD-DFT) quantum chemical calculations were performed in order to gain deeper insight into the electronic structures of alkenylruthenium-triarylamine conjugates in their various accessible oxidation states. These compounds were experimentally scrutinized in their neutral, mono- and dicationic states by infrared, UV/Vis/near-infrared and electron paramagnetic resonance (EPR) spectroscopy. Our combined experimental and computational data provide detailed information on the impact of the triarylamine substituents on the charge and spin density distributions in the mixed-valent radical cations.

## 1 Introduction

Electron-rich triarylamines exhibit similar (electronic) properties as alkenylruthenium compounds of the type [aryl-CH=CH-Ru(CO)Cl($PiPr_3$)$_2$], such as reversible one-electron oxidations at low potentials, electrochromism with intense NIR absorption in the oxidized state, and resolved hyperfine splittings in EPR experiments [1]. This raises the question as to how the charge and spin densities are (de)localized in oxidized forms of alkenylruthenium-triarylamine conjugates, in particular in their mixed-valent radical cations. In previous work [2, 1], the radical cation of the di(p-anisyl)amine derivative has been shown to exhibit full delocalization despite the presence of two chemically equivalent redox sites. We here explore the effect of introducing electron withdrawing substituents at the triarylamine entity.

## 2 Computational Method and Comparison to experimental data

The structures of the neutral complexes and their mono- and dioxidized forms were DFT-optimized with the Gaussian09 [3] program using the PBE1PBE basis sets (6-31G(d), Ru: MWB28) [4], pseudo-potentials and the polarizable continuum model (PCM) [5] to account for solvation effects. Calculated IR data for the neutral (blue) and the mono-oxidized states (red) of the complexes, using the charge-sensitive CO stretch of the ruthenium-bonded carbonyl

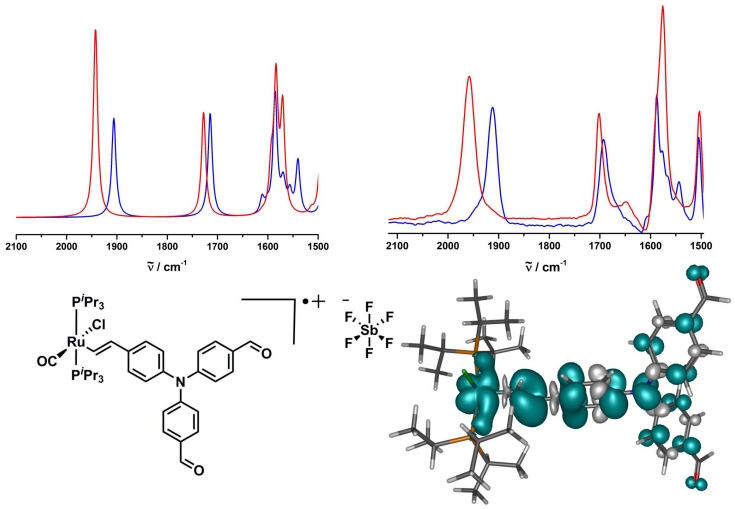


Figure 1: Comparison between exp. and calc. IR spectra (top), calculated spin density (bottom).

ligand and the amine bonded formyl groups, were compared with experimental data and display good levels of agreement, which confirms computational reliability (Figure 1).

DFT calculations also provide insight into spin density distributions in the different oxidized states (green and white colors). Computational data compare well with the experimentally observed EPR hyperfine splitting constants, which were extracted by simulation with the MATLAB Easyspin program suite. TD-DFT calculations provide insight into the underlying electronic transitions observed in the vis/NIR. Introducing electron withdrawing substituents has the consequence of changing the electronic structures of the radical cations from fully to partially delocalized with higher contributions from the alkenyl ruthenium moiety.

## 3 Conclusions

Calculated IR, EPR and UV/vis/NIR data on neutral and oxidized alkenylruthenium triarylamine conjugates agree well with experimental results. In particular, they show how electron-withdrawing substituents at the triarylamine site shift the charge and spin density of the associated radical cations onto the alkenylruthenium site. This allows us to study the spectroscopic consequences of tuning the radical cations from fully to partially delocalized mixed-valent systems.

## Acknowledgements

This work was financially supported by the ”Deutsche Forschungsgemeinschaft” (grant WI1262/13-1). We also thank the bwHPC facilities for providing access to their computing clusters.

## References

[1] Polit, W.; Mücke, P.; Wuttke, E.; Exner, T.; Winter, R. F., Organometallics 2013, 32, 5461-5472.

[2] Polit, W.; Exner, T.; Wuttke, E.; Winter, R. F., BioInorganic Reaction Mechanisms 2012, 8 (3-4), 85-105.

[3] Frisch, M. J.; Trucks, G. W.; Schlegel, H. B.; Scuseria, G. E.; Robb, M. A.; Cheeseman, J. R.; Scalmani, G.; Barone, V.; Mennucci, B.; Petersson, G. A.; Nakatsuji, H.; Caricato, M.; Li, X.; Hratchian, H. P.; Izmaylov, A. F.; Bloino, J.; Zheng, G.; Sonnenberg, J. L.; Hada, M.; Ehara, M.; Toyota, K.; Fukuda, R.; Hasegawa, J.; Ishida, M.; Nakajima, T.; Honda, Y.; Kitao, O.; Nakai, H.; Vreven, T.; Montgomery Jr., J. A.; Peralta, J. E.; Ogliaro, F.; Bearpark, M. J.; Heyd, J.; Brothers, E. N.; Kudin, K. N.; Staroverov, V. N.; Kobayashi, R.; Normand, J.; Raghavachari, K.; Rendell, A. P.; Burant, J. C.; Iyengar, S. S.; Tomasi, J.; Cossi, M.; Rega, N.; Millam, N. J.; Klene, M.; Knox, J. E.; Cross, J. B.; Bakken, V.; Adamo, C.; Jaramillo, J.; Gomperts, R.; Stratmann, R. E.; Yazyev, O.; Austin, A. J.; Cammi, R.; Pomelli, C.; Ochterski, J. W.; Martin, R. L.; Morokuma, K.; Zakrzewski, V. G.; Voth, G. A.; Salvador, P.; Dannenberg, J. J.; Dapprich, S.; Daniels, A. D.; Farkas, Ö.; Foresman, J. B.; Ortiz, J. V.; Cioslowski, J.; Fox, D. J.; Gaussian, Inc.: Wallingford, CT, USA, 2009.

[4] Andrae, D.; Haeussermann, U.; Dolg, M.; Stoll, H.; Preuss, H., Theor. Chim. Acta 1990, 77, 123-141.

[5] Cossi, M.; Rega, N.; Scalmani, G.; Barone, V., J. Comput. Chem. 2003, 24, 669-681.

# Bioinformatics and Astrophysics Cluster (BinAC)

Jens Krüger[1], Volker Lutz[1], Felix Bartusch[1], Werner Dilling[1], Anna Gorska[2], Christoph Schäfer[3], and Thomas Walter[1]

[1]Zentrum für Datenverarbeitung, Eberhard Karls Universität Tübingen
[2]Algorithms in Bioinformatics, Eberhard Karls Universität Tübingen
[3]Computational Physics, Institut für Astronomie und Astrophysik, Eberhard Karls Universität Tübingen

BinAC provides central high performance computing capacities for bioinformaticians and astrophysicists from the state of Baden-Württemberg. The bwForCluster BinAC is part of the implementation concept for scientific computing for the universities in Baden-Württemberg. Community specific support is offered through the bwHPC-C5 project.

## 1 Introduction

The bwForCluster BinAC offers cutting edge computing capabilities for users from the scientific domains of bioinformatics, astrophysics and related fields [1]. In both domains, scientific challenges are addressed through highly demanding computational approaches. As thus, the need for efficient and highly performant compute resources was immanent during the procurement phase for BinAC. Anyhow, the precise requirements from individual user groups dealing with particular use cases led to a broad spectrum of desired characteristics.

## 2 Resources and Architecture

Maximum performance on single cores, low latency network connections for improved scaling and the most recent GPU technology were the most prominent requests. All of BinAC's 300 individual nodes have a common base configuration. Each node holds two Intel Xeon E5-2680v4 (Broadwell) making a total of 28 cores available on each node. Aggregated over all 11,184 cores this leads to a nominal peak performance of more than 534 Tera-Flop/s, which put BinAC briefly on the TOP500 list of the world fastest supercomputers [2]. Additionally, each node provides 128 GB

DDR4-RAM of memory and a 256 GB local SSD harddisk. Also, 60 nodes of BinAC are equipped with two Nvidia Tesla K80 cards each. As each of these GPU accelerators has two Kepler GK210 Chips a total of 4 GPUs are available on each of the GPU nodes. Furthermore, to cope with high memory jobs, four SMP nodes with 40 cores each were equipped with 1 TB DDR4-RAM of memory. In order to provide interactive visualization capabilities of simulation data four dedicated nodes are available. They are equipped with NVIDIA Quatro M4000 graphic cards.

As depicted in Figure 1, all compute nodes are part of a low-latency high-bandwidth FDR Infiniband fabric and connected with the outside world through a 10 GBit/s uplink. The global workspace file system is based on the scalable parallel file system BeeGFS providing up to 720 TB raw storage space.

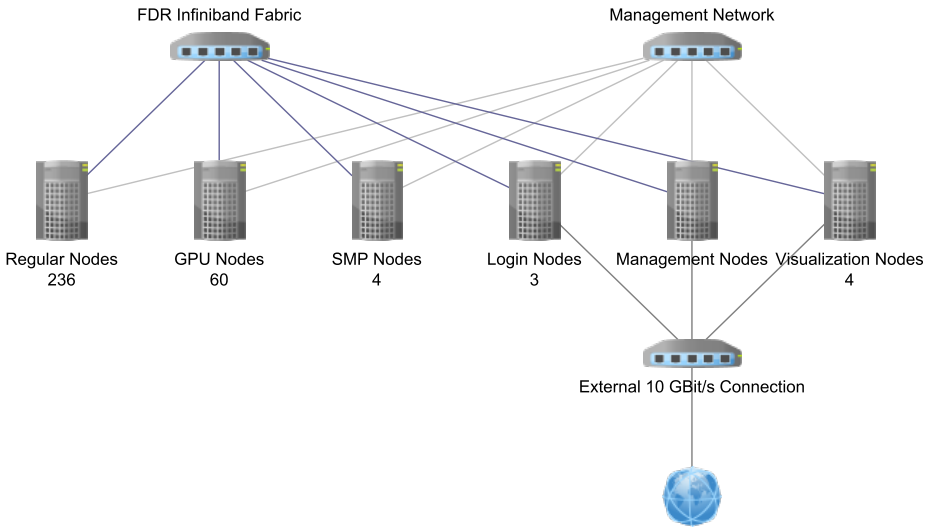


Figure 1: Architecture overview of the BinAC Cluster environment. All nodes are part of a low-latency high-bandwidth FDR Infiniband fabric and connected to the outside world through a 10 GBit/s connection.

## 3 Application Show Cases

The following examples illustrate the effectiveness of BinAC to address current scientific questions from different fields.

A classical approach for the metagenomic analysis of the human gut microbiome is to compare reads against the chosen database and then analyze the counts of reads assigned to the certain taxa [3]. In the case of phages this approach is not feasible since there are not enough known phage genomes to compare against. Therefore, one first needs to assemble the reads to be able to analyze long stretches of the phage genomes instead of the short reads. Assembly, especially of big datasets, is computationally expensive. For the case at hand, the sequencing reads were pulled together, resulting in two datasets, one per participant, comprising 134 million and 110 million reads. The assembly program Ray was run on 112 CPUs on BinAC cluster, 13 times (different k-mer size) for each participant (see Table 1). The authors of Ray have tested it on a

| k-mer | A | B | k-mer | A | B |
|---|---|---|---|---|---|
| 19 | 2h 24m 3s | 3h 34m 59s | 33 | 2h 19m 34s | 4h 9m 3s |
| 21 | 2h 7m 27s | 3h 44m 35s | 35 | 2h 21m 6s | 4h 8m 24s |
| 23 | 2h 8m 31s | 4h 16m 23s | 37 | 2h 19m 15s | 3h 22m 32s |
| 25 | 3h 40m 12s | 3h 23m 53s | 39 | 2h 18m 35s | 4h 9m 39s |
| 27 | 3h 40m 31s | 4h 9m 8s | 55 | 2h 20m 4s | 4h 7m 54s |
| 29 | 2h 17m 17s | 4h 7m 52s | 77 | 4h 3m 15s | 3h 21m 34s |
| 31 | 2h 17m 41s | 3h 22m 16s | | | |

Table 1: Runtimes for the assembly of reads using Ray.

roughly four times bigger dataset. Using 128 cores it took them 13 hours to complete [4]. But the datasets are not directly comparable, since they used a simulated metagenome dataset with entire bacterial genomes, therefore the resulting contigs were much larger.

Ray is not the only program applicable for this use case. Thanks to BinAC it is possible to construct a pipeline comprising several steps, (1) Ray (assembly), (2) Bowtie2 (read mapping back to the assembled scaffolds), (3) Blast (comparison to the Viral and CARD databases), (4) Prodigal (gene prediction) and (5) Aragorn (tRNA gene prediction), and run it in one go, with various parameters. Such an approach would be impossible using other resources, not only because of the CPU and memory usage, but also because it would not be possible to occupy a lab server completely for longer periods of time.

Gromacs is a molecular dynamics package intended for the simulation of biochemical molecules like proteins, lipids and nucleic acids [5]. It supports CUDA-based GPU acceleration. Benchmarking the alcohol dehydrogenase protein (ADH) system with 130,000 atoms using a rectangular box and PME (http://www.gromacs.org/GPU_acceleration) already results in a simulation speed of 23 ns/day just using the 28 CPU cores available on a single compute node. When adding one GPU the speed is amplified by factor 2 (47 ns/day) without any further optimization. When simulating larger systems the effect is even more pronounced. A membrane system with two ion channels consisting of 430,000 atoms (rectangular box, PME) can be simulated with 6.0 ns/day just using CPU cores. Using all four GPUs available a speed of 24.3 ns/day can be reached which corresponds to a speedup of 4. Hence, the GPU nodes of BinAC enable researchers to simulate their large biomolecular systems on biological relevant time scales which had been much more challenging before.

The smooth particle hydrodynamics (SPH) equations allow to model gas, liquids and elastic, and plastic solid bodies. The approach is used for the simulation of the collision between Ceres-sized objects. Schäfer et. al. implemented a GPU version of this method also considering self-gravity of the simulated objects [6]. Comparing the runtimes of the new implementation to an existing OpenMP version they can report a speedup of at least two orders of magnitude for all relevant substeps of the SPH method. Given that the runtime evaluation was 'only' carried out on a single Nvidia GTX Titan even larger speedup and further parallelization options arise from the four K80 GPU cores available on each of BinAC's GPU nodes.

## 4 Access and Support

Generally all academic users who have some kind of affiliation with a research institution within the state of Baden-Württemberg are eligible to apply for access to BinAC. In order to provide optimal assistance to researchers looking for high performance compute resources, a lightweight application system was introduced by the bwHPC initiative (https://www.bwhpc-c5.de/zas_info_bwforcluster.php). The researchers are asked to provide a short description of the planned research, desired compute resources and software environments. This information serves as basis for an appropriate resource allocation so the task can be distributed to the compute center which is best suited to handle it. The bwHPC-C5 partners, including the team at the compute center of the University of Tübingen, provide assistance and consulting for all questions related to the usage of BinAC (hpcmaster@uni-tuebingen.de). Some scientific communities might require more effort to enable an appropriate research environment, like installing special software packages or enabling access to external data sources. For this purpose the bwHPC-C5 partners offer the opportunity to form Tigerteams offering extended support through experts from the associated compute centers and experts from the affected scientific fields.

## 5 User Perspective

The queues on BinAC are filling up fast. Users are encouraged to apply quickly for an appropriate entitlement. The highly motivated HPC team at the ZDV is supporting users from the related communities, trying to provide the necessary software environment, stable operation of the underlying hardware and consequently a positive user experience. Recent additions to the module environment used for handling the simulation software covers machine learning applications such as Tensorflow and Caffe.

## 6 Conclusions

BinAC offers state of the art compute capabilities accompanied by result oriented support through the bwHPC-C5 project. A powerful research tool is offered to the users from the research areas of bioinformatics and astrophysics, enabling them to carry out their cutting edge research.

## Acknowledgments

The bwHPC-C5 project has been funded by the Ministry of Science, Research and the Arts of the state of Baden-Württemberg, Germany. The Universities of Freiburg, Heidelberg, Hohenheim, Konstanz, Mannheim, Stuttgart, Tübingen and Ulm, the Karlsruhe Institute of Technology, as well as the Universities of Applied Sciences in Stuttgart and Esslingen are the partners carrying out the project.

## References

[1] H. Hartenstein, T. Walter, and P. Castellaz. “Aktuelle Umsetzungskonzepte der Universitäten des Landes Baden-Württemberg für Hochleistungsrechnen und datenintensive Dien-

ste." Praxis der Informationsverarbeitung und Kommunikation, Band 36, Heft 2 (2013): 99-108.

[2] https://www.top500.org/system/178843 (accessed 2017-02-02)

[3] M. Willmann, M. El-Hadidi, D. H. Huson, M., Schütz, C. Weidenmaier, I. B. Autenrieth, and S. Peter. "Antibiotic selection pressure determination through sequence-based metagenomics." Antimicrobial Agents and Chemotherapy, 59(12) (2015): 7335-7345. http://doi.org/10.1128/AAC.01504-15

[4] S. Boisvert, F. Raymond, E. Godzaridis, F. Laviolette, and J. Corbeil. "Ray Meta: scalable de novo metagenome assembly and profiling." Genome Biology, 13(12), (2012) R122. http://doi.org/10.1186/gb-2012-13-12-r122

[5] M. J. Abraham, T. Murtolad, R. Schulz, S. Páll, J. C. Smith, Berk Hess, and E. Lindahl. "GROMACS: High performance molecular simulations through multi-level parallelism from laptops to supercomputers" SoftwareX, Volumes 1–2 (2015): 19–25.

[6] C. Schäfer, S. Riecker, T. I. Maindl, R. Speith, S. Scherrer, and W. Kley. "A smooth particle hydrodynamics code to model collisions between solid, self-gravitating objects" Astronomy and Astrophysics 590, A19 (2016).

# Research Data Management and Virtual Research Environments. Presentation of new collaborating E-Science Projects

Volodymyr Kushnarenko[1], Petra Enderle[2], Stefan Kombrink[2], Franziska Ackermann[2], Uli Hahn[2], Christopher B. Hauser[1], Jörg Domaschka[1], Pia Schmücker[2], and Stefan Wesner[1,2]

[1]Institute of Information Resource Management (IOMI), Ulm University
[2]Communication and Information Centre (kiz), Ulm University

One of the challenges for scientists today is how to handle research data in a way that makes their research reproducible and transparent. This includes storing data, tools and environments, as well as publishing them and making them available for re-use, so experiments can be reproduced under similar conditions at a later date. The four E-Science projects CiTAR, SARA, RePlay-DH and ViCE of Ulm University and its partners aim to provide answers to support scientists in the areas of Research Data Management and Virtual Research Environments.

## 1 CiTAR

The CiTAR project (Citing and Archiving Research) develops a scientific service for the long-term archiving of Virtual Research Environments. The service focuses on the reproducibility of research data, which scientific publications rely on. Archiving Virtual Research Environments allows long-term traceability of scientific experiments after their original realization. For users in the field of High Performance Computing (HPC) the project will deliver new tools which can be easily implemented into well-established scientific workflows. With these tools data centres extend their service provision and will be able to provide a long-term citable and reproducible availability of research data, tools and scientific methods. This new and interdisciplinary service is developed by three of the four bwForCluster operators of Baden-Wuerttemberg and operates in the field of scientific High Performance Computing.

**Web page:** https://www.alwr-bw.de/kooperationen/bwzwm

## 2 SARA

The SARA project (Software Archiving of Research Artefacts) aims to develop a new scientific service to make research data as well as software tools generating the data available in the

long-term. In the discipline of biology measured data is captured and processed with the aid of computers. In electrical engineering and information technology, source code of software is generated numerously and must be stored in its different versions. The scientific service planned in the project reflects the workflows of the scientists and allows them to record their intermediate results already during the research process. Thereby scientists will be able to access immediately the process history and the versions of the research tools, which are often modified by the scientists themselves. The new service aims to make the gained research data and the different versions of the involved software tools also comprehensible for later scientific research. The service, in the long term, is intended to be available for other scientific disciplines as well.

**Web page:** https://www.alwr-bw.de/kooperationen/bwfdm-soft

## 3 RePlay-DH

The RePlay-DH project realizes a platform and surrounding services in Research Data Management for the scientific community of the Digital Humanities. Scientists of the Digital Humanities are supported in their scientific work with scripts by the RePlay-DH platform in the publication and archiving process to provide citable long-term research data. This enables the re-use of research data and the easy tracking of changes ("Replay") with no extra effort for scientists such as learning of complex version control systems. The RePlay-DH graphic user interface operates on the surface of these systems, simplifies the application and provides completeness and compliance. Metadata, which is important for the re-use of research data, will be archived during the scientific process. The platform can be used by different scientific disciplines as an open source instrument for long-term available research data.

**Web page:** https://www.alwr-bw.de/kooperationen/replay-dh

## 4 ViCE

The ViCE project (Virtual Open Science Collaboration Environment) supports scientists in various disciplines in providing and adapting Virtual Research Environments. As an important basic infrastructure a comprehensive collaboration platform is built, which provides a long-term re-use of research results especially with regard to new scientific issues. Scientists are supported in the documentation of various versions of their Virtual Research Environments and research data and are able to share them with others during the origination process. The platform is provided exemplarily for the communities of English Studies, Business Information Systems, Life Sciences and Particle Physics by the infrastructure partners Freiburg, Tübingen and Mannheim (HPC, bwCloud, bwLehrpool). The scientific service will be also available for other disciplines and can be deployed in teaching and in the future integration of junior scientists.

**Web page:** https://www.alwr-bw.de/kooperationen/vice

## Acknowledgement

The authors would like to thank all collaboration partners from Ulm University, University of Freiburg, University of Tübingen, University of Mannheim, University of Konstanz, University of Stuttgart and Karlsruhe Institute of Technology for their support and cooperation, and the Ministry of Science, Research and the Arts of the state of Baden-Wuerttemberg, Germany, for the funding of the projects involved in this publication.

# Accretion outbursts in massive star formation

D. M.-A. Meyer[1], E. I. Vorobyov[2,3], R. Kuiper[1], and W. Kley[1]

[1]Institut f. Astronomie und Astrophysik, Universität Tübingen, Germany
[2]Department of Astrophysics, The University of Vienna, Austria
[3]Southern Federal University, Rostov-on-Don, Russia

Using the HPC resources of the state of Baden-Württemberg, we modelled for the first time the luminous burst from a young massive star by accretion of material from its close environment. We found that the surroundings of young massive stars are shaped as a clumpy disk whose fragments provoke outbursts once they fall onto the protostar and concluded that similar strong luminous events observed in high-mass star forming regions may be a signature of the presence of such disks.

## 1 An FU-Orionis-like burst from a high-mass protostar

Accretion-driven luminosity outbursts are a vivid manifestation of variable mass accretion onto protostars. They are known as the so-called FU Orionis phenomenon in the context of low-mass protostars (Vorobyov & Basu 2006). More recently, this process has been found in models of primordial star formation (Hosokawa et al. 2016). In Meyer et al. (2017), using numerical radiation hydrodynamics simulations of a collapsing 100 $M_\odot$ pre-stellar cores rotating with a ratio of kinetic by gravitational energy of 4% that produces a central massive protostar (cf. Kuiper et al. 2011), we stress that present-day forming massive stars also experience variable accretion (Fig. 1) and show that this process is accompanied by luminous outbursts induced by the episodic accretion of gaseous clumps migrating from the circumstellar disk onto the protostar (Fig. 2).

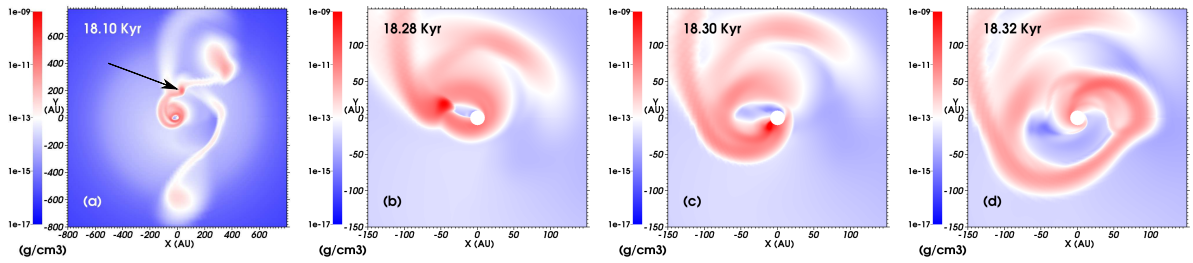


Figure 1: Midplane density in the center of the computational domain around the time of the outburst. (a) The region when a clump forms in a spiral arm. Panel (b-c) display zooms to illustrate the migration and accretion of a part of the clump.

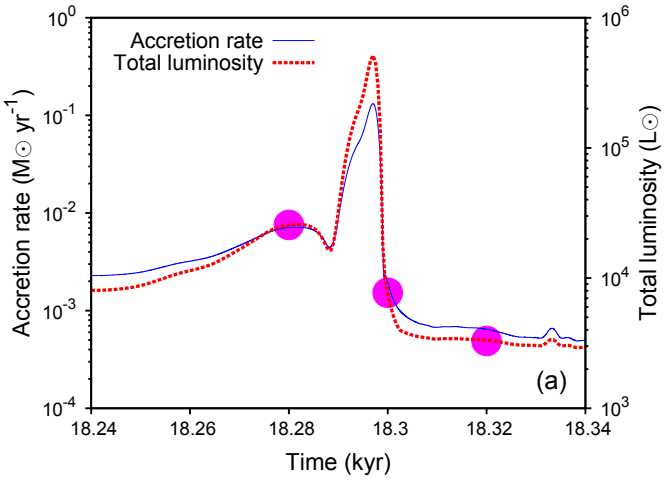


Figure 2: Accretion rate onto the protostar (in $M_\odot\,yr^{-1}$) and total luminosity of the protostar (in $L_\odot$) during the burst. Magenta dots mark the times of Fig. 1b-d.

## 2 Observational implications

We conjecture that luminous flares from regions hosting forming high-mass star may be an observational implication of the fragmentation of their accretion disks, i.e. that those flares constitute a possible tracer of the fragmentation of their accretion disks. This may apply to the young star S255IR-NIRS3 that has recently been associated to a 6.7 GHz methanol maser outburst (Fujisawa et al. 2015, Stecklum et al. 2016) but also to the other regions of high-mass star formation from which originated similar flares (Menten et al. 1991) and which are showing evidences of accretion flow associated to massive protostars, see e.g. in W3(OH), W51 and W75.

## Acknowledgements

This study was conducted within the Emmy Noether research group on "Accretion Flows and Feedback in Realistic Models of Massive Star Formation" funded by the German Research Foundation under grant no. KU 2849/3-1. E.I.V. acknowledges support from the Austrian Science Fund (FWF) under research grant I2549-N27 and RFBR grant 14-02-00719.

## References

[1] Fujisawa K., Yonekura Y., Sugiyama K., et al., 2015, ATel, 8286

[2] Hosokawa T., Hirano S., Kuiper R., et al., 2016, ApJ, 824, 119

[3] Kuiper R., Klahr H., Beuther H., Henning T., 2011, ApJ, 732

[4] Menten K. M., 1991, ApJ, 380, L75

[5] Meyer D. M.-A., Vorobyov E. I., Kuiper R., Kley, W., 2017, MNRAS 464, L90–L94

[6] Stecklum B., Caratti o Garatti A., Cardenas M. C., et al., 2016, ATel, 8732

[7] Vorobyov E. I., Basu S., 2006, ApJ, 650, 956

# *Drosophila melanogaster* linker histone (dH1) binding to the nucleosome

Mehmet Ali Öztürk[1,2], Vlad Cojocaru[3,4], and Rebecca C. Wade[1,5,6]

[1]Molecular and Cellular Modeling Group, Heidelberg Institute for Theoretical Studies (HITS), Heidelberg, Germany
[2]The Hartmut Hoffmann-Berling International Graduate School of Molecular and Cellular Biology (HBIGS), Heidelberg University, Heidelberg, Germany
[3]Computational Structural Biology Laboratory, Department of Cellular and Developmental Biology, Max Planck Institute for Molecular Biomedicine, Münster, Germany
[4]Center for Multiscale Theory and Computation, Westfälische Wilhelms University, Münster, Germany
[5]Center for Molecular Biology (ZMBH), DKFZ-ZMBH Alliance, Heidelberg University, Heidelberg, Germany
[6]Interdisciplinary Center for Scientific Computing (IWR), Heidelberg, Germany

Linker histone proteins are key players in the structuring of chromatin for the packing of DNA in eukaryotic cells. The common fruit fly (*Drosophila melanogaster*) has a single isoform of the linker histone (dH1). It is thus a useful model organism to investigate the effects of the linker histone (LH) on nucleosome compaction and the configuration of the chromatosome, the complex formed by binding of a LH to a nucleosome. The structural and mechanistic determinants of how LH proteins bind to nucleosomes are not fully understood. Here, we apply Brownian dynamics simulations to compare the binding of dH1 and the chicken (*Gallus gallus*) LH H5 isoform to identify residues in the LH that critically affect the configuration of the chromatosome.

## 1 Introduction

In eukaryotic cells, DNA is packed by formation of nucleosomes consisting by stretches of $\sim 146$ bp of DNA wrapped around a core histone protein octamer. Compaction and various cellular

processes, including gene expression are regulated by the binding of linker histone (LH) proteins to nucleosomes, forming chromatosomes. While many organisms have more than one LH isoform, the model organism *Drosophila melanogaster* has a single H1 isoform (dH1) which facilitates experimental studies on the phenotypic effects of dH1. LHs are $\sim$ 200 amino acid (aa) proteins composed of a short flexible N-terminal tail ($\sim$ 25 aa), a globular DNA binding domain ($\sim$ 80 aa), and a long C-terminal domain ($\sim$ 100 aa). Previous experiments have shown that nucleosome binding is primarily determined by the LH globular domain and removal of the N- and C-domains affects the affinity of the binding but not the binding site on the nucleosome. In this report, we investigated the effect of single mutations on globular domain dH1 - nucleosome binding by means of Brownian dynamics simulations. The results are compared with the nucleosome binding configurations of the globular domain of a chicken (*Gallus gallus*) H5 mutant isoform.

## 2 Methods

8 different structures of a nucleosome, previously generated by molecular dynamics simulation and representing a range of linker DNA (L-DNA) conformations, were used for Brownian dynamics simulation-based docking of dH1 and H5 globular domains to the nucleosome [1]. The structures of the globular domains of dH1 (kindly provided by Dr. Yawen Bai, [2]) and *Gallus gallus* H5 (Chain B PDB ID: 1hst, [3]) shown in Figure 1 were used. Docking was performed as described in Öztürk et al. [1] for the wild-type (WT) globular domains and for the single point mutants shown in Figure 1. The mutations are at sites that are important for DNA binding or have very different physiochemical properties in the two proteins.

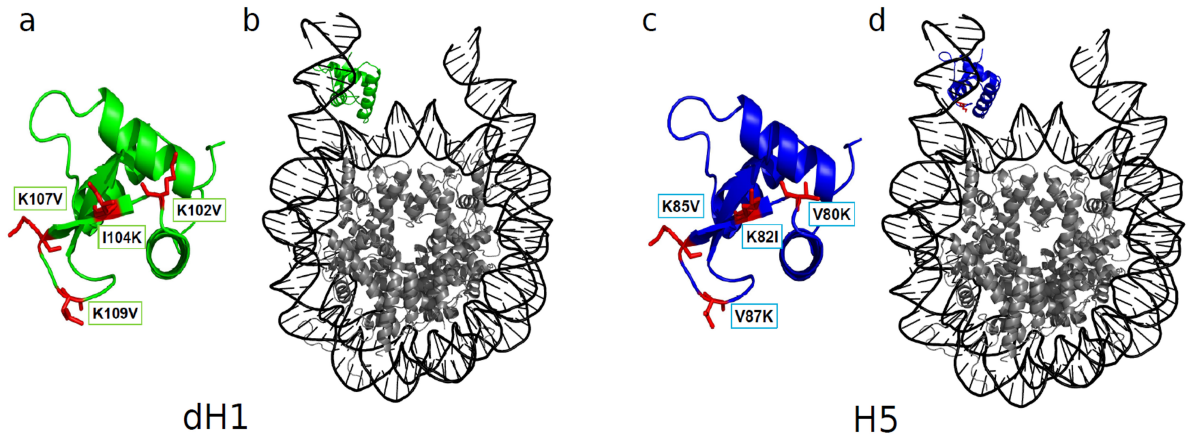


Figure 1: Structures of the globular domains of the linker histone proteins, dH1(a-green) and H5 (c-blue), and the locations of the mutations (red) evaluated by computational docking to a nucleosome. Selected Brownian dynamics docking simulation results for WT dH1(b) and V87K mutant of H5 (d) bound to nucleosome (gray) in off-dyad form.

## 3 Results

Experiments have revealed structures of the chromatosome with gH5 bound in an on-dyad configuration and dH1 bound in an off-dyad configuration. Docking of the WT and mutant

variants of the globular domains of dH1 and H5 to the nucleosome revealed that, depending on the extent of opening of the linker-DNA arms, a range of configurations of the chromatosome is possible. Of the single-point mutations, K107V and I104K resulted in the most significant changes in configurations compared to WT dH1, whereas K82I and V87K had the greatest effects compared to WT H5. Interestingly, for a subset of nucleosome conformations, the V87K mutant of H5 docked in similar configurations to WT dH1.

## 4 Conclusions

Our Brownian dynamics simulations reveal that chromatosome configurations depend on the extent of opening of the linker DNA arms. Certain single residue mutations of dH1 and H5 can significantly change the binding mode. These results may help to explain the evolutionary emergence of various LH isoforms having different cellular functions and provide a basis for mutagenesis experiments to understanding the mechanisms of chromatin packing.

## Acknowledgements

We gratefully acknowledge the support of the Klaus Tschira Foundation and the State of Baden-Württemberg for provision of computing resources.

## References

[1] Öztürk M. A., Pachov G. V., Wade R. C., Cojocaru V. “Conformational selection and dynamic adaptation upon linker histone binding to the nucleosome” Nucl. Acids Res. 44 (2016) 414: 6599-6613.

[2] Zhou B.R., Feng H., Kato H., Dail L., Yang Y., Zhou Y., Bai Y. “Structural insights into the histone H1-nucleosome complex” Proc. Natl. Acad. Sci. (2013) 110:19390-5.

[3] Ramakrishnan, V., Finch, J.T., Graziano, V., Lee, P.L., Sweet, R.M. “Crystal structure of globular domain of histone H5 and its implications for nucleosome Binding” Nature (1993) 362: 219-223.

# bwForCluster MLS&WISO

Sabine Richling[1], Martin Baumann[1], Stefan Friedel[2], and Heinz Kredel[3]

[1]Computing Centre, Heidelberg University
[2]Interdisciplinary Center for Scientific Computing, Heidelberg University
[3]Computing Centre, University of Mannheim

The bwForCluster MLS&WISO provides high performance compute resources for the Universities in Baden-Württemberg with focus on the research fields Molecular Life Science (MLS), Economics and Social Sciences (WISO) as well as on the development of methods for scientific computing in general. The different requirements of the communities are met by a distributed cluster concept with various node types. The cluster is connected to the scientific data storage SDS@hd with high bandwidth which facilitates the data management of complex and data-intensive workflows.

## 1 Introduction

The bwForCluster MLS&WISO is an entry level (Tier 3) system within the state of Baden-Württemberg's bwHPC concept for high performance computing [1]. The system is financed by the Ministry of Science, Research, and the Arts Baden-Württemberg (MKW) and the German Research Foundation (DFG) as well as the Interdisciplinary Center for Scientific Computing (IWR) of Heidelberg University. The bwForCluster MLS&WISO is a joint project of the Computing Centre (URZ) and the Interdisciplinary Center for Scientific Computing (IWR) of Heidelberg University and the Computing Centre of the University of Mannheim (RUM). The system consists of two separate clusters: The development part (Linpack performance 222.7 TFLOP/sec) and the production part (Linpack performance 291.3 TFLOP/sec). In 2015 both parts were present in the TOP500 list of the most powerful computer systems in the world [2].

## 2 Development Part

The development part of bwForCluster MLS&WISO (Fig. 1) is a high performance compute cluster with about 400 identical nodes and a fully non-blocking Infiniband network of speed QDR (40 GBit/sec) [3]. This cluster part is designed for compute activities related to method development in all research fields. The hardware is located in Heidelberg. The system is operated by the IWR. The development part provides a flexible service with short response times for massively parallel jobs with high scalability. The operating concept is such that it is possible to use the whole machine for a single job.

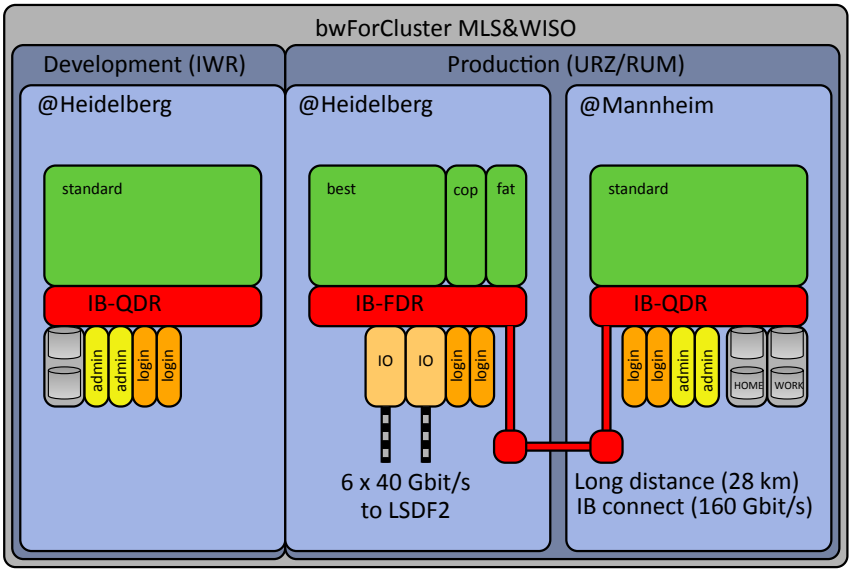


Figure 1: bwForCluster MLS&WISO: Development part and production part.

## 3 Production Part

The production part of bwForCluster MLS&WISO (Fig. 1) is a high performance compute cluster with about 700 nodes. The hardware is located partly in Heidelberg and partly in Mannheim. Both sites are interconnected by a long-distance Infiniband link effectively forming one single system which is jointly operated by URZ and RUM. The production part is intended for compute activities in the research fields Molecular Life Science (MLS), Economics, and Social Sciences (WISO). It provides a stable service for a large throughput of production jobs using up to 128 nodes.

All components of the cluster are connected to a high-speed Infiniband fabric for MPI communication and storage access. The Infiniband fabric in Mannheim is of speed QDR (40 GBit/sec) and fully non-blocking across all 'standard' nodes. The Infiniband fabric in Heidelberg is of speed FDR (56 Gbit/sec) and also fully non-blocking across all 'best', 'fat', and 'coprocessor' nodes. The different node types allow a high diversity of jobs: 'best' nodes have more memory and faster CPUs than 'standard' nodes, 'fat' nodes are equipped with a large amount of memory (1 TB and 1.5 TB), and 'coprocessor' nodes are equipped with GPUs (Nvidia K80) or MICs (Xeon Phi). A complete description of the node types is available in the bwHPC Wiki [4]. Two separate storage systems provide storage space for home directories (36 TB) and for workspaces (384 TB). Both storage systems are equipped with the parallel cluster file system BeeGFS [5].

## 4 Long-distance Infiniband Link

The long-distance Infiniband link permits the operation of the production part as one single cluster. Fig. 2 shows the interconnection in more detail. The 28 km distance between the cluster sites in Heidelberg and Mannheim is linked via a 10 GE optical fibre. Both ends are equipped with a DWDM multiplexer allowing the simultaneous transmission of different colours over one fibre. We use 16 colours to serve the two Mellanox MetroX TX6240 LongHaul appliances at each site which in turn are connected with 4 × 40 GBit/sec links to the Infiniband fabric. The total

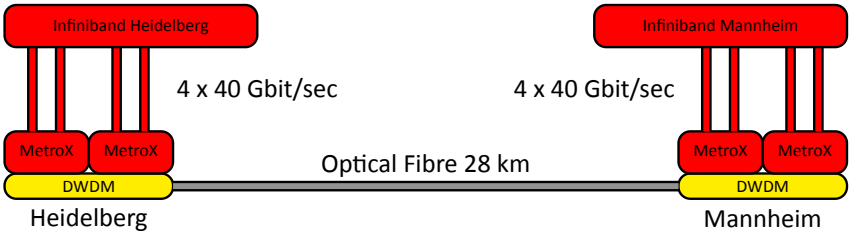


Figure 2: bwForCluster MLS&WISO: Long-distance Infiniband interconnect.

bandwidth of the long-distance interconnection is 160 GBit/sec. Latency is only slightly above the hard limit set by the speed of light. The bandwidth is broad enough to allow parallel accesses to the storage systems. For production operation, it is not allowed to use nodes from both sides for a single job, because in general only parallel jobs with low communication requirements run with sufficient performance across the long-distance link. One advantage of a two-site cluster is a higher availability. Because of the high power consumption, the compute nodes are not connected to the uninterruptible power supply. In the case of power failures or cooling problems at one site, the cluster keeps running with the compute nodes of the other site.

## 5 Access to SDS@hd

SDS@hd is a Scientific Data Storage for data with frequent access ('hot data') [6]. The data is stored on the second generation hardware of the Large Scale Data Facility (LSDF2) which is financed by MWK and DFG and is part of the state of Baden-Württemberg's bwDATA concept for data-intensive services [1]. The service is open to all scientist at Baden-Württemberg's Universities. Supported access protocols are NFSv4 with Kerberos, SMB 2.x/3.x as well as SSHFS.

Access to SDS@hd from all bwHPC clusters is in preparation and in case of the bwForCluster MLS&WISO already established for production use. A special feature of bwForCluster MLS&WISO is the direct and high-bandwidth connection to SDS@hd which is possible due to the physical proximity of the two systems. This allows the generation of data, e.g. with a microscope in a lab, the data analysis on the cluster, and pre- and postprocessing at the office PC of a scientist without keeping several copies of the same data and without annoying

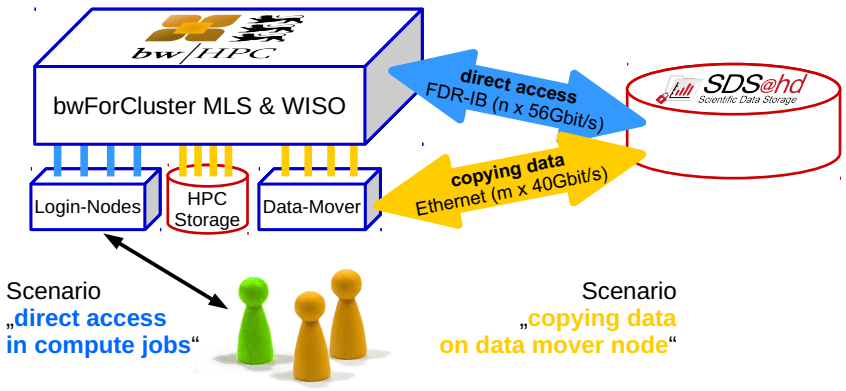


Figure 3: bwForCluster MLS&WISO: Access to SDS@hd.

manual data synchronization. For this scenario SDS@hd is mounted at the compute nodes via Infiniband (blue arrows in Fig. 3) for direct access to SDS@hd in compute jobs. If the workflow or the access pattern benefit from the parallel cluster file system, a fast data transfer via data mover nodes (IO nodes) from SDS@hd to the cluster file system is possible (yellow arrows in Fig. 3). SDS@hd is mounted at the data mover nodes via separate broad band Ethernet links to prevent copy processes from interfering with SDS@hd accesses in running jobs. Kerberos ticket management is done on the data mover nodes and is supported by e-mail notification to remind of expiring tickets.

## 6 bwHPC competence center MLS&WISO

User support for the bwForCluster MLS&WISO is provided by the bwHPC competence center MLS&WISO as part of the project bwHPC-C5 [7]. General support activities include assistance in access and usage of the cluster as well as in providing software for the user communities. The bwHPC competence center MLS&WISO organizes regularly the user meeting bwForTreff and an introductory HPC workshop. It also hosts workshops of external lecturers on specific software or method related topics.

In the research fields economics and social sciences many user groups apply statistical methods using software packages like R, Stata, and Matlab. The research projects deal for example with asset pricing, corporate taxation, political reforms, empirical accounting, household models, risk management, structural changes in agriculture, and energy system analysis. In social sciences data mining and language processing are fields with increasing compute demands. Here the competence center provides migration support and assists in the setup of workflows.

Scientists working in the field of molecular life science apply a broad spectrum of methods such as molecular dynamics, bioinformatics, bio-medical image processing and statistics as well as computational fluid dynamics (CFD). With the help of these methods research groups from various biological and medical institutes investigate for example structure formation processes in biological systems, folding and aggregation phenomena of proteins, membrane reorganization, evolution of vertebrate gene expression, molecular phylogenetics of birds, morphological plasticity and protein composition of neurons, biological images from fluorescent microscopy or cryo-electron microscopy, and the blood or air flow in human organs. The different node types of the cluster offer suitable hardware for the diverse methods. For example molecular dynamics and fluid dynamics jobs need many cores and benefit from the fast non-blocking Infiniband network. 'fat' nodes enable image processing to analyse very large datasets en bloc. 'coprocessor' nodes speed up the work, since more and more software packages provide GPU-enabled versions for example in molecular dynamics and image processing.

The growing number of users, high-level support teams, and community-specific software modules shows that the bwForCluster MLS&WISO has become an important tool for scientists in the fields of molecular life science, economics, and social sciences.

## Acknowledgements

The bwForCluster MLS&WISO is funded by the state of Baden-Württemberg through bwHPC, by the German Research Foundation (DFG) through grant INST 35/1134-1 FUGG, and by the IWR of Heidelberg University.

## References

[1] Hartenstein, H., T. Walter, and P. Castellaz. "Aktuelle Umsetzungskonzepte der Universitäten des Landes Baden-Württemberg für Hochleistungsrechnen und datenintensive Dienste." Praxis der Informationsverarbeitung und Kommunikation, Band 36, Heft 2 (2013): 99-108. http://dx.doi.org/10.1515/pik-2013-0007

[2] TOP500 Site: Heidelberg University and University of Mannheim. https://www.top500.org/site/50564

[3] bwHPC-Wiki: bwForCluster MLS&WISO Development. https://www.bwhpc-c5.de/wiki/index.php/BwForCluster_MLS&WISO_Development_Hardware

[4] bwHPC-Wiki: bwForCluster MLS&WISO Production. https://www.bwhpc-c5.de/wiki/index.php/BwForCluster_MLS&WISO_Production_Hardware

[5] BeeGFS – The Leading Parallel Cluster File System. https://www.beegfs.io/content

[6] SDS@hd – Scientific Data Storage. https://sds-hd.urz.uni-heidelberg.de

[7] bwHPC-C5: Coordinated Compute Cluster Competence Centers. http://www.bwhpc-c5.de

# Computational Methods to Describe the Magnetic Properties of SMM Systems

Asha Roberts and Peter Comba

Institute of Inorganic Chemistry and Interdisciplinary Center for Scientific Computing, Heidelberg University

Because the magnetic and electronic properties of SMMs are dictated by the ligand field, they are theoretically predictable. In order to elucidate the subtle effects of the ligand field on the magnetic properties, two mononuclear dysprosium(III) complexes have been investigated. The ligands employed are comprised of two bidentate donors (1-hydroxy-pyridine-2-one-1,2-HOPO) with a linking chain of various lengths [1]. Depending on the identity and length of the chain, a different geometry can be enforced. Preliminary calculations indicate that such geometrical changes significantly impact the magnetic properties, revealing high sensitivity of the ground and excited states.

## 1 Introduction

Single molecule magnets (SMMs) are a class of compounds that contain one or more magnetic centres (d- or f-block metals). The unique magnetic behaviour of such compounds, simply put, is the ability of each individual molecule to retain its own magnetic field. The challenge faced in this field is preventing magnetic relaxation and the various paths by which this relaxation can occur. Using computational methods it is possible to predict whether relaxation will occur and by which pathway. In this regard, there are three criteria that must be met. Firstly, the ion must be of Ising-type character, i.e. should be highly anisotropic ($g_x = g_y = 0$, $g_z = 20$) in order to prevent quantum tunnelling of magnetization (QTM). Secondly, there must be a large enough energy barrier between the different states to prevent thermal relaxation of magnetism. Thirdly, the magnetic axes of the states must be aligned in order to suppress Orbach relaxation.

## 2 Computational Methods

Complete active space self-consistent field (CASSCF) wave functions are generated using the restricted active space self-consistent field (RASSCF) module provided by the MOLCAS 8.0 package [2]. All atoms were described using the ANO-RCC-VDZP basis sets included in the MOLCAS package [3]. Because of lanthanide contraction, accurate results are achievable by restricting the active space to the nine electrons in the seven 4f orbitals. Furthermore, as no additional electron correlation is required, the CASSCF wave functions are used without further

perturbations. Spin-orbit coupling is introduced using the state interaction program RASSI (restricted active space state interaction) using 21 sextet, 50 doublet and 50 quartet states for the $f^9$ ion. The spin-orbit multiplets are then used by the SINGLE_ANISO program to calculate the relevant magnetic properties. The calculations were carried out using optimised structures, as published by Daumann *et al.* [1]. The ligands employed are presented in Figure 1. Depending on the length of the chain, a different geometry is enforced, and it is the effect of this change on the magnetic properties that is being investigated.

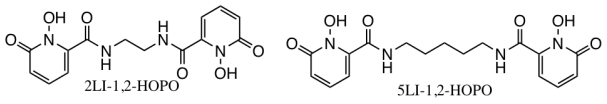


Figure 1: Ligands employed in this study.

## 3 Results

Both the 2LI and 5LI complexes show insufficient splitting of the $M_J$ states to prevent thermal relaxation of magnetisation (44 and 55 $cm^{-1}$, respectively). While the anisotropy of the 5LI complex ($g_z = 19.12$) would be sufficient to suppress QTM, the magnetic axes of the excited states are perpendicular to each other, allowing Orbach relaxation to occur. On the other hand, the 2LI complex appears to show little Ising-type character ($g_x = 1$, $g_y = 2$, $g_z = 16$) but the local magnetic axes are parallel.

## 4 Conclusions

While neither complex appears to have potential as an SMM, the results illustrate notable sensitivity of the ground and excited Kramers doublet states to changes in the ligand field. Despite the small ligand field of lanthanides, it is clear that it is of central importance for molecular magnetism.

## Acknowledgements

AR acknowledges the financial support provided by the Heidelberg Graduate School of Mathematical and Computational Methods of the Sciences (HGS MathComp).

## References

[1] Daumann, L. J. *et al.*, *Inorg. Chem.* **2016**, *55*(1), 114-124.

[2] B. O. Roos *et al.*, *Chem. Phys.* **1980**, *48*, 157.; F. Aquilante *et al.*, *J. Comput. Chem.* **2010**, *31*, 224.

[3] B. O. Roos *et al.*, *J. Phys. Chem. A* **2005**, *109*, 6575.

# Cost Optimization for Simulations in the Cloud

Oleksandr Shcherbakov[1], Kai Polsterer[1], and Volodymyr Svjatnyj[2]

[1]Heidelberg Institute for Theoretical Studies
[2]Donetsk National Technical University

The growing popularity of cloud service providers is driven by their affordability and flexibility. For scientific purposes the possibility of obtaining unused resources with a substantial discount (spot instances), for computational intensive tasks that do not require real-time simulation, seems to be attractive. We are developing an approach for cost optimization and a framework supporting all stages of running simulations in a cloud in the most efficient way.

## 1 Introduction to the DPSE framework

Distributed Parallel Simulation Environment (DPSE) [1, 2, 3] is a system organization that specifies how high performance computing resources and system / modeling software can be brought together. It focuses on a user-friendly way to develop and implement computational models that operate in distributed parallel environments.

## 2 Cost optimization

Assume, we want to launch a simulation on the cloud cluster and minimizing its computation costs. The simulation has been previously benchmarked with test data on different types and numbers of instances. This benchmark serves as a basis for deciding which resources are more economical/best performing for the simulation at hand. For simplification, we take into account only two types of Amazon Web Services (AWS) EC2 spot-instances: *c4.large* and *c4.8xlarge*. *Frankfurt* is chosen as an AWS region. The execution time of this simple benchmark model is shown in table 1. Table 2 shows a price comparison for one simulation running on the *onDemand*- and on *spot*-instances. Full utilization is assumed. Average spot prices were computed by the spot-market analysis tool of DPSE. Values for 6 *c4.large* instances are removed as they are redundant and will wrongly increase a calculation of the resulting ratio.

When comparing the price per run on on-demand instances with the price per run on spot-instances, the latter turn out to be 6.5 times cheaper. Running a benchmark on different types of instances an additional cost improvement of factor 1.4 can be achieved when choosing the best performing one (see tables 1, 2). In combination this yields a cost improvement of factor 9.1.

| Number of instances | Instance type | Duration (min) | Simulation runs per hour |
|---|---|---|---|
| 1 | c4.large | 14 | 4.3 |
| 2 | c4.large | 8 | 7.5 |
| 3 | c4.large | 6 | 10 |
| 4 | c4.large | 5 | 12 |
| 6 | c4.large | 5 | 12 |
| 1 | c4.8xlarge | 1 | 60 |

Table 1: Simulation benchmarking for different types of instances

| Number of instances | Instance type | *OnDemand* price/run *(USD)* | *Spot* price/run *(USD)* |
|---|---|---|---|
| 1 | c4.large | 0.0312 | 0.0048 |
| 2 | c4.large | 0.0357 | 0.0055 |
| 3 | c4.large | 0.0402 | 0.0062 |
| 4 | c4.large | 0.0447 | 0.0068 |
| 1 | c4.8xlarge | 0.0356 | 0.0066 |

Table 2: Prices per run for the benchmarked model

## 3 Conclusions

A prototype of DPSE providing support for all phases of model and simulation development of dynamic network objects and other models was developed. Running DPSE entirely on cloud resources (as opposed to using in-house resources) provided us with further experiments on whether using cloud resources for different classes of simulations can deliver an economical and performance benefit.

An example of saving up to 910% of simulation costs when running a certain simulation in a cloud, shows the potential of our research. This was achieved by choosing an optimal type of instance for the presented simulation model and by automatically monitoring the prices on the spot-market. This benefit will differ for other types of models.

Calculations were made without taking into account the prices for EBS storage, EBS I/Os and data transfer for downloading the results of the simulations. This will be done in future research.

## References

[1] L.P. Feldmann, V.A. Svjatnyj, M. Resch, and M. Zeitz. “Forschungsgebiet: Parallele Simulationstechnik.” In ASIM 2014 22. Symposium Simulationstechnik (2014): 3-7.

[2] V. Svjatnyj, V. Kushnarenko, O. Shcherbakov, and M. Resch. “Dekomposition der verteilten parallelen Simulationsumgebung.” Scientific papers of Donetsk National Technical University. Series “Problems of modeling and design automation” (2012): 227-234.

[3] O. Shcherbakov and V. Svjatnyj. “Decomposition into subsystems and organization of work of distributed parallel simulation environment on the web.” Informatics and Computer Technologies (2010): 192-194

# Brainware for Science – the Hessian HPC Competence Center

Dörte C. Sternel and Alexandra Feith

Hessisches Kompetenzzentrum für Hochleistungsrechnen, Darmstadt

In 2013 the Hessian HPC-Competence Center (Hessisches Kompetenzzentrum für Hochleistungsrechnen, HKHLR) was founded by the five universities of Hesse (TU Darmstadt, Goethe-Universität Frankfurt, Justus-Liebig Universität Gießen, Universität Kassel, Philipps Universität Marburg), to close the so called "software gap".

This article gives an overview about the Hessian HPC infrastructure as well as the tasks and methods of the Hessian Competence Center for High Performance Computing.

## 1 Motivation for founding HKHLR

High performance computing (HPC) is a key technology for scientific advancement of more and more research fields. But in the context of engineering sciences, many TOP500[1] systems achieve only a fraction of their peak computation capability [1]. In other sciences one observes a similar behaviour.

Additionally, the lifespan of a typical research code is four to five times longer than the lifespan of a computing system, with generations of researchers working on a code within their research field [2]. Thus, software development often lags behind hardware development with the result that expensive hardware is often not utilised efficiently. This is called the "software gap" [3]. Only if researchers are able to realise their ideas with a justifiable amount of effort in parallel codes that can also routinely be ported to new hardware architectures, scientific computing on high performance computers can unlock its real potential.

So, one key issue for efficient computing on codes with scientific relevance and not only on benchmarks, software competence and software specialists need to be a part of the HPC ecosystem. In [4], this human expertise was called "brainware".

Another key issue is to make researchers and their supervisors aware of the advantages of a good performance and support them to achieve knowledge about their code performance. A third issue is to enable researchers to use HPC hardware in the most efficient way according to their programming experience.

In the end the "brainware" of full time employees in HPC support saves operational costs of high performance computers, while the hard- and software runs under best possible conditions.

[1] http://www.top500.org

The idea of the Hessian Competence Center for High Performance Computing (Hessisches Kompetenzzentrum für Hochleistungsrechnen, HKHLR) is to make HPC expertise available for all Hessian scientists.

# 2 HPC Ecosystem in Hesse

## 2.1 HPC Hardware access in Hesse

The network of Hessian High Performance Computing consists of two tier 2 high performance computers in Darmstadt (Lichtenberg High Performance Computer) and Frankfurt (LOEWE-Cluster) with a complementary hardware architecture[2] as well as local tier 3 high performance computers in Giessen, Kassel, and Marburg. The clusters in Darmstadt and Frankfurt are open for all research projects in Hesse; for both clusters a proposal is necessary. In Darmstadt the access underlies a scientific review procedure, which is controlled by a steering committee.

## 2.2 The Hessian Competence Center for High Performance Computing, HKHLR

The funding of the first period (2013–2016) of the Hessian Competence Center for High Performance Computing was fully financed by the Hessian State Ministry of Higher Education, Research and the Arts (HMWK). After the successful evaluation by the DFG (Deutsche Forschungsgemeinschaft) in 2015, the second period has been started in 2016, which is funded again by HMWK and with a growing share by the five Hessian universities. The funding allows the employment of seven full time researchers and a management position and includes also a budget for the organisation of tutorials, workshops, trainings, and public relations. The staff is distributed over the five locations; this offers a local HPC support for the researchers. A steering committee, in which all universities are represented, decides about the focus of the HKHLR.

The coordination of the Hesse-wide work is organized by the management located in Darmstadt. In regular meetings, for example weekly web conferences as well as bimonthly meetings at one of the locations, the management and staff members report about their ongoing work, discuss local events, and future tasks.

### 2.2.1 The HKHLR online survey

With a yearly online survey, the HKHLR monitors the user demands for support, training, and hardware infrastructure. In 2016 239 researchers participated in that survey. In the following, selected results are presented. Figures 1(a) and (b) show an overview about affiliation and disciplines of the participants.

One issue of the survey is the self-assessment about the importance of code development and parallel performance of the used software. Fig. 2 shows some results to this aspect. 72% answered that code development is part of their scientific work (Fig. 2(a)), 83% answered that the parallel performance is part of their research or important for the success of their research (Fig. 2(b)) and more than 80% gave an assessment of their code behaviour (Fig. 2(c)). Looking at Fig. 3, which visualizes the answers to the questions about further education, a gap to the previous answers becomes evident: More than 50% answered, that they are interested in workshops on the topic "What is serial/parallel performance?" (>20% "high interest", >30% "nice to have"), and more than 60% on the topic "How to measure code performance?" (>20% "high interest,

[2]hardware details: http://www.hhlr.tu-darmstadt.de and https://csc.uni-frankfurt.de/

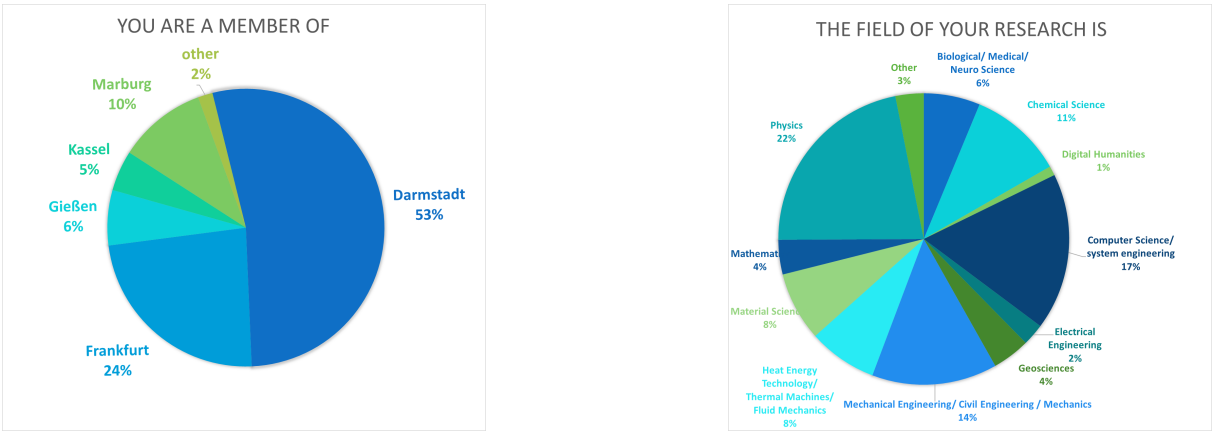


(a) (b)

Figure 1: Participants of the online survey 2016. 239 answers.

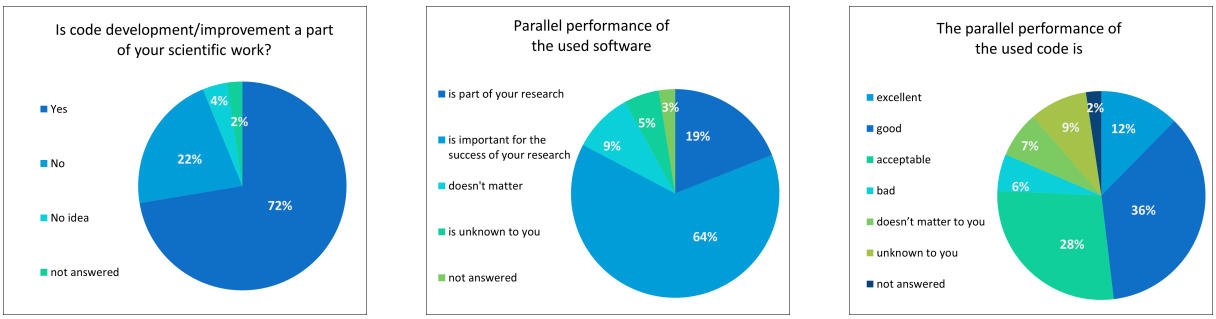


(a) (b) (c)

Figure 2: Code development and parallel performance. HKHLR-Online Survey 2016, 239 participants.

40% "nice to have"). This implies that many participants more or less estimated the parallel performance of their code.

About 20% of the users declare that they have a high interest in courses at beginner level, and additionally 40% of the users think that these courses are "nice to have" (Fig. 3). This shows, that for a high number of HPC users, there is a big need of courses at a relatively low level.

### 2.2.2 Monitoring of HPC usage

For optimizing the usage of the Hessian HPC facilities, the HKHLR management initiated a central monitoring, which will be continuously improved.

This job monitoring, in its current form, is used to detect imbalances between required and used resources. In case of imbalances, the HKHLR staff can contact the user to clarify the reasons, and help to improve the usage.

Furthermore, to give tuning experts the information where substantial performance improvements can be achieved, monitoring helps to identify "power users". Figure 4 shows the accumulated resource demands of the projects at Lichtenberg High Performance computer, ordered by decreasing resource demands. The first 10 users request around 50% of the complete cluster (cf. [4], with a similar situation).

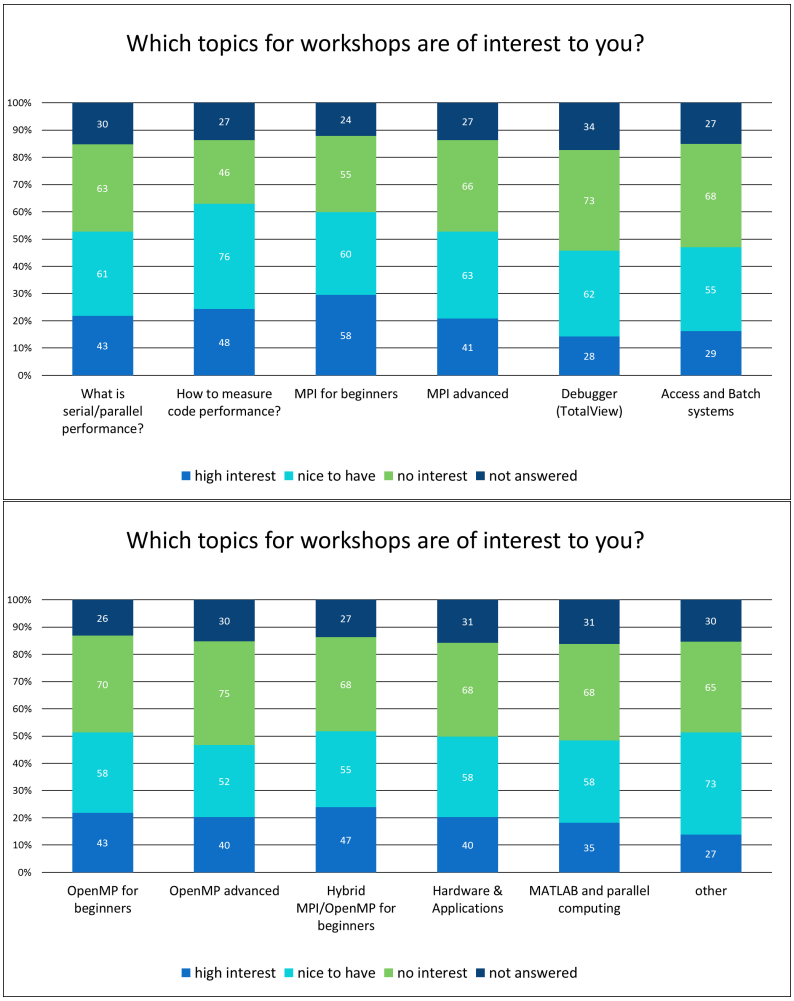


Figure 3: Demands for advanced trainings. HKHLR-Online Survey 2016, 197 answers.

Another advantage of a central monitoring in Hesse is to control free resources. When there is an overload on one location and free resources on one of the others, it is often possible to satisfy short term necessities.

### 2.2.3 Personal support

A user can request personal support of HKHLR via the ticket system of the local HPC cluster.

If the HKHLR staff identifies potential candidates for performance improvement by the analysis of the monitoring data (see section 2.2.2), they will contact the user. In most cases small changes in the batch script or of the compiler options can save a lot of resources.

The support of power users is a greater challenge. Here, the researchers are addressed directly. Together with HKHLR staff members, the parallel performance of the code will be analyzed, bottlenecks identified, and suggestions for improvement developed.

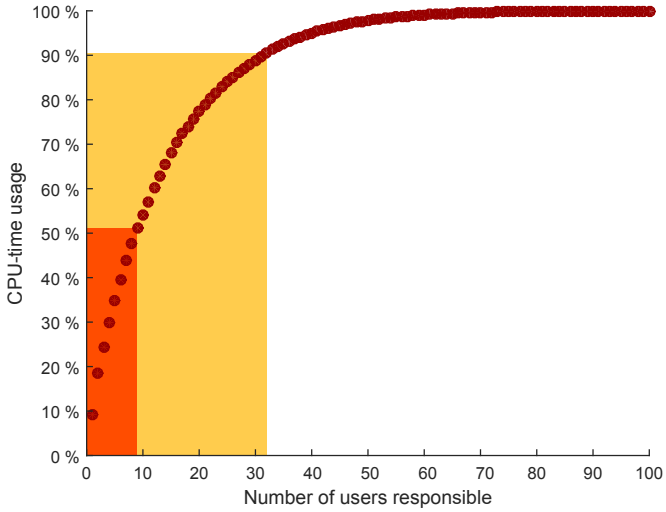


Figure 4: Accumulated resource demands of the users at Lichtenberg High Performance Computer.

### 2.2.4 Workshops, training, courses and networking

The workshop series HiPerCH (High Performance Computing Hesse) takes place two times a year. The experience of the last two years showed that researchers prefer local workshops. Therefore, the location of HiPerCH workshops alternates. The topics of HiPerCH are chosen by the user demands extracted from the online survey, from experience of HKHLR staff, or from direct user requests. These workshops cover basic as well as advanced topics for specific audiences.

As a result of the online surveys, HKHLR initialized introductory courses for new users of the Hessian HPC clusters, covering information about general access, available hardware, and usage. Basic introductions to Linux, shell scripting, and other basic tools are part of the introductory courses and are completed by offering more detailed knowledge by the HiPerCH workshop series.

On demand, the HKHLR organizes special trainings as well as user group meetings.

### 2.2.5 Unified Usage

To simplify the use of other hessian HPC clusters, the HKHLR aspires to unify the systems, whenever it is reasonable and technically feasible. One first step is to use the same scheduler at all locations as soon as possible.

To push that process, the HKHLR organizes regular meetings of the Hessian HPC-system administrators.

### 2.2.6 Tools

With the funding of the HMWK, the HKHLR provides the license for the performance analysing tool Vampir[3] and the debugger Totalview[4] for all Hessian Universities. Those tools and individual user support, either on request by users or by identifying power users (see section 2.2.1),

[3] https://www.vampir.eu/
[4] http://www.roguewave.com/products-services/totalview

foster competences in analyzing or tuning parallel tools. Local trainings empower the researchers in the use of these tools.

### 2.2.7 Public relations

Besides scientific publication, the awareness of Hessian research on HPC in public is one aim of HKHLR. Therefore, HKHLR offers a platform for HPC in Hesse. The Web page (http://www.hpc-hessen.de) summarizes information about the goals and benefits of HKHLR and gives an overview of Hessian research by HPC reports, current research projects as well as video portraits of Hessian researchers. HKHLR assists researchers by the distribution of their research for the general public. In addition, it is the first point of contact for new users and offers helpful links, flyer material, and an event calendar. Since 2015, HKHLR has an own booth at ISC High Performance in Frankfurt (http://isc-hpc.com/).

## Acknowledgements

HKHLR is funded by the Hessian State Ministry of Higher Education, Research and the Arts.

## References

[1] D.F. Harlacher, S. Roller, F. Hindenlang, C.-D. Munz, T. Kraus, M. Fischer, K. Geurts, M. Meinke, T. Klühspies, V. Metsch, and K. Benkert. "Highly Efficient and Scalable Software for the Simulation of Turbulent Flows in Complex Geometries", in W.E. Nagel et al. (eds): High Performance Computing in Science and Engineering, Part 5, pp. 289-307, DOI 10.1007/978-3-642-23869-7_22, Springer Verlag, 2012.

[2] D.E. Post, R.P. Kendall, Software project management and quality engineering practices for complex, coupled multiphysics, massively parallel computational simulations: lessons learned from ASCI. Int. J. High Perform. Comput. Appl. 18, pp. 399-416, 2004.

[3] Computational Science: Ensuring America's Competitiveness, President's Information Technology Advisory Committee. https://www.nitrd.gov/pitac/reports/20050609_computational/computational.pdf, 2005.

[4] C. Bischof, D. an Mey, and C. Iwainsky, "Brainware for green HPC", Computer Science – Research and Development, DOI 10.1007/s00450-011-0198-5, Springer, 2011.

# Simulating climate change adaptation and structural change in agriculture using microsimulation and agent-based modeling

Christian Troost and Thomas Berger

Land Use Economics Group, Institute of Agricultural Sciences in the Tropics, University of Hohenheim

We present MPMAS, a software package for agent-based modeling and microsimulation in agricultural economics. The modeling package uses mixed integer programming to represent farm and farm household decisions and is designed for *ex ante* policy analysis in the context of agricultural production. We present the internal modeling sequence, our approaches to parallelization and case studies that use the software in the context of the analysis for climate change adaptation in agriculture.

## 1 Introduction

Originally developed for the analysis of innovation diffusion and the effects of trade policy on irrigation agriculture in Chile [1], the MPMAS software has developed into a versatile modeling package for agent-based modeling (ABM) in the context of agricultural production and land use decisions that has been used in a variety of case studies around the world [2, 3]. It is targeted at scientific applications that specifically require taking into account heterogeneity of farms and farming households (microsimulation) and/or interactions between farms (ABM). Farm management is modeled as a sequence of pre- and post-production-season decisions. Management decisions have consequences on the farm and its social, natural and economic environment. These effects are evaluated using internal or externally coupled biophysical, social and market models and feedback recursively on the next decision steps (cf. Fig. 1).

## 2 Uncertainty analysis and parallelization

Recent development of MPMAS focused on improving the options for uncertainty analysis with MPMAS. Uncertainty in MPMAS simulations stems from epistemic uncertainty due to incomplete knowledge on decision parameters and population characteristics and the uncertainty of future climatic and socioeconomic development, but also from aleatory uncertainty due to the inherently stochastic nature of certain farm events (e.g. death and birth of household members). Robustness of simulation results is assessed using sampling-based sensitivity analysis. Experimental designs (Latin-hypercube sampling, Sobol' sequences, elementary effect screening) are

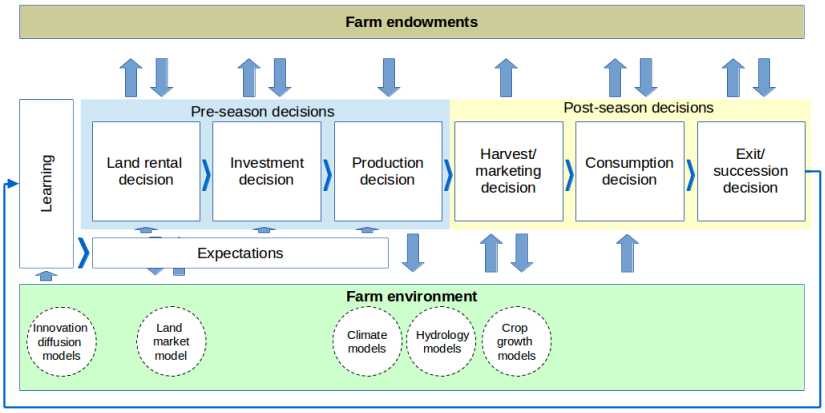


Figure 1: Sequencing of farm agent decisions in MPMAS

used to keep the number of model repetitions feasible. Still, considerable numbers of repetitions are necessary [4]. Two approaches to parallelization are used: With smaller applications, where the runtime of each individual repetition remains within acceptable time limits, trivial parallelization, i.e. running each run on one processor, is most efficient as it avoids the overhead of multiple processes/threads. For larger applications (e.g. with many land market interactions), MPMAS uses MPI to parallelize agent decisions. A common random numbers scheme has been implemented to ensure consistency of stochastic events across repetitions and parallel processes [5].

## 3 Applications

Scientific application of MPMAS currently has a strong focus on agricultural policy analysis in the context of climate change adaptation and mitigation. For example, Troost & Berger [4] demonstrated the importance of taking farm-level processes into account when assessing the consequences of climate change adaptation in agriculture in Southwest Germany.

## Acknowledgements

Part of this research was funded by DFG as part of the Research Unit DFG-FOR1695 “Agricultural Landscapes under Global Climate Change - Processes and Feedbacks on a Regional Scale”. Computations were performed on bwUniCluster funded by the Ministry of Science, Research and the Arts Baden-Württemberg and the Universities of the State of Baden-Württemberg, Germany, within the framework program bwHPC-C5.

## References

[1] Berger, T. “Agent-based models applied to agriculture: a simulation tool for technology diffusion, resource use changes and policy analysis.” Agricultural Economics Volume 25, Issue 2/3 (2001): 245-260.

[2] Schreinemachers, P. and T. Berger. "An agent-based simulation model of human environment interactions in agricultural systems." Environmental Modelling & Software Volume 26 (2011): 845-859.

[3] Berger, T. and C. Troost. "Agent-based Modelling of Climate Adaptation and Mitigation Options in Agriculture." Journal of Agricultural Economics, Volume 65 (2014): 323-348.

[4] Troost, C. and T. Berger. "Dealing with Uncertainty in Agent-Based Simulation: Farm-Level Modeling of Adaptation to Climate Change in Southwest Germany." American Journal of Agricultural Economics, Volume 97 (2015): 833–854.

[5] Troost, C. and T. Berger. Advances in probabilistic and parallel agent-based simulation: Modelling climate change adaptation in agriculture. In: Sauvage, S., Sánchez-Pérez, J.M., Rizzoli, A.E. (Eds.), 2016. Proceedings of the 8th International Congress on Environmental Modelling and Software, July 10–14, Toulouse, France. (2016)

# Many-body effects in simulations of ionic liquids

Frank Uhlig, Jens Smiatek, and Christian Holm

Institute for Computational Physics, University of Stuttgart

Room temperature ionic liquids are salts that are molten below 373 K, and show promise for many industrial applications. The aim of this project is to investigate them computationally using both ab initio methods and empirical potentials. We parametrized an explicitly polarizable, coarse-grained force field for the ionic liquid 1-butyl-3-methyl-imidazolium hexafluorophosphate. The force field lacks atomistic resolution, yet simulations using it are able to accurately reproduce many-body effects in the electronic polarizability as observed in ab initio simulations.

## 1 Introduction

Room temperature ionic liquids are an interesting class of solvents that have received significant scientific interest in the past decades [1]. These liquids exhibit, among other beneficial properties, low vapor pressures, high thermal stability, and large electrochemical windows. These features make them interesting for potential applications in fuel cells [2] or (super-)capacitors [3].

Ionic liquids are also notoriously difficult to model computationally, because of large particle numbers and long simulation times needed to obtain converged results in molecular simulations [4]. In the aforementioned applications explicit treatment of polarizability may play an important role, but also puts additional computational effort on top of the common computational experiment. Hence, in this contribution we focus on explicitly polarizable coarse-grained (CG) models that reduce the overall number of degrees of freedom, similar to previously published, but non-polarizable models [5]. These models allow to explicitly include electronic polarizability while keeping the computational effort reasonable. We find compelling, semi-quantitative agreement between simulations using our CG force field, and the ab initio methodology for many-body effects, exemplified here by the electronic polarizability.

## 2 Methods

We performed both ab initio molecular dynamics (AIMD) based on density functional theory using CP2K (`https://www.cp2k.org`), and force-field based molecular dynamics (FFMD) using LAMMPS (`http://lammps.sandia.gov/`). The AIMD simulations used the revised Perdew-Burke-Ernzerhof density functional approximation [6] and a double-$\zeta$ basis set with polarization functions [7]. Please see ref. [8] for more computational details. The AIMD simulations serve to provide reference data, and also to obtain averaged geometries of the species in the liquid phase which is input to our model parametrization. The chemical structures of our system of interest,

1-butyl-3-methyl-imidazolium hexafluorophosphate ($[C_4C_1Im][PF_6]$), are shown in Fig. 1. Also shown in Fig. 1 is a snapshot from a bulk simulation of the final coarse-grained model.

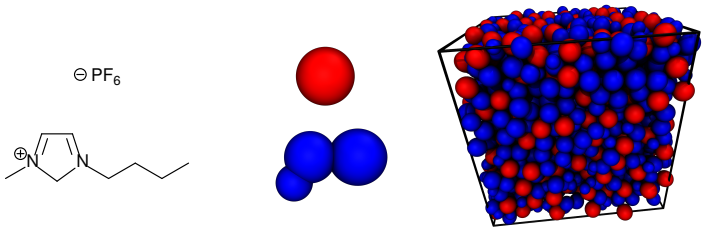


Figure 1: Chemical structure of 1-butyl-3-methyl-imidazolium hexafluorophosphate (left). Coarse-grained representation of respective ions in the middle. The anion is represented by a single red sphere. The three-site model of the cation shown in blue. A snapshot from a simulation of 500 ion pairs of the coarse-grained model is shown on the right.

## 3 Results and Discussion

We calculated the electronic polarizability along trajectories obtained with both AIMD and FFMD. The polarizability was obtained using finite differences of the dipole moment under applied electric fields in x, y, and z direction. Histograms of the polarizability of an individual $C_4C_1Im^+$ ion embedded in the liquid environment and in the gas phase are shown in Fig. 2. The difference in mean polarizabilities between AIMD and FFMD is between 5-7 %. The polarizability is enhanced in the bulk liquid compared to a single ion in the gas phase. On average this effect amounts to an about 14 % and 24 % higher polarizability in the bulk liquid in AIMD and FFMD, respectively. The effect is larger in the simulations using the CG force field, likely due to a lack of explicit modelling of Pauli repulsion effects.

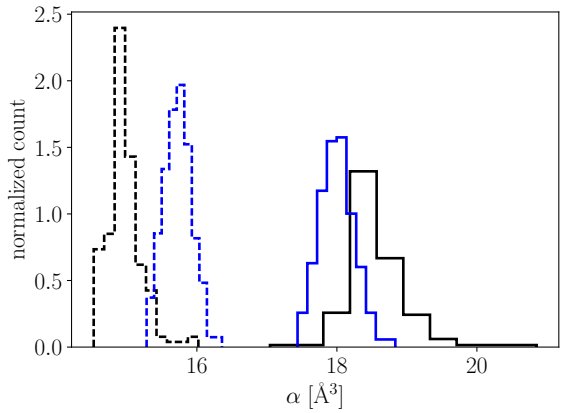


Figure 2: Histograms of polarizability $\alpha$ for $C_4C_1Im^+$ obtained from ab initio (blue) and coarse-grained force field simulations (black). Polarizabilities were calculated for a single $C_4C_1Im^+$ ion, both in the $[C_4C_1Im][PF_6]$ liquid (solid lines), and in the gas phase (dashed lines).

## 4 Conclusions

We investigated the performance of an explicitly polarizable, coarse-grained force field for the ionic liquid 1-butyl-3-methyl-imidazolium. The electronic polarizabilities were extracted from ab initio, and force field molecular dynamics simulations. Semi-quantitative agreement between both types of simulations is found, although the coarse-grained force field lacks atomistic resolution. Hence, the coarse-grained model reproduces many-body effects as observed in the ab initio simulations. Moreover, with this new force field one can model large systems that are out of reach with ab initio methodologies and force fields with atomistic resolution.

## Acknowledgements

The authors gratefully acknowledge resources provided from bwHPC, DFG: INST 40/467-1 FUGG and funding from DFG SFB 716.

## References

[1] Hayes, R., Warr, G.G., Atkin, R., "Structure and Nanostructure in Ionic Liquids", Chem. Rev., Volume 115 (2015): 6357–6426

[2] Yasuda, T., Watanabe, W. "Protic ionic liquids: Fuel cell applications", MRS Bulletin, Volume 38 (2013): 560-566

[3] Breitsprecher, K., Košovan, P., Holm, C., "Coarse grained simulations of an ionic liquid-based capacitor I: density, ion size, and valency effects", Journal of Physics: Condensed Matter, Volume 26 (2014): 284108

[4] Gabl, S., Schröder, C., Steinhauser, O., "Computational studies of ionic liquids: Size does matter and time too", J. Chem. Phys., Volume 137 (2012): 094501

[5] Roy, D., Patel, N., Conte, S., Maroncelli, M., "Dynamics in an Idealized Ionic Liquid Model", J. Phys. Chem. B, 114 (2010): 8410–8424

[6] Zhang, Y., Yang, W., "Comment on ‚Generalized Gradient Approximation Made Simple'", Phys. Rev. Lett., Volume 80 (1998): 890

[7] VandeVondele, J., Hutter, J., "Gaussian basis sets for accurate calculations on molecular systems in gas and condensed phases", J. Chem. Phys., Volume 127 (2007): 114105

[8] Uhlig, F., Zeman, J., Smiatek, J., Holm, C., *in preparation*

# Overview on governance structures in bwHPC

Dirk von Suchodoletz[1], Bernd Wiebelt[1], Gerhard Schneider[1], Thomas Walter[2], and Stefan Wesner[3]

[1]University of Freiburg
[2]University of Tuebingen
[3]University of Ulm

In Baden-Württemberg, the implementation of the bwHPC concept has created efficient, distributed research infrastructures involving scientists, grant giving organizations and HPC operators at various sites. To ensure the operation of HPC resources in a successful, efficient and fair way for all involved parties, several governance structures were created and further developed. The ALWR-BW and the bwHPC-Lenkungskreis ("steering committee") are the superordinate structures for decisions concerning the bwHPC strategy. They rely on subordinate governance structures, such as the bwHPC-C5 Kernteam ("core team"), the bwHPC-C5 CAT ("cluster selection team") and the bwHPC-TAB ("technical advisory board") for the actual decision making process. Scientific governance is provided by a state-wide user committee composed of Baden-Württemberg scientists. The implementation of bwHPC is an example for the federated provisioning and control of large resources across several research and teaching institutions.

## 1 Federated HPC cluster governance

State-wide distributed infrastructures providing HPC services require appropriate governance structures. HPC resources are used by various scientific communities for research, teaching and training. The resources are financed by different money granting organizations. In the cooperative model, the interests and goals of the various stakeholders and shareholders have to be taken into consideration and balanced against each other. To this end, advisory and decision-making committees had to be created. These committees identify and address arising questions. At the same time they implement and moderate decision making processes.

The development of these governance structures was accomplished in parallel to the technical procurement, acquisition and deployment of the HPC resources and with the involvement of all related parties. The central governance structures encompass all affected HPC resources, taking strategic decisions. Additionally, dedicated and modular governance structures were established which directly address the needs of scientific communities or specific HPC sites.[1]

[1]See e.g. the example for the governance of the bwForCluster NEMO discussed in these proceedings.

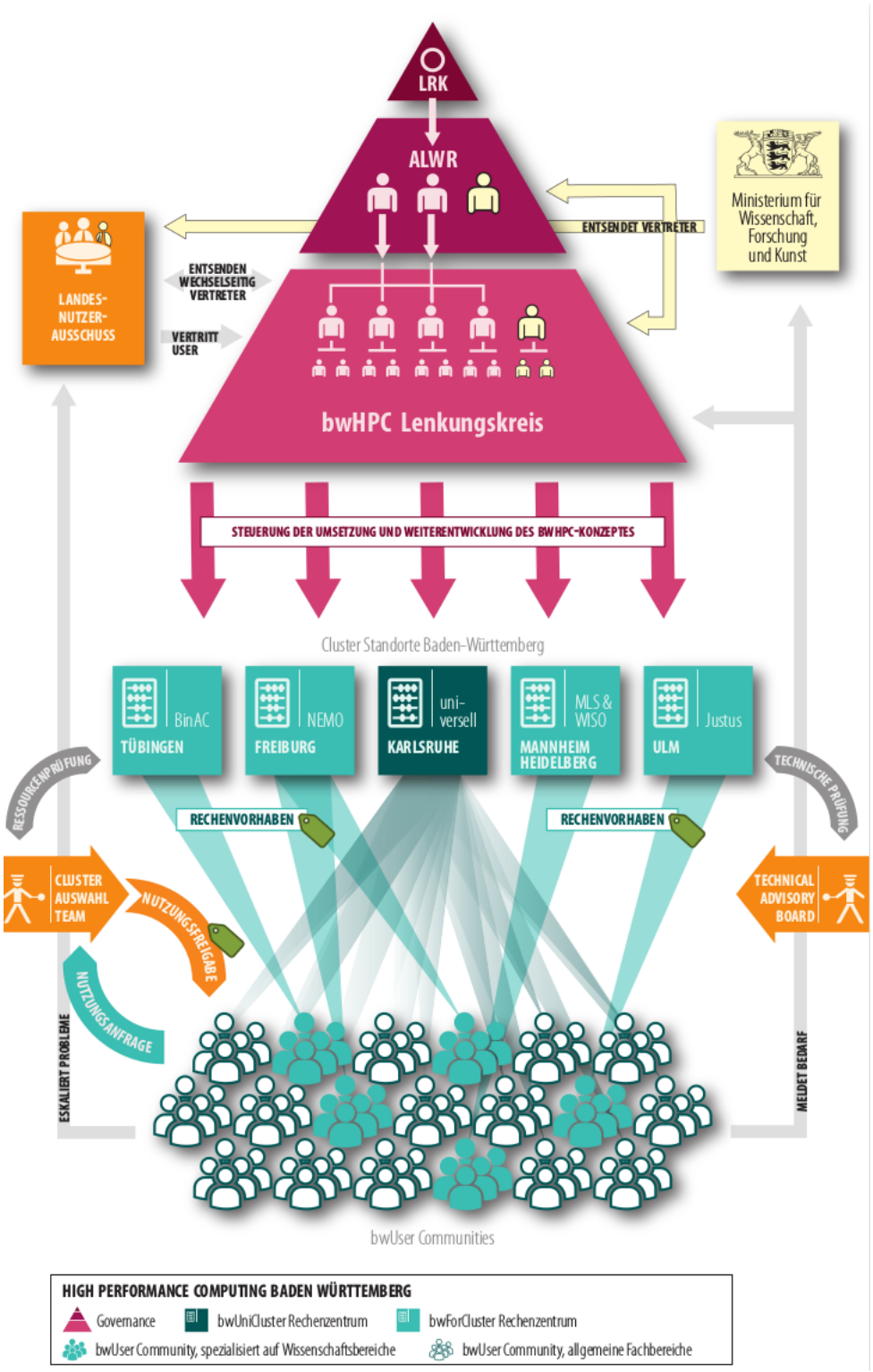


Figure 1: bwHPC governance structural overview [1].

The *ALWR-BW* and the *bwHPC-Lenkungskreis* are the superordinate governance entities of the bwHPC initiative. The *ALWR-BW* is composed of all directors of scientific computing centers at universities in the state of Baden-Württemberg. Together with representatives of the users and the *Ministry of Science, Research and the Arts Baden-Württemberg*, they form the *bwHPC-Lenkungskreis* (bwHPC steering committee). Both governance structures lay out the general policies and take strategic decisions with respect to bwHPC. Technical and administrative tasks are delegated to subordinate governance bodies, such as the bwHPC-TAB (technical advisory board), the *bwHPC-CAT (cluster selection team)* the bwHPC competence centers and the bwHPC cluster sites. In principle, as many governance decisions as possible should be taken in the subordinate bodies.

For the overall scientific governance of bwHPC, a dedicated state-wide user committee, the *Landesnutzerausschuss Baden-Württemberg (LNA-BW)* was established. For each university, a representative is suggested by the vice president of the university responsible for research. This person is then appointed by the ministry as a member of the state-wide user committee. Additionally, a representative of the ministry is invited as permanent guest to each meeting of LNA. The LNA user committee gets together at least twice per year, consolidating and moderating the manifold of HPC user expectations. It advises the ALWR-BW and the bwHPC-Lenkungskreis on their decisions and sends a representative to the steering committee. For organizational purposes, there is an LNA office which is located at the Karlsruhe Institute of Technology.

The *bwHPC-C5-Kernteam* (core team) represents the steering committee of the *bwHPC-C5 project*, which bundles HPC support activities through its bwHPC competence centers. It is composed of the bwHPC-C5 project leaders, the bwHPC-C5 work package responsibles and representatives of the HPC cluster sites. Additional members can be invited as permanent guests by way of a majority vote. The core team is responsible for the coordination of the activities of the bwHPC competence centers and development of the federated HPC solutions. Furthermore, the core team monitors the deployed infrastructure mechanisms to provide risk assessment and quality assurance. It regularly reports to LNA, bwHPC-Lenkungskreis and ALWR-BW.

The *bwHPC-C5 Clusterauswahlteam* (CAT, cluster selection team) is the governance body which takes care of directing the users to the HPC resources best suited for them. In the federate setting of bwHPC, users are not limited to HPC resources at their home university. In fact, it is often the case that the HPC competence center and the HPC resources for a specific scientific fields are concentrated at another site. The procedure to apply for bwHPC resources is designed to be lightweight in that the application is done via a simple web form and there is no in-depth scientific review. Instead, mainly a routing decision is taken by the cluster selection team. The cluster selection team is composed of two representatives of each bwHPC competence center and experts from the scientific fields.

The *bwHPC-TAB* is a state-wide committee to assure a technical and operational common ground for bwHPC resources. It reports to the superordinate governance bodies and prepares strategic decisions on operational parameters by evaluating existing alternatives, e.g. for the standard operating system or the standard scheduler used in the HPC systems. While still allowing individual solutions (where appropriate) this offers a uniform user experience on either of the distributed HPC resources.

## 2 Conclusions and future development

Starting from the initial bwHPC initiative proposition, foremost individual and university-bound HPC resources have been turned into state-wide service providing infrastructures for their respective scientific communities. To make this mode of operation sustainable, the governance entities that have been created and deployed constitute an indispensable component. However, the development of governance structures in the bwHPC project cannot be considered concluded. While the tasks of several committees (e.g. the bwHPC-Lenkungskreis) have been well defined, some other structures are still in the process of adapting to the demands of shareholders and stakeholders. Due to the multitude of interested parties involved on various levels, the overall structure is at first sight not as transparent as one might wish for. However, this is subject to further optimizations, incorporating all experience and feedback acquired so far.

## References

[1] Wesner, S., Walter, T., Wiebelt, B., von Suchodoletz, D., Schneider, G. "Strukturen und Gremien einer bwHPC-Governance – Momentaufnahmen und Perspektiven." Kooperation von Rechenzentren Governance und Steuerung – Organisation, Rechtsgrundlagen, Politik, de Gruyter (2016): 315–329.

# Flexible HPC: bwForCluster NEMO

Bernd Wiebelt, Konrad Meier, Michael Janczyk, and Dirk von Suchodoletz

Rechenzentrum, Universität Freiburg

Traditional High Performance Computing on *bare metal* is based on the paradigm of *maximum usage of resources* whereas Cloud Computing relies on virtualization and is considered as a shift towards *flexible usage of resources*. The bwForCluster NEMO is a HPC system that offers virtualized research environments as an additional mode of operation, thus spanning a bridge between both paradigms. The important achievement is that for the HPC scheduler, a virtual machine instance is *just another job*. There is no static partitioning necessary and the HPC scheduler keeps control over accounting and fair-share.

## 1 Motivation

The bwForCluster NEMO, part of the bwHPC initiative of the state of Baden-Württemberg, was designed and procured as a High Performance Computing system serving the scientific domains of Elementary Particle Physics, Neurosciene and Microsystems Engineering. During the procurement period of the system it became clear that the classic HPC model of operation would not be sufficient to satisfy the demands of all those scientific communities. In particular, the Particle Physics community had requirements regarding reproducibility that would have been hard to implement and sustain by installing, maintaining, running and ultimately binding the software directly to the underlying hardware. Therefore, while procuring the final HPC system, research was done in the framework of the bwHPC-C5 project [1] whether virtualization technology could be applied and integrated to allow additional usage profiles for a HPC system.

## 2 Virtualized Research Environments

In the classic HPC model the software environment is heavily optimized towards the acquired HPC hardware. This is done to achieve the maximum possible performance for the individual compute tasks to be accomplished. In turn, usage of the optimized software environment without the HPC hardware becomes cumbersome or impractical. On a different hardware, the software environment has to be completely redeployed. Optimizations that benefited the software running on the original hardware might turn out to yield inferior results on the new hardware. In any case, since the newer hardware typically needs newer versions of the operating system and system libraries, even by using the same version of the application software, reproducible results cannot be guaranteed.

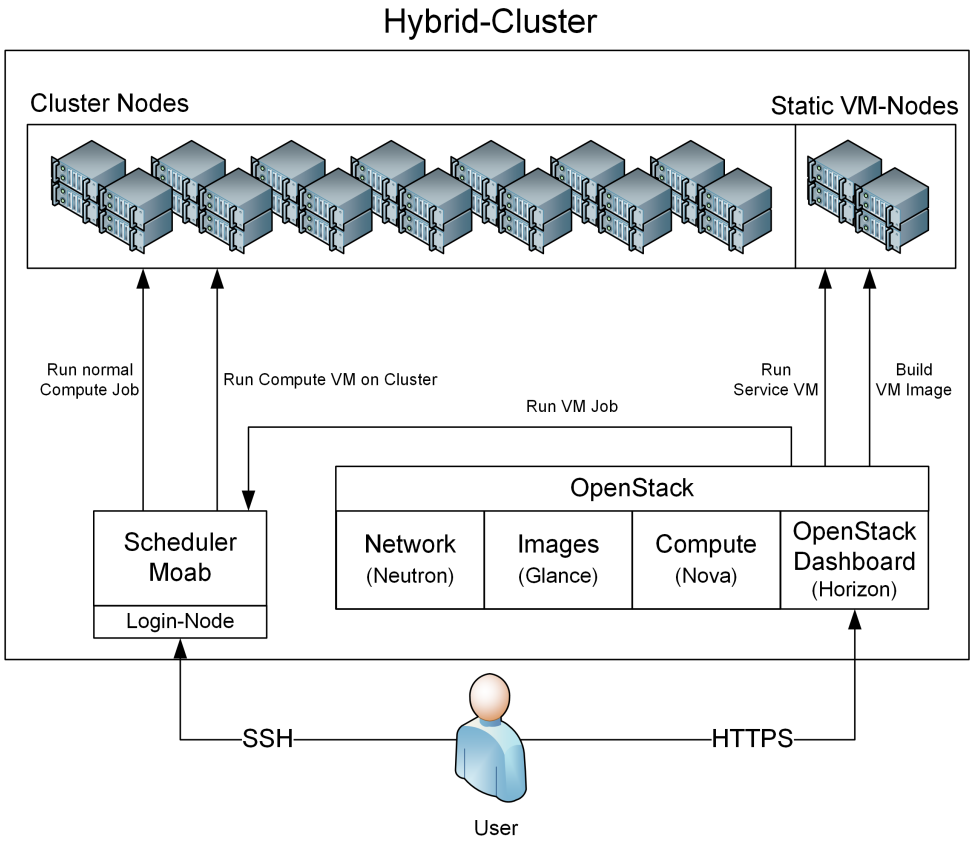


Figure 1: NEMO HPC/Cloud interface [3].

Cloud Computing, by abstracting the software environment from the underlying hardware, is known to solve these problems. Virtualized research environments can be created as virtual machine images. Once created, they are ready to run inside the virtualization framework, yielding the same results no matter how often the underlying hardware changes. As immediate additional benefits, virtualized research environments can be easily versioned, copied, archived and referenced.

The caveat is that there is a performance loss due to the virtualization overhead. However, this is perfectly acceptable if the benefits of virtualized research environments outweigh the loss in performance for an individual use case or an entire scientific work flow.

General feasibility and provisioning of virtualized research environments for scientific communities is a research topic currently investigated by the Baden-Württemberg VICE project [2].

## 3 NEMO HPC/Cloud

The bwForCluster NEMO is running virtualized research environments on the HPC hardware orchestrated by an OpenStack server. For the HPC scheduler, virtual machine instances are ”just another job”. There is no static partitioning necessary and the HPC scheduler keeps control over accounting and fair-share. Scientists who would like to use the virtualization feature need to provide their own custom VM images. They modify the script *startVM.py* and add it as an

instruction in their job description file. The script allocates the job resources, starts the virtual machine instance via the OpenStack nova interface and then waits for the virtual machine instance to be finished, e.g. by the user issuing a halt operation inside the virtual machine [3].

## 4 Future HPC Virtualization Concepts

Using virtualization inside an HPC system opens up the possibilities for several interesting features. While their implementation would require tighter integration between HPC scheduler and virtualization framework, they could solve several classic problems with HPC systems, especially those designated for novice HPC users.

Snapshot and migration functionality for running virtual machine instances are a typical feature of virtualization frameworks. This means that running processes can be stopped, possibly moved to a different node in the virtualization cluster and then resumed. For an HPC system, this would be practical for two use cases. The first one concerns long running monolithic jobs. These are, for very practical reasons, non favored jobs in HPC environments, assuming they are permitted in the first place. However, the costs to adapt a particular workflow based on such monolithic tasks to a HPC system, e.g. by parallelizing and partitioning it manually, may sometimes exceed the practical use of the resulting solution. If the monolithic job could automatically be stopped, checkpointed and resumed at regular intervals, this might very well constitute a more economic procedure. In the second use case, if there is a mix of pleasingly parallel high throughput jobs (using only single cores or nodes) and massively parallel high performance jobs (using several nodes), the second class of jobs should be concentrated on nodes that share optimal high performance network communication paths. Typically this is accomplished by high investments in the network topology or sophisticated tuning of the job queue. However, if jobs could be moved around the physical machines (i.e. "de-fragmented"), optimal high performance network communication paths can be guaranteed by concentrating massively parallel jobs on the same or adjacent high performance network switches.

Last but not least, to make an HPC system capable of processing sensitive data, the usual strategy is to isolate it from other systems. However, this also means that the HPC resources cannot easily be shared. Virtualization of HPC resources could in principle enable the creation of isolated safe data center partitions inside a shared HPC system.

## References

[1] http://www.bwhpc-c5.de

[2] https://www.alwr-bw.de/kooperationen/vice

[3] K. Meier, G. Fleig, T. Hauth, M. Janczyk, G. Quast, D. von Suchodoletz, and B. Wiebelt "Dynamic provisioning of a HEP computing infrastructure on a shared hybrid HPC system." Journal of Physics: Conference Series, Volume 762(1):012012, 2016

# bwHPC Governance of the ENM community

Bernd Wiebelt, Dirk von Suchodoletz, and Michael Janczyk

Rechenzentrum, Universität Freiburg

The bwForCluster NEMO is an entry-level (Tier-3) HPC resource for researchers in the state of Baden-Württemberg. It was designed to offer high performance compute resources to the scientific domains of Elementary Particle Physics, Neuroscience and Microsystems Engineering (ENM). The expectations of these heterogeneous user communities have to be respected and tended to. Usage profiles vary from work group to work group. For some users, this is their first encounter with computation beyond the desktop. Other users are more experienced, coming from (smaller) HPC systems of their own. Furthermore, some scientists have extended NEMO with a financial contributions of their own and thus have become shareholders. For the smooth, fair and harmonic operation of the system it is imperative to balance the interests of the various scientific communities and shareholders. This is accomplished by offering the opportunity to participate on all levels of the decision making processes and to jointly moderate and develop the operating model. To this end, two consulting governance bodies have been established. On the one hand, there is the *NEMO Nutzerversammlung* (general user assembly), meeting at least once per year to gather feedback from all users. On the other hand, there is the *NEMO Cluster-Beirat* (advisory board) composed of representatives from the scientific communities and the shareholders. The advisory board meets more often and can therefore discuss and advise more timely on current topics.

## 1 Managing a shared resource

The bwForCluster NEMO and the corresponding HPC competence center ENM are located in Freiburg, offering their services to all scientists in Baden-Württemberg working in the scientific fields of Elementary Particle Physics, Neuroscience and Microsystems Engineering (ENM). NEMO was financed by the *Ministry of Science, Research and the Arts Baden-Württemberg* and the *German Research Foundation*. NEMO was procured with the intention of providing researchers from these scientific fields an entry-level (Tier-3) HPC resource which gives them the opportunity to start progressing beyond the limits of desktop-bound computing. The acquisition and deployment of the NEMO hardware was accompanied by the installation of the HPC competence center ENM in the framework of the bwHPC-C5 project [1]. The competence center ENM offers service and support to further the scientists' efforts in adapting their applications to HPC environments.

During the application phase, scientists from the ENM communities have supplemented NEMO with financial resources of their own, consequently becoming shareholders of the final system. Serving three scientific communities and the shareholders, the user community of the bwForCluster NEMO has become large and heterogeneous. This heterogeneous community does not necessarily have coherent objectives with respect to the initial setup of an HPC system. Therefore, during the procurement phase, there were already lots of interactions and consultations between all involved parties to balance these interests and find a joint mode of operation. This cooperation has continued since NEMO became operational. The governance structures outlined herein aim to formalize those already established and well tested ways for acting cooperatively and towards a common goal.

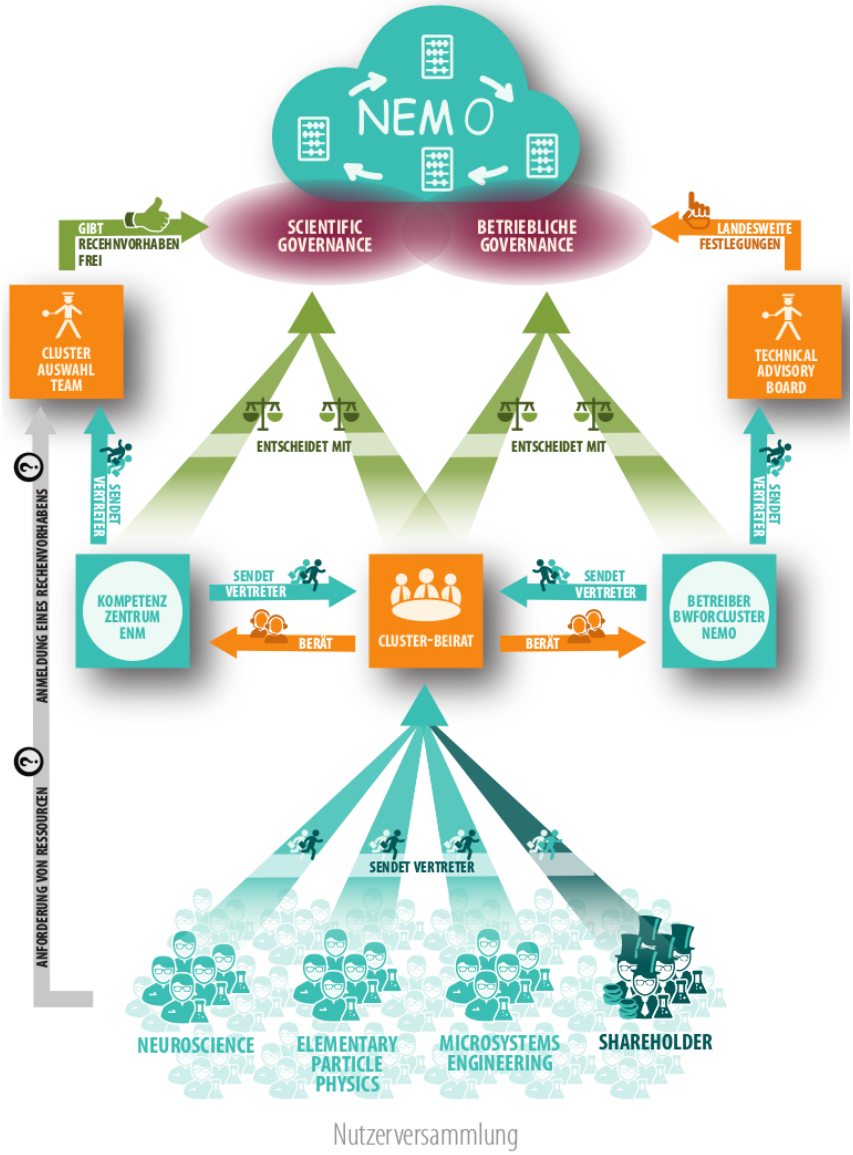


Figure 1: bwForCluster NEMO governance [3].

The bwHPC initiative has dedicated superordinate governance bodies that specify the basic

policies that bwHPC resources – such as the bwForCluster NEMO – have to adhere to [2]. However, avoiding micro-management, these policies are deliberately not chosen to encompass each and every parameter of operation. Thus, there are decisions which have to be taken by the operators of a bwHPC resource in accordance with their respective user communities.

For the bwForCluster NEMO, a twofold approach was chosen [3] based on the experience acquired during the procurement phase of NEMO. Two governance bodies have been created, with either taking a designated role for the gathering of community feedback and getting recommendations for taking scientific and technical decisions:

- The NEMO general user assembly ("NEMO Nutzerversammlung") is taking place biannually. The event is widely announced on various websites and mailing lists and all current and prospective NEMO users are invited to participate. The aim is to report on the current status, gather broad feedback coming from the actual user base and inform on current and future developments with respect to NEMO. Common ideas and problems from users can be addressed and discussed at this meeting.
- The NEMO advisory board ("NEMO Cluster-Beirat") is a committee composed of representatives of NEMO's scientific communities and its shareholders. It is complementary to the general user assembly in the sense that the board's meetings happen more often and can be convoked on demand. It is thus able to give advice if immediate or short-term decisions have to be taken. Additionally, the board members serve as contact partners for their respective communities. In this way, common issues can be consolidated and addressed in a concerted fashion, instead of dealing with each individually. Last but not least, it is the task of the advisory board to reconcile the diverging interests of the affected scientific communities and shareholders.

## 2 Fair-share and Quality of Service

A supercomputer such as the bwForCluster NEMO enforces a time sharing policy, meaning there is no individual user who has exclusive and unlimited access to all provided resources at all times. Instead, the user specifies the required resources (CPU cores, RAM, etc.) in a job description file which also states for how long the said resources will be needed. A scheduling software monitors the available computing resources and executes the job as soon as the requirements can be met.

In the default mode of operation, each user has an equal chance to allocate resources for his jobs. Once resources get scarce, the decision for resource allocation is based on a fair-share heuristic, which takes the usage history into account. In principle, this means that chances to allocate resources are higher for users that have previously not used the system as intensely as other users. The fair-share mechanism thus balances the concurrent demands of all users based on previous usage.

Compute resources (i.e. processor clock cycles) are highly volatile. At any given time, they are either used or not used. Unused compute resources are lost. Therefore, incrementation of fair-share priority ("saving of compute resources") can only be allowed up to a certain threshold. Otherwise, users who have not been using the system for an extended period of time would be able to monopolize and block the system for other users at a later time. To prevent this, fair share priorities will be reduced by a decay function over time.

Beyond the default fair-share mode of operation, it is possible to provide more fine grained usage rights, going so far as to give de facto exclusive rights to selected users on parts of the

HPC resource. This can be accomplished in multiple technical ways described by quality of service policies. In general, shareholders would be given a fixed percentage of compute resources representing their share. The interesting question is what happens with shareholder compute cycles that are not used. The following strategies are possible, including mixes and variations:

- Do not offer unused shareholder compute cycles to other users. Unfortunately, this is also the least efficient policy, wasting precious resources.
- Define a quality of service policy with guaranteed availability windows via rollback reservations. For example, a shareholder QoS policy could guarantee availability of 10% of the shareholder part in 1 hour, 50% of the share in 4 hours and 100% of the share in 24 hours.
- Guarantee 100% of the shareholder resources immediately. However, the resources are part of a preemptive scheduler queue, which can be used by other users with a zero QoS guarantee, meaning that jobs in this queue are not guaranteed to finish at all. This would still be useful for backfilling with smaller jobs, provided that experienced users can cope with prematurely terminated jobs by having a solid checkpointing strategy.

In the last two cases, the shareholder will be compensated by the right to use more resources than his share allows at times when there are a free compute cycles available.

## 3 Conclusions

The NEMO governance structures follow common practices established in research institutions. The first general user assembly was held on August 14th 2016 and the first NEMO advisory board meeting took place on December 14th 2016. Both events provided valuable feedback and resulted in several operational adjustments. Fair-share and quality of service have been approved as technical instruments to balance the competing interests of the three scientific communities and shareholders.

## References

[1] http://www.bwhpc-c5.de

[2] Wesner, S., Walter, T., Wiebelt, B., von Suchodoletz, D., Schneider, G. “Strukturen und Gremien einer bwHPC-Governance – Momentaufnahmen und Perspektiven.” in Kooperation von Rechenzentren Governance und Steuerung – Organisation, Rechtsgrundlagen, Politik, de Gruyter (2016): 315–329.

[3] Wiebelt, B., Janczyk, M., von Suchodoletz, D., Aertsen, A., Rotter, S., Schuhmacher, M., Greiner, A., Quast, G. “Strukturvorschlag für eine bwHPC-Governance der ENM-Community.” in Kooperation von Rechenzentren Governance und Steuerung – Organisation, Rechtsgrundlagen, Politik, de Gruyter (2016): 343–354.